Nuclear Science
NEA/NSC/R(2022)4
November 2022
www.oecd-nea.org

Treatment of Volatile Fission Products

OECD
BETTER POLICIES FOR BETTER LIVES

NEA
NUCLEAR ENERGY AGENCY

Nuclear Energy Agency

NEA/NSC/R(2022)4

Unclassified

English text only

23 November 2022

NUCLEAR ENERGY AGENCY
NUCLEAR SCIENCE COMMITTEE

Treatment of Volatile Fission Products

This document is available in PDF format only.

JT03508455

ORGANISATION FOR ECONOMIC CO-OPERATION AND DEVELOPMENT

The OECD is a unique forum where the governments of 38 democracies work together to address the economic, social and environmental challenges of globalisation. The OECD is also at the forefront of efforts to understand and to help governments respond to new developments and concerns, such as corporate governance, the information economy and the challenges of an ageing population. The Organisation provides a setting where governments can compare policy experiences, seek answers to common problems, identify good practice and work to co-ordinate domestic and international policies.

The OECD member countries are: Australia, Austria, Belgium, Canada, Chile, Colombia, Costa Rica, the Czech Republic, Denmark, Estonia, Finland, France, Germany, Greece, Hungary, Iceland, Ireland, Israel, Italy, Japan, Korea, Latvia, Lithuania, Luxembourg, Mexico, the Netherlands, New Zealand, Norway, Poland, Portugal, the Slovak Republic, Slovenia, Spain, Sweden, Switzerland, Türkiye, the United Kingdom and the United States. The European Commission takes part in the work of the OECD.

OECD Publishing disseminates widely the results of the Organisation's statistics gathering and research on economic, social and environmental issues, as well as the conventions, guidelines and standards agreed by its members.

NUCLEAR ENERGY AGENCY

The OECD Nuclear Energy Agency (NEA) was established on 1 February 1958. Current NEA membership consists of 34 countries: Argentina, Australia, Austria, Belgium, Bulgaria, Canada, the Czech Republic, Denmark, Finland, France, Germany, Greece, Hungary, Iceland, Ireland, Italy, Japan, Korea, Luxembourg, Mexico, the Netherlands, Norway, Poland, Portugal, Romania, Russia (suspended), the Slovak Republic, Slovenia, Spain, Sweden, Switzerland, Türkiye, the United Kingdom and the United States. The European Commission and the International Atomic Energy Agency also take part in the work of the Agency.

The mission of the NEA is:

– to assist its member countries in maintaining and further developing, through international co-operation, the scientific, technological and legal bases required for a safe, environmentally sound and economical use of nuclear energy for peaceful purposes;

– to provide authoritative assessments and to forge common understandings on key issues as input to government decisions on nuclear energy policy and to broader OECD analyses in areas such as energy and the sustainable development of low-carbon economies.

Specific areas of competence of the NEA include the safety and regulation of nuclear activities, radioactive waste management and decommissioning, radiological protection, nuclear science, economic and technical analyses of the nuclear fuel cycle, nuclear law and liability, and public information. The NEA Data Bank provides nuclear data and computer program services for participating countries.

Foreword

Under the auspices of the Nuclear Energy Agency (NEA) Nuclear Science Committee (NSC), the Working Party on Scientific Issues of Advanced Fuel Cycles (WPFC) was established to co-ordinate scientific activities related to advanced nuclear fuel cycles, including fuel cycle scenarios, innovative fuels and materials, separation chemistry, waste disposal and coolant technologies. Various expert groups have been established to cover these topics.

The Expert Group on Fuel Recycling and Waste Technology (EGFRW) – previously known as the Expert Group on Fuel Recycling Chemistry (EGFRC) – was created in 2012 and focuses on the separation processes relevant to recycling technologies for spent nuclear fuel, including reprocessing, waste treatment, recycling and reuse of spent fuel components but excluding long-term (dry/wet) spent fuel storage technologies.

After the publication of a state-of-the-art report on the progress of separation chemistry (NEA, 2018), the expert group initiated work on the different treatment systems capable of selectively trapping volatile fission products that are released during the reprocessing of spent nuclear fuel. The study primarily focused on technologies deployed or under research and development in member countries. This report presents the results of that study.

Acknowledgements

The NEA would like to acknowledge the efforts of past and present members of the EGFRW who have contributed to this report. Particular appreciation is expressed for the contributions of Giorgio De Angelis (retired from the National Agency for New Technologies, Energy and Sustainable Economic Development, Italy) who initiated the project; Pascal Baron (French Alternative Energies and Atomic Energy Commission, retired), the previous Chair of the expert group; and Stéphanie Cornet (NEA). Thanks to Jonathan Austin (National Nuclear Laboratory, United Kingdom) for the production of Figures 5.4, 5.5, 5.6 and 5.7.

Contributing authors

Pascal Baron (French Alternative Energies and Atomic Energy Commission [retired], France), past-Chair of the Expert Group on Fuel Recycling Chemistry

Emeroy Collins (Oak Ridge National Laboratory, United States)

Stéphanie Cornet (NEA), former Secretary of the Expert Group on Fuel Recycling Chemistry (until October 2020)

Giorgio De Angelis (National Agency for New Technologies, Energy and Sustainable Economic Development [retired], Italy)

Bill DelCul (Oak Ridge National Laboratory, United States)

Gabriele Grassi (NEA), Secretary of the Expert Group on Fuel Recycling and Waste Technology

Viktor Ignatiev (Kurchatov Institute, Russia)

Masatoshi Iizuka (Central Research Institute of Electric Power Industry, Japan)

In-Tae Kim (Korea Atomic Energy Research Institute, Korea)

Jack Law (Idaho National Laboratory, United States)

Tatsturo Matsumura (Japan Atomic Energy Agency, Japan)

Manuel Miguirditchian (French Alternative Energies and Atomic Energy Commission, France)

Yasuji Morita (Japan Atomic Energy Agency, Japan)

Robin Taylor (National Nuclear Laboratory, United Kingdom), Chair of the Expert Group on Fuel Recycling Chemistry/Expert Group on Fuel Recycling and Waste Technology

Joshua Turner (National Nuclear Laboratory, United Kingdom)

Jan Uhlíř (Research Centre Řež, Czech Republic)

Brian Wilson (National Nuclear Laboratory, United Kingdom)

Table of contents

List of tables

List of figures

List of abbreviations and acronyms

µSv/y	Micro sieverts per year
Ag@ZSM-5	Silver-loaded Zeolite Socony Mobil-5
AHTGR	Advanced high-temperature gas-cooled reactor
ALARA	As low as reasonably achievable
ANL	Argonne National Laboratory
ATLAS	Vitrification active pilot plant to study volatility
AVH	Atelier de vitrification de La Hague
AVM	Atelier de vitrification de Marcoule
BAT	Best available technique
BNFP	Barnwell Nuclear Fuel Plant
Bq/year	Becquerels per year
CCIM	Cold crucible induction melter
CEA	French Alternative Energies and Atomic Energy Commission
CETE	Complete End-To-End
CSTF	Coolant Salt Technology Facility
DF	Decontamination factor
DFcv	Decontamination factor for the calciner outlet
DOE	Department of Energy (United States)
DOG	Dissolver off-gas
EARP	Enhanced Actinide Removal Plant
EGFRW	Expert Group on Fuel Recycling and Waste (NEA)
FMOF-Cu	Fluorinated Metal Organic Framework
FP	Fission product
GDF	Geological disposal facility
GWd/MTIHM	Gigawatt day per metric tonne of irradiated heavy metal
HEPA	High efficiency particulate air
HIP	Hot isostatic press
HLLW	High-level liquid waste
HLW	High-level waste
HT	Tritiated hydrogen
HTO	Tritiated water
HTPT	High-temperature pre-treatment

HZ	Hydrogen mordenite
IAEA	International Atomic Energy Agency
ICPP	Idaho Chemical Processing Plant
INL	Idaho National Laboratory
JAEA	Japan Atomic Energy Agency
JHMM	Joule heated metal melter
KAERI	Korea Atomic Energy Research Institute
KfK	Karlsruhe Nuclear Research Centre
KIT	Karlsruhe Institute of Technology
kPa	Kilopascals
KRF	Krypton Recovery Facility
LLW	Low Level Waste
M	Concentration in moles per litre
MOF	Metal organic framework
MOR	Mordenite
MSR	Molten Salt Reactor
MSRE	Molten Salt Reactor Experiment
MOX	Mixed oxide
NEA	Nuclear Energy Agency
NiDOBDC	Nickel dioxobenzenedicarboxylic acid
NNL	National Nuclear Laboratory
NOx	Nitrogen oxide
NSC	Nuclear Science Committee (NEA)
OECD-NEA	Organisation for Economic Co-operation and Development – Nuclear Energy Agency
ORNL	Oak Ridge National Laboratory
PAMELA	Pilot installation at Mol for the vitrification of high active liquid waste undergoing conversion for the processing of part of the historic HRA/solarium waste
PAN	Polyacrylonitrile
PEV	Inactive vitrification pilot plant containing a full-scale replica of a La Hague vitrification line
PIVER	A batch vitrification process that did not employ a separate calcination step
PNC	Power Reactor and Nuclear Fuel Development Corporation
PNNL	Pacific Northwest National Laboratory
ppm	Part per million

TGA	Thermogravimetric analysis
PWR	Pressurised water reactor
SA	Silica alumina
THORP	Thermal oxide reprocessing plant
TRP	Tokai Reprocessing Plant
UNF	Used nuclear fuel
V/ENH	Electrode potential in volts compared with the standard hydrogen electrode
VEK	Verglasungseinrichtung Karlsruhe
VFP	Volatile fission product
VOG	Vessel off-gas
vol.	Volume
VULCAIN	Early French facility for glass fabrication
WAK	Karlsruhe Reprocessing Plant
WPFC	Working Party on Scientific Issues of Advanced Fuel Cycles (NEA)
wt.%	Weight per cent
WVP	Waste Vitrification Plant
ZIF	Zeolitic Imidazolate Framework

Executive summary

This report brings together the life cycle story of key volatile species that are released in the reprocessing of used nuclear fuel (UNF), from their generation to ultimate disposal. Only once that entire picture is understood can decisions be taken on the best methods for managing volatile fission products (VFPs). This area represents a major challenge that has been the subject of a substantial body of research and technology development over the last few decades. The scope of this report, therefore, has been limited to providing an overview of the challenges caused by VFPs, the main abatement technologies used or investigated, and their consequent immobilisation into suitable waste forms. For more detailed information, the reader is directed towards the wider body of literature cited in the references for each chapter.

Chapter 2 discusses the generation of volatiles (H-3, C-14, Kr-85 and I-129) and semi-volatiles (Tc-99, Ru-106, Cs-137, etc.). While it is correct that the majority of volatiles are released in the head-end section of a reprocessing plant, it is too simplistic to concentrate attention there, especially if aiming for a near-zero discharge process. Downstream of head end, the processes themselves can change the chemistry of the volatiles, as is the case for iodine, or introduce significant quantities of semi-volatiles into the off-gas. Semi-volatiles are most prevalent for high-temperature processes such as those found in high-level waste (HLW) treatment. A high-temperature head-end step, originally designed as a route to tritium management, can be used to drive off many of the volatile species, potentially making off-gas capture an easier proposition. The challenges associated with VFPs in pyroprocessing differ to aqueous processes, most significantly for the fluoride volatility method, although the chloride method also has differences caused by the fundamental change in process relative to classical reprocessing techniques. The need to manage VFPs can be shown to be present across the whole reprocessing plant, whether that is a classical aqueous process or a pyrochemical one.

Chapter 3 explores the different techniques that can be used to remove volatiles from the off-gas stream. There are three main concepts, if particulates are discounted, that describe the approaches taken: 1) liquid adsorption; 2) solid adsorption; and 3) distillation. Of these three, solid adsorption is seen as preferable as it removes the difficulties of managing liquid effluent. Furthermore, the solid sorbent can be designed to be readily converted into a final disposal form.

Chapter 4 focuses on the waste forms that enable the final disposal of captured volatiles. While there are unique challenges faced for each of the different volatile and semi-volatiles, I-129 poses perhaps the greatest challenge. Its long half-life and high mobility means that an iodine-containing waste form may need to be stable on the order of 10^7 years within a geological repository.

Chapter 5 presents nanomaterials as one of the ways to increase the control of volatiles. These materials can be synthesised with great control over their physical structure, leading to greater levels of selectivity. In addition, a move away from relying on liquid effluents to manage volatiles means that volatile species can be readily converted into final waste forms without the additional need to treat the effluent.

Further to what is presented in Chapter 5, advances in on-plant monitoring coupled to the use of modelling and simulation, forming what is known as “digital twins”, will help future operators better manage their plant to minimise off-gas generation. It is also key to integrate the development of abatement and final waste form technologies to ultimately minimise

the steps required to convert waste into a waste form ready for storage and disposal. Reducing the number of different plants or plant stages will reduce the footprint of a reprocessing site, which reduces the upfront capital expense. There are further broader ambitions for advanced reprocessing that have been presented, which also apply to the treatment of volatile fission products (Table ES.1).

Table ES.1. Volatile fission product requirements for advanced reprocessing.

Strategic objective	Fuel cycle requirement	Potential implications for reprocessing plant flowsheets
Process safety	– Safer processes	
Waste management and environmental impact	– Reduced impact of fuel cycle on repository footprint (radiotoxicity and heat loading) – Reduced waste generation and lower environmental impact	– Reduced number and volumes of aqueous waste streams – Target "near-zero" emissions – Capture of volatile species (H-3, C-14, Kr-85 and I-129) – New waste forms
Economics of advanced reprocessing	– Reduced capital costs through smaller plant footprint – Greater flexibility of process	– Intensified processing – Fewer waste streams – Process light water reactor, mixed oxide and fast reactor fuels – Feed variations (carbide, nitride and metal fuels as well as oxides) – Higher burnup – Short cooled fast reactor, very long cooled light water reactor fuels – depends on scenario

Source: Selected from Table 1 in reference [202].

This report focuses on technologies, but it is impossible to separate the implementation of a technology from the regulations which govern aerial discharges. National approaches to environmental regulation differ, but are often based on applying the principles of best available technique (BAT) and as low as reasonably achievable (ALARA) to guide decision making on whether to abate a radionuclide and to what level. To further guide new plant development, regulatory bodies may state a maximum dose to the critical group (e.g. 150 µSv/y in the United Kingdom for new build). Furthermore, in the United Kingdom, there is a preference for concentrate and contain over dilute and disperse, coupled with a requirement for a continuous reduction in discharges. In contrast, in the United States, the regulatory environment is specific for some species, such as I-129 and Kr-85. However, looking at current regulations only gives a picture of the world today, but advanced recycling is expected in the medium-term future. It is therefore not certain what the environmental standards will be and consequently the levels of performance that new or emerging technologies will have to meet.

Looking back on the history of nuclear programmes for perspective, what was once good practice at the time of a plant's design can be quickly eclipsed by improving environmental standards. The impact of changes over time has meant that there are examples of reprocessing plants that were retrofitted with abatement systems to reduce discharges to meet those increasing standards. The Enhanced Actinide Removal Plant (EARP) at Sellafield in the United Kingdom was one such plant, built to treat effluent to remove long-lived actinides. Considering Pu-239/240, this led to approximately a fourfold

reduction in discharge despite an increase in reprocessing activity. In hindsight, any additional plant added to a process after design of the reprocessing plant is suboptimal. Efficiencies are lost relative to considering incorporating those abatement facilities during the original design and build. Therefore, when developing new technologies today, the focus should be on providing options for the abatement of volatile and semi-volatile species to meet a wider variety of future scenarios, e.g. from a business-as-usual scenario to a "net zero" emissions scenario. The challenging ambition of aiming for net zero, as articulated by the Nuclear Energy Agency, helps to guide researchers towards developing technologies of the future.

Finally, the treatment of VFPs should be considered in the context of the wider recycle plant and associated waste treatment. The better this can be modelled and understood prior to design, the more optimised the facility can be to deliver reduced costs and reduced discharges relative to the plants of today. By developing improved technologies for the treatment of VFPs that reduce environmental impacts and waste generation, credible options for spent fuel recycling in future closed fuel cycles are enhanced. Such abatement technologies support both aqueous reprocessing and pyrochemical processing of spent fuels for either generation III+ thermal reactors or deployment of generation IV reactors and their associated fuel cycles.

1. Introduction

A by-product of nuclear fission is the formation of a large array of activation and fission product (FP) species, some of which form compounds that can readily move into the gaseous phase, commonly referred to as off-gases. Typical reactors today generate approximately 2-5 wt.% of FP in UNF. The quantity of FPs generated is proportional to the burnup during irradiation (typically expressed as burnup per metric tonne of irradiated heavy metal, GWd/MTIHM). Other factors such as fuel properties and cooling time will affect the distribution of FPs. A small proportion of the FPs and some activation products contained in the UNF are volatile at elevated temperatures. Those species that do enter the off-gas need to be understood and appropriately managed to minimise the environmental impact. UNF management is either through direct disposal in a geological repository (the open fuel cycle) or through reprocessing and recycling of reusable materials, with only residual wastes sent to the repository (the closed fuel cycle). The challenges associated with off-gas management have been the subject of substantial reviews over the years [1-5].

There are two main facilities where gaseous species are released: the reactors and reprocessing plants. These facilities must be equipped with abatement systems to manage these gaseous FPs and ensure any releases are strictly kept within authorised discharge limits. The focus of this review is how these VFPs (used as a generic term in this report to also include the activation products, tritium and C-14) can be abated during current or future reprocessing activities.

The elements involved in aerial discharge from reprocessing can be split into three categories (where elements readily fit into multiple categories, they have been placed in the more volatile category, e.g. Cs in semi-volatile instead of particulate):

1. volatiles: C, H, I, Kr;
2. semi-volatiles: Ag, Au, Bi, Cd, Cs, Ge, In, K, Mo, Na, Pb, Po, Pt, Rb, Re, Rh, Ru, Sb, Se, Sn, Tc, Te, Tl, Zn;
3. particulates: Am, Ce, Cm, Co, Eu, Fe, Nb, Ni, Np, Sr, Zr, Pu, U.

Since the focus of this report is on volatiles, only volatile and semi-volatile species will be considered. For a good summary on the management of particulates in nuclear reprocessing plants see reference [5].

When considering what defines a volatile and a semi-volatile FP, it is not immediately clear where the boundary exists, a problem recognised by Jubin et al. in 2014 [4]. To attempt a useful definition, semi-volatiles are inorganic and organometallic species that can become gaseous under operating conditions within a reprocessing facility or have vapour pressures to enable noticeable concentrations in the vapour phase above process liquors. Volatile species are those that readily enter the gaseous phase at ambient conditions or have extremely high vapour pressures that facilitate facile volatilisation. It is challenging to define these terms independent of the process in which they are applied. This issue becomes clear when considering pyrochemical processes in Section 2.3 in Chapter 2, where the categorisation of semi-volatile and volatile changes due to the different plant operating conditions. Unless the text is discussing a pyrochemical process, the categorisation as defined above will be used.

Among the VFPs, H-3, C-14, Kr-85 and I-129 constitute the main environmental concern if released to the environment during spent fuel processing. Longer term storage (>10 years) of used fuel prior to reprocessing allows the short-lived isotopes (e.g. $T_{1/2}$(H-3) = 12.32 y, $T_{1/2}$(Kr-85) = 10.76 y) to decay significantly. However, depending on regulatory limits, they may remain an environmental concern even up to about 50-100 years of fuel storage [6]. In contrast, the release of the highly mobile I-129 and C-14 remains important to consider over geological timescales ($T_{1/2}$(I-129) = 15.7 million years, $T_{1/2}$(C-14) = 5 730 y).

The speciation of the "volatile radionuclides", which include H-3, C-14, Kr-85 and I-129, is important to understand. In aqueous UNF reprocessing, these radionuclides are most commonly expected to evolve into off-gas streams as tritiated water (HTO or T_2O), radioactive CO_2, noble gases (mainly krypton) and iodine (HI, I_2 or organic iodides). These volatile radionuclides will be discharged to the environment if no off-gas capture processes are included to limit their release. As an example, Table 1.1 shows the amount of selected volatile gases contained in a unit quantity of UNF irradiated to a burnup of 55 GWd/MTIHM after five years of storage.

Regulatory requirements for the capture of volatile fission gases are dependent on the environmental regulations specific to the country of operation. For example, in the United States, required decontamination factors were estimated based on current regulations and are presented in Table 1.2 [7]. In other countries, such as the United Kingdom, the approach to setting discharge limits is less prescriptive and based around the concepts of BAT and ALARA [8].

In commercial-scale reprocessing plants across the world today, such as Sellafield and La Hague, the management of VFPs follows a similar theme [5]. Xenon and krypton are released, unabated to the environment, via an off-gas stack. Iodine is removed from the off-gas stream, typically through caustic scrubbing, but can also be abated by solid silver-based sorbents. It is then converted into a liquid waste and discharged to the sea using the principle of isotopic dilution. C-14 is scrubbed from the gas phase and either discharged to the sea or converted to a solid carbonate and encapsulated in a solid waste form such as cement. The semi-volatiles are typically abated by liquid scrubbers and only become important in waste vitrification processes, where abatement is mostly achieved through the use of liquid scrubbing. As technology advances, the options available for an advanced reprocessing plant will increase. In addition, it is also to be expected that discharge limits will become more restrictive.

In any future "advanced" reprocessing plant, minimising plant discharges will be paramount to continue to demonstrate compliance with national and international environmental regulations and standards. These plants should therefore maximise the capture of volatile and semi-volatile species and dispose of the secondary wastes in improved waste forms that achieve the performance required for final disposal. The increase in control required to abate these volatiles adds a variety of technological challenges that need to be overcome to achieve a vision of "near-zero" environmental impact.

This report will give an understanding, through contributions from experts from NEA member countries, of where volatiles are generated within reprocessing; the methods that can be used to trap these species from the gas phase; their conversion to a final waste form; and, finally, a summary of innovative technologies being considered for the future. Specifically, Chapter 2 will describe where major releases of volatile and semi-volatile species are expected within reprocessing. It considers volatile release from tritium pre-treatment, nitric acid dissolution, pyrochemical processing and waste treatment. Chapter 3 focuses on technologies used to remove important radioisotopes from the gas phase. Each

important radioisotope will be considered in turn: H-3, I-129, C-14, Kr-85 and semi-volatiles. Chapter 4 outlines the final disposal waste forms for the trapping technologies described in Chapter 3. Finally, promising developments such as nanomaterials, likely to influence the future of volatile treatment technologies, are considered in Chapter 5.

Table 1.1. Quantity and activity of selected radioactive volatile gases contained in used nuclear fuel irradiated at a burnup of 55 GWd/MTIHM* after 5 years of storage

Isotope	Activation products		Fission products		Activation + fission products	
	(g/MTIHM)	(Bq/MTIHM)	(g/MTIHM)	(Bq/MTIHM)	(g/MTIHM)	(Bq/MTIHM)
H-3	2.19E-2	7.81E12	6.84E-2	2.44E13	9.03E-2	3.22E13
C-14	1.66E-1	2.74 E10	4.38E-5	7.22E6	1.66E-1	2.74E10
Kr-85	0	0	2.96E+1	4.29E14	2.96E+1	4.29E14
I-129	7.24E-13	4.74E-6	2.35E+2	1.54E9	2.35E+2	1.54E9

* Oak Ridge National Laboratory Isotope Generation and Depletion Code (ORIGEN) calculation based on pressurised water reactor fuel at a burnup of 55 GWd/MTIHM and cooling time of five years.
Notes: GWd/MTIHM: gigawatt day per metric tonne of irradiated heavy metal; g: gramme; Bq: becquerels.

Table 1.2. Estimated decontamination factors required for the volatile radionuclides for different selected types of used fuels and burnups based on US regulations

	Dose limit = 25 µSv/y and 75 µSv/y to thyroid (40 CFR 190)			Dose limit = 2.5 µSv/y and 7.5 µSv/y to thyroid (10% of 40 CFR 190 limits)		
	PWR/UOX BU = 60 GWd/MTIHM	PWR/MOX BU = 100 GWd/MTIHM	AHTGR BU = 100 GWd/MTIHM	PWR/UOX BU = 60 GWd/MTIHM	PWR/MOX BU = 100 GWd/MTIHM	AHTGR BU = 100 GWd/MTIHM
H-3	25 (1 after 57 y cooling)*	160 (1 after 90 y cooling)*	42 (1 after 66 y cooling)*	600 (1 after 110 y cooling)*	720 (1 after 120 y cooling)*	590 (1 after 110 y cooling)*
C-14	1	1	4	10	15	30
Kr-85	9 (1 after 34 y cooling)*	4.2 (1 after 22 y cooling)*	9.2 (1 after 34 y cooling)*	18 (1 after 45 y cooling)*	13 (1 after 40 y cooling)*	62 (1 after 64 y cooling)*
I-129	380	630	650	3 800	8 000	6 600

* The number of years of cooling for no abatement to be required (DF = 1).
Notes: µSv/y: micro sieverts per year; PWR: pressurised water reactor; UOX: uranium oxide; BU: burn-up; GWd/MTIHM: gigawatt day per metric tonne of irradiated heavy metal; MOX: mixed oxide; AHTGR: advanced high-temperature gas-cooled reactor; DF: decontamination factor.

2. Generation of volatiles

Within a reprocessing plant, there are a number of key locations where substantial quantities of volatiles can be generated. Major sources include during a pre-treatment step, head-end aqueous dissolution, pyrochemical processing and waste treatment plants involving elevated temperatures. Understanding where volatile species are generated is key to selecting an appropriate abatement method.

2.1. Tritium pre-treatment

2.1.1. Introduction

Under the effect of a thermal gradient, tritium formed in the fuel during irradiation migrates to the cooler parts of the fuel. The diffusion of tritium in the fuel rod is thus directly linked to the temperature and to the linear power of the irradiation. In fast reactor fuels, the thermal gradient is very high and almost all the tritium (99%) diffuses out of the oxide and stainless steel clads and is found in the sodium coolant. In light water reactor fuels, roughly half of the tritium diffuses out of the oxide and is trapped in the Zircaloy clads. The zirconia layer (ZrO_2) formed on the surface of the cladding material during the irradiation behaves as a barrier, preventing the migration of tritium to the coolant.

Tritium pre-treatment is a dry head-end method initially developed for removing tritium from UNF prior to aqueous processing. This avoids introducing the tritium into the aqueous systems where it would accumulate and/or might be released to the environment.

2.1.2. Standard tritium pre-treatment

During standard tritium pre-treatment, the monolithic fluoritic UO_2 transforms to orthorhombic α-U_3O_8 powder. This phase transformation serves to release volatiles and remove the pelletised UNF from the cladding.

Tritium is released into the head-end off-gas as tritiated water. In addition, there is a significant release of other volatiles (e.g. Kr, Xe, C-14 [as $^{14}CO_2$]) and may include trace release of semi-volatiles depending on the conditions used. A review of the literature [9] indicates releases as follows:

~50% C-14 (as CO_2);

~6% Kr and Xe;

~1% I (Br may behave similarly);

< 0.2% Ru-106, Sb-125, Cs-134-Cs-137.

However, studies at the Oak Ridge National Laboratory (ORNL) during the "Complete End-To-End (CETE)" project showed a higher fraction of Kr, and Xe by analogy (up to 50% Kr), and undetectable amounts of gamma-emitting fission products beyond a high efficiency particulate air (HEPA) filter that separated the tritium pre-treatment system from the off-gas system. In any case, release of noble gases and iodine is certainly not complete. Advanced pre-treatment processes that are in development have shown near complete volatile and semi-volatile release, primarily through a collaboration between Canada, Korea and the United States [10-14].

2.1.3. NO_2-based tritium pre-treatment

As discussed above, in standard tritium pre-treatment, monolithic fluoritic UO_2 transforms to orthorhombic α-U_3O_8 powder. The NO_2 oxidation process allows for additional release of volatile and semi-volatile FPs during pre-treatment and proceeds with higher reaction rates at temperatures lower than those employed in standard temperature pre-treatment processes [15, 16]. A mixture of NO_2 and O_2 is used as the oxidant at lower temperatures (<350°C), leading to a faster process than just using air or O_2 oxidation at elevated temperatures (t >500°C).

Additionally, consumed NO_2 used in the oxidation reactions can be easily regenerated in a closed loop system, where oxygen back-reacts with the by-product NO to regenerate the dioxide in the cooler regions. In effect, NO_2 could be described as an oxygen carrier since it is not consumed in the overall set of reactions in which O_2 is the consumable reagent:

$$2NO(g) + O_2(g) \longrightarrow 2NO_2(g)$$

The use of a closed loop system results in a potential reduction of the total volume of off-gas requiring treatment to remove VFPs. This could reduce the size of a head-end off-gas system, since the volume to be treated is in the order of a few m^3 compared to >1 000 m^3 per tonne of fuel as in a conventional tritium pre-treatment system. Xe and Kr would be present at a concentration of a few vol.% compared to parts per million (ppm) that could translate into a potentially simplified recovery and separation system.

Recent studies on an advanced tritium pre-treatment process using nitrogen dioxide have shown the removal of iodine in addition to tritium [15, 16]. This may provide a means to limit the distribution of iodine to other streams within the plant. Iodine is believed to be found in UNF primarily as CsI, which has been observed to react with NO_2 to produce $CsNO_3$, liberating iodine as shown by:

$$2CsI(s) + 4NO_2(g) \longrightarrow 2CsNO_3(s) + I_2(g) + 2NO(g)$$

The near complete removal of iodine was confirmed by cold tests using natural CsI and spiked $Cs^{125}I$ on unirradiated UO_2 pellets. This has also been carried out at a gram scale with irradiated fuel, but not yet corroborated at bench scale [16]. For the gram scale, tests with irradiated fuel neutron activation and low-energy gamma spectroscopy were used to analyse for ^{129}I and were found to be effective methods when combined with an appropriate separation procedure for both surrogate and UNF samples. Iodine must be separated from the matrix to avoid interferences in low-energy gamma spectroscopy and to limit the heat generated upon activation. If the near complete release of iodine could be achieved in a dry head-end process, this would eliminate the need for, or simplify, the subsequent trapping of iodine from other off-gas streams present in a reprocessing facility.

2.1.4. Alternative tritium control techniques

Without an upfront temperature pre-treatment step, the tritium in UNF is converted into tritiated water and diluted when the fuel is dissolved. This dilution makes the control of tritium substantially more challenging. There are two primary approaches to controlling the discharge of tritium from the fuel processing plant to the environment: 1) isotopic separation of HTO from H_2O; or 2) capture and treatment of all water discharges. Other alternatives depend on one of these methods in combination with either the degree of water recycle or placement of the process within the plant.

Dissolution of UNF following shearing would contaminate the plant water with tritiated water. Isotopic separation of HTO from the process water is technically possible. A plant processing 1 000 metric tonnes per year of UNF would receive only about 90 g/year of

tritium (3.2×10^{16} Bq/year). If totally converted to water, the mass of HTO would be 330 g/year. This small amount would be diluted in the plant water inventory; the inventory might be in the range of 50 000 kg. HTO concentrations in the range of around 6 ppm would result. Separation of the tritium by isotopic separation could require very large equipment and be very expensive to operate. An earlier assessment indicated this to be the case; however, the economics could be significantly improved by recycling the plant water to permit a build-up of tritium concentration in the plant water inventory, coupled with continuous processing of a small bleed stream [17]. There is a risk for build-up of other impurities, which could negatively impact separation efficiencies in any portion of the plant where the recycled water is used. This would be an additional consideration for this method to become viable.

A technique to capture and treat all water discharges is another option. Water removed from the plant could be immobilised such that it is suitable for disposal; for example, mixing the water with grout for deep-well injection where it would solidify [18]. Two approaches to implementing this can be considered. In one approach, a controlled water discharge to a holding tank at a rate equal to the amount of water produced by chemical reaction would be used to collect a sufficient volume for a batch disposal, which would occur at regular intervals.

2.2. Nitric acid dissolution

2.2.1. Dissolution of chopped fuel

In conventional fuel recycling, the heavy end pieces and hardware are removed from the fuel element. The fuel pins, comprised of UO_2 fuel pellets in Zircaloy tubing, are sheared (or chopped) either individually or as a bundle into short segments ranging from 0.5 cm to 5.0 cm long. These segments are fed into a basket-type dissolver where the fuel components are leached from the cladding segments, leaving the acid-resistant empty Zircaloy cladding segments (hulls) behind. Leaching rates depend on the nitric acid concentration, solution temperature and the length of the chopped fuel segments. Mass transfer between the open ends of the chopped segment and the surface of the enclosed fuel pellet is improved by agitation, but complete dissolution may take up to four hours. Nitric acid oxidises and converts the UO_2 fuel to uranyl nitrate and considerable quantities of nitric oxide (NO) and nitrogen dioxide (NO_2) are evolved during the process. See the reaction stoichiometry below:

$$\text{For } [HNO_3] < 2 \text{ M:} \quad 3UO_2 + 8HNO_3 \rightleftharpoons UO_2(NO_3)_2 + 2NO + 4H_2O$$

$$\text{For } [HNO_3] > 8 \text{ M:} \quad UO_2 + 4HNO_3 \rightleftharpoons UO_2(NO_3)_2 + 2NO_2 + 2H_2O$$

In typical operational conditions today, the nitric acid concentration is ~3 moles per litre, so the average reaction stoichiometry is**:**

$$UO_2 + 3HNO_3 \rightleftharpoons UO_2(NO_3)_2 + 0.5NO + 0.5NO_2 + 1.5H_2O$$

During this operation, most fission and activation products are present as nitrates in solution. The dissolver system usually includes a means to rinse the defueled cladding hulls to recover the fuel solution and decontaminate the hulls for further processing (e.g. drying, compaction and/or entombment in grout).

2.2.2. Tritium behaviour

If tritium is not removed by a dedicated treatment (see Section 2.1), the tritium remaining in the oxide is mainly released in the nitric solution as HTO during the fuel dissolution. Only a very small fraction of tritium (0.5%) is volatile and is present in the off-gas as tritiated hydrogen (HT) gas. Once in an aqueous phase, tritium release is distributed throughout the plant.

2.2.3. Iodine behaviour

Iodine, formed by fission in the fuel, reacts with highly electropositive elements such as caesium, which is very abundant. Stabilised as CsI, iodine remains in the oxide during the shearing of the fuel elements. At higher burnup, Cs_2O and I_2 migrate to the cooler regions of the fuel, further promoting the formation of CsI. In metal fuels, in addition to reacting with Cs, iodine can also react with the abundant uranium forming UI_3. During the dissolution step in nitric medium, iodides are then oxidised into elemental iodine (I_2) through the following reactions:

$$2I^- + NO_3^- + 2H^+ \longrightarrow I_2 + NO_2^- + H_2O$$

$$2I^- + 2NO_2^- + 4H^+ \longrightarrow I_2 + 2NO + 2H_2O$$

The oxidation can be extended beyond iodine with formation of non-volatile species, such as iodates (IO_3^-). However, the presence of nitrous acid in the dissolution solution prevents this reaction, which is anyway very slow in nitric medium. Nitrous acid is formed during UO_2 dissolution and buffers the redox potential of the solution around 1 V/NHE stabilising iodine under its volatile form I_2 as depicted in Figure 2.1.

Figure 2.1. Phase diagram showing concentration of iodine (M) and redox potential (V/NHE) for an iodine-water system (T = 100°C, [H^+] = 3 M)

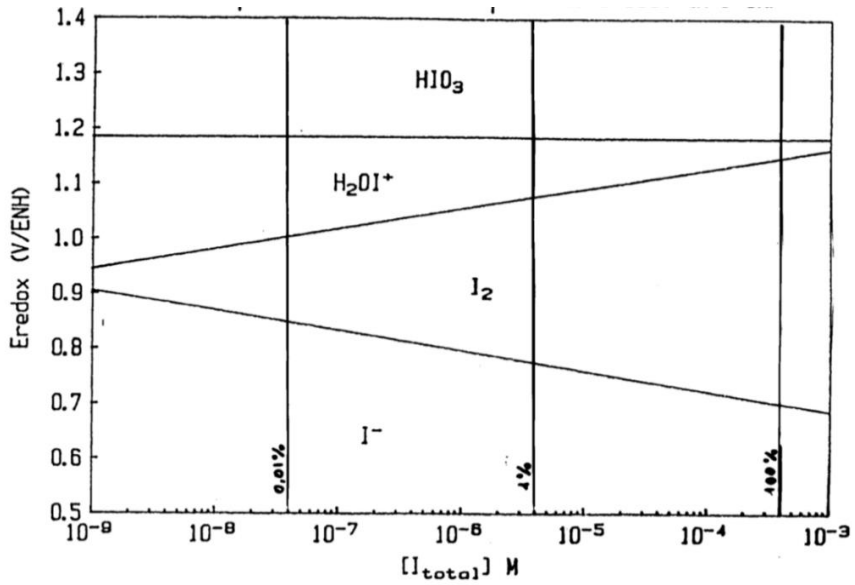

Source: Courtesy of CEA-Orano.

Most of the iodine is therefore released with the off-gases from fuel dissolution reactions as I_2. To optimise the management of iodine in the process, it is very important to minimise the residual amount of iodine in the dissolution solution. The method depends on the type of dissolution process:

- In a discontinuous dissolver, where the fuel is fed by batches, the standard procedure consists of extending the boiling time of the solution dissolution to complete iodine desorption from the solution. If the objective is to lower the residual iodine quantity to less than 1% of the initial quantity in the solution, the limiting factor is the presence of iodates, organic iodides (reaction with trace organic contaminants in the nitric acid) and colloidal iodine species (e.g. AgI and PdI2). Reduction of the remaining trace iodates is limited when the solution contains no more nitrous acid, produced by dissolution of fuel pellets.
- In a continuous dissolver (e.g. rotating dissolver; see Figure 2.2), the process is at a steady state and the residual concentration of iodine in the outlet solution depends on the operating conditions. A complementary step is generally needed to reach a residual iodine content less than 1% of the initial quantity. This is performed in the La Hague reprocessing plants through an iodine desorber located in series with the dissolver. This device extends the boiling of the dissolver solution with a possible injection of nitrous fumes to stabilise iodine.

Figure 2.2. Rotating dissolver of La Hague UP3 and UP2-800 Orano's plants

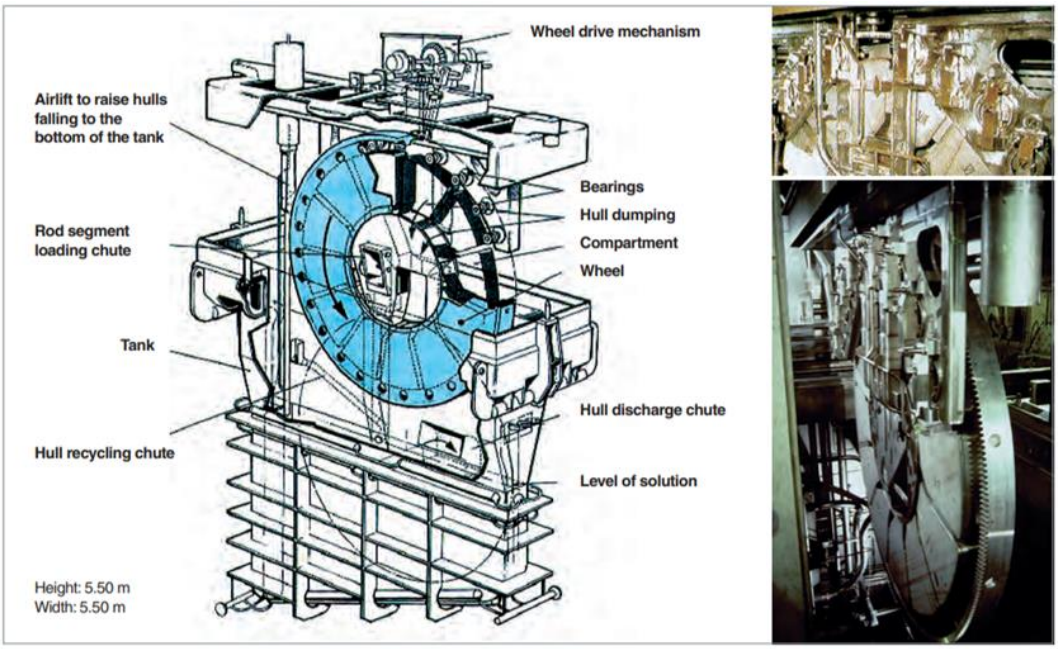

Source: CEA-Orano (2008).

Despite the small quantity remaining, iodine is also released downstream of the dissolver and can contribute similar quantities of off-gas to environmental discharges. This is due to the relative inefficiencies of abating iodine in the vessel vent off-gas systems. It is therefore important to understand what causes iodine to be released downstream of head end and what can be done to reduce the discharge. One challenge is that by addition of organic solvent in the chemical separations part of a reprocessing plant, iodine species can move from the aqueous to the organic phase. As the solvent breaks down due to radiolysis, it

produces radicals which can react to form organic iodides [19]. These organic species are not well abated by typical caustic scrubbers, due to reduced solubility and slower reaction rates, and therefore are released essentially unabated.

2.2.4. Carbon-14 behaviour

C-14 is mainly an activation product formed by neutron capture on N-14 (n,p reaction) and O-17 (n,α reaction). As N-14 is an impurity of the fuel, the amount and the chemical form (gaseous CO_2, CO, carbides, graphite, etc.) of C-14 present in the fuel are difficult to determine precisely.

Studies carried out at the French Alternative Energies and Atomic Energy Commission (CEA) showed, however, that less than 1% of C-14 would be released during the shearing of the fuel elements while the major fraction of C-14 would be released as $^{14}CO_2$ (and ~1% as ^{14}CO) during the dissolution in nitric acid (highly diluted in non-active CO_2). A small fraction of the C-14 remains in the solution post-dissolution. Studies are in progress to determine precisely the distribution of C-14 depending on the conditions of dissolution. In the United Kingdom, <2% of the C-14 remains in the dissolver product.

While the majority of C-14 is released into the dissolver off-gas, it is also important to consider other points of C-14 release. This is because abatement systems in downstream processes are typically less efficient than in the head end. In the Thermal Oxide Reprocessing Plant (THORP), the C-14 treatment plant, which receives caustic scrubbing liquors and adds barium nitrate to precipitate barium carbonate, contributes a significant portion of the total C-14 aerial discharge.

2.2.5. Krypton, xenon behaviour

As expected for noble gases. krypton and xenon, formed during irradiation, are not chemically bound to the fuel and are typically unreactive. Depending on the burnup and the temperature, a certain content of Kr and Xe remains occluded in the oxide while the other part is released into the expansion chamber. If the fuel is allowed to cool, the majority of the short-lived noble gas isotopes are allowed to decay, leaving only non-active Xe and Kr-85.

In the case of light water reactor fuels, around 5% of Kr and Xe would be released in the off-gas during the shearing step and 95% during the dissolution step. The fraction of Kr and Xe released during the shearing of fast reactor fuels is, however, much higher (e.g. 80% or more).

2.3. Pyrochemical processes

Pyrochemical, unlike nitric acid-based aqueous processing, does not utilise differences in solubility as a primary method of separation. Instead, partitioning of species in UNF is controlled by electrochemical differences between elements and thermally induced volatility. There are two main pyrochemically based processing methods: a fluoride volatility and a chloride electrochemical-based process.

2.3.1. Fluoride volatilisation processes

Fluoride volatilisation processes are the “dry” pyrochemical separation techniques based on the specific property of uranium, neptunium and partially plutonium to form volatile hexafluorides. This property can be exploited mainly for the separation of uranium and plutonium from the spent nuclear fuel by the fluoride volatility method or for the separation

of uranium from the liquid molten salt fuel by the fused salt volatilisation technique. Both processes also generate volatile fission products in the chemical form of volatile fluorides.

The **fluoride volatility method** is based on the direct fluorination of spent fuel by fluorine gas. The technology converts the elements present in spent fuel in oxide or metallic form into fluorides, which are either solid, semi-volatile or highly volatile. Most FPs present in the typical spent fuel from light water reactors or fast reactors form solid fluorides, but an appreciable part of the fission product inventory forms volatile fluorides, which must be separated from volatile actinides and be subsequently treated [20-22]. Table 2.1 lists the distribution of FPs into the solid and volatile fluorides.

Table 2.1. Distribution of fluorinated spent fuel according to the volatility

Group I (highly volatile)			Group II (volatile)			Group III (non-volatile)		
Agent	**m.p. °C**	**b.p. °C**	**Agent**	**m.p. °C**	**b.p. °C**	**Agent**	**m.p. °C**	**b.p. °C**
Kr	–157.2	–153.4	IF_7	5	4	RhF_3	subl.	600
Xe	–111.8	–108.1	IF_5	9.4	98	UNF_4	subl.	705
TeF_6	subl.	–38.6	MoF_6	17.6	33.88	ZrF_4	912	918
SeF_6	subl.	–34.5	TcF_6	37.9	55.2	CsF	703	1 231
			SbF_5	6	142.7	RbF	760	1 410
			NbF_5	80	235	YF_3	1 136	2 230
			RuF_5	101	280	BaF_2	1 353	2 260
			RuF_6	51	70	EuF_3	1 276	2 280
			RhF_5	95.5	n/a	GdF_3	1 380	2 280
			RhF_6	70	73.5	CeF_4	838	decomp.
						CeF_3	1 430	2 330
						PmF_3	1 410	2 330
						SmF_3	1 306	2 330
						SrF_2	1 400	2 460

Notes: subl.: sublimation; decomp.: decomposition. Boiling (b.p.) and melting points (m.p.) under standard conditions have been provided.
Source: Based on [23].

However, the UNF must be pre-treated before reprocessing by the fluoride volatility method. Before the fluorination process, the fuel has to be converted into a powdered form suitable for the flame fluorination reaction. High-temperature pre-treatment (described in Section 2.1) is the most suitable technology for disintegration of the spent fuel.

VFPs generated during reprocessing by the fluoride volatility method are generally fluorides, which can be trapped and fixed in the solid form only by sorption onto a suitable sorbent. Sodium fluoride in the form of NaF pellets is the main sorbent used successfully within the process. The columns of pelletised NaF can be eventually supplemented by the columns of LiF, MgF_2 and alkaline absorber/mixture of $Ca(OH)_2$ and NaOH or KOH.

Whereas the columns with NaF can quantitatively sorb all volatile fluorides of FPs and all volatile actinides (UF_6, NpF_6, PuF_6) at temperatures close to 100°C, MgF_2 can be used as a selective sorbent for some volatile FP fluorides (e.g. MoF_6, IF_5, TeF_6) in those cases when the sorption of UF_6 is not desirable.

The sorption of volatile fluorides on NaF pellets is usually done at 100°C and the eventual desorption of these fluorides from the complex is possible in the fluorine flow at about 400°C. These processes were verified on the laboratory and semi-pilot level during the research and development studies devoted to the development of reprocessing technology by the fluoride volatility method

In addition to the generation of VFPs, the process also generates gases, which leave the system in the off-gas stream. Surplus fluorine gas, nitrogen used as auxiliary gas and oxygen generated during the fluorination reaction go to the off-gas system. Here the fluorine gas can be captured at the sorption columns filled by alumina (Al_2O_3) and alkaline absorber [$Ca(OH)_2$ and NaOH or KOH]; the remaining gases leave the system to the hot cell off-gas ventilation.

The **fused salt volatilisation** was developed by the ORNL within the Molten Salt Reactor Program to remove uranium from carrier molten fluoride salt (LiF-BeF_2 eutectics, often called FLIBE salt). The method is based on the introduction of fluorine gas into fluoride molten salt and on the removal and separation of emerging volatile fluorides. In the molten salt reactor technology, this method was proposed for the extraction of uranium from the carrier molten salt as uranium is converted from the soluble form (UF_4) into volatile UF_6 [24-26].

The FPs present in the molten salt reactor carrier salt are converted during the fused salt volatilisation into volatile and non-volatile fluorides as in the fluoride volatility method, according to the distribution listed in Table 2.1. If the molten salt reactor operates with the Th-232 – U-233 fuel cycle, plutonium will be present only in minor amounts and americium and curium will, therefore, also be in small quantities. Instead, there will be thorium in the stable non-volatile form of ThF_4 and protactinium primarily in the non-volatile form of PaF_4. A small quantity of the volatile but unstable PaF_5 is present, but readily decomposes back to PaF_4.

Concerning the formation of VFPs in the molten salt reactor system, those can be divided into two categories. The first consists of fission products that tend to leave the carrier salt spontaneously as they are either almost insoluble in the fluoride salt (Kr, Xe), or they do not form stable fluorides in the carrier salt under the molten salt reactor operating conditions (Nb, Mo, Ru, Sb, Te). These elements, usually named noble metals, tend to leave the salt during a gas extraction step, which was designed in the Molten Salt Reactor Experiment (MSRE) to extract xenon and krypton from the fuel salt [27]. The second category consists of FPs which are present in fluoride salt as stable soluble compounds and which form volatile fluorides only by the fused salt volatilisation process. This group consists of elements which leave the salt together with uranium (in the form of UF_6). Here, the typical FPs are I, Rh, Tc and also any remaining species from Group I in Table 2.1. As the fused salt volatilisation is a strong oxidative process, the volatile fluorides of actinides (UF_6, NpF_6 and PuF_6) and of fission products can also be accompanied by some volatile fluorinated components of the structural material. The structural material tends to be nickel alloys, typically containing chromium and molybdenum. However, during the fluorination process, both elements can be extracted from the surface of the alloy in the form of volatile fluorides (CrF_4, CrF_5, MoF_6), which are then mixed with the original VFP fluorides.

2.3.2. Chloride pyrochemical processes

A typical process flow sheet for chloride-based pyroprocessing of U-Pu-Zr or U-Zr metallic and oxide fuels is shown in Figure 2.3. Broadly, after a head-end pre-treatment step (see Section 2.1), it contains steps relating to pre-conditioning of the oxide fuel (Step I), primary separations of the FPs from the actinides (Step II), actinide processing (Steps III, IV and VIII), actinide recovery from waste (Steps IV and V) and waste treatment (Steps V, VI, VII and VIII).

To process light water reactor spent fuels, they are transformed to metals by electrochemical reduction (Step I) in molten LiCl electrolyte at 650°C [28]. Spent metallic fuel dismantled from a fast reactor is disassembled and irradiated fuel pins are mechanically chopped into small pieces. In contrast to oxide fuel, the chopped metal fuel pins are sent

directly to the molten salt electrorefining step (Step II), where the actinides are decontaminated from the FPs and recovered in LiCl-KCl eutectic melt at 500°C [29-31]. The electrolytic reduction (Step I) product is also fed to the electrorefining step (Step II). In the electrorefining step, two kinds of cathodes are used to obtain different streams of products. One is a solid cathode made of iron, where uranium is selectively collected due to its higher standard electrode potential compared with other actinide elements [32-35]. The other cathode is a liquid cadmium cathode, where transuranics are collected together with uranium, taking advantage of low activity coefficients and subsequent chemical stabilisation of transuranics in liquid cadmium [36].

The cathode products taken out from the electrorefining apparatus are accompanied by the solvents (chlorides and cadmium metal). In the high-temperature distillation step, called cathode processing (Step III), those solvents are distilled off, and the cathode products are consolidated into dense metal ingots at the same time [37, 38]. The products of the cathode-processing step are adequately blended with other products and supplementary zirconium to make the fuel composition, then sent to the injection casting step to fabricate the recycled fuel slug [39].

The anode residue of the electrorefining is sent to the anode processing step (Step IV) [40], where remaining actinides are removed to LiCl-KCl melt by oxidation with $CdCl_2$. After that, the anode residue consisting of noble metal FPs, zirconium and stainless steel cladding is consolidated into a stable metal waste.

Alkali, alkaline earth and rare earth FPs in the spent fuels accumulate in the electrorefiner in the form of their chlorides. These FPs are separated from co-existing actinides by the counter current reductive-extraction step (Step V) in molten salt/liquid cadmium system [41]. The actinide elements recovered in the cadmium phase are recycled to the electrorefiner. The FPs remaining in the actinide-free salt after the reductive extraction are absorbed in zeolite filled in columns in series (Step VI) [42]. The zeolite loaded with FPs is then mixed with glass material and pressed at high temperature to fabricate a stable ceramic waste called glass-bonded sodalite, which is a natural analogue of the chlorine-containing mineral (Step VII) [43].

Figure 2.3. Generic process flow sheet of the chloride pyro-reprocessing for metallic and oxide fuels

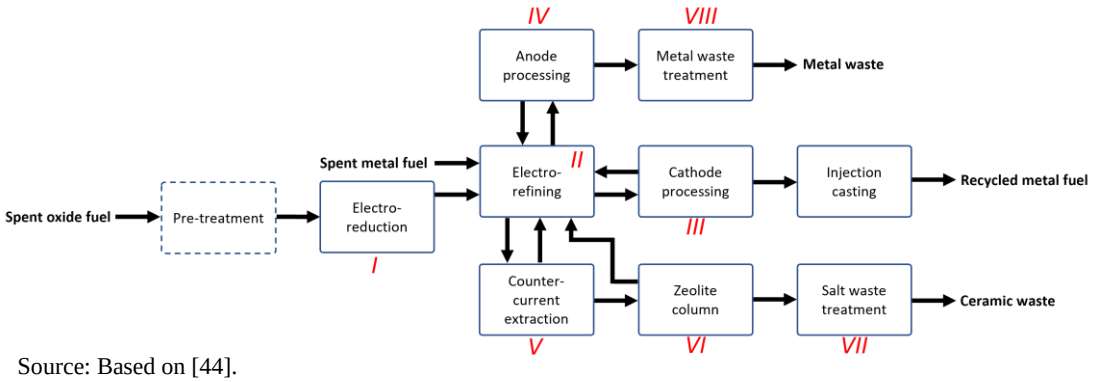

Source: Based on [44].

There is an option to add a pre-treatment involving voloxidation and a compaction/sintering step before the electroreduction to separate the spent oxide fuel from the cladding material and to obtain pellet material suitable for handling in the subsequent steps, i.e. the electroreduction and electrorefining. During the pre-treatment and compaction/sintering steps, FPs such as noble gases, halogens, alkalis and some of the noble metals are volatilised from the fuel, as described in Section 2.1 [45-47].

The Korea Atomic Energy Research Institute (KAERI) developed a high-temperature pre-treatment step which results in volatiles (Kr-85, Xe, C-14 and H-3, etc.) and semi-volatiles (Tc-99, I-129, Cs-134, Cs-137, etc.) being released. Their abatement will be discussed in Chapter 3. Using high-temperature pre-treatment to fabricate feed materials that are supplied to the oxide reduction process has several advantages, over direct addition to the pyrochemical steps:

- a greater fraction of the fuel can be separated from the cladding;
- the particle size of spent fuel material can be controlled in a better manner to improve the efficiencies of subsequent processes;
- volatile and semi-volatile fission products including Cs, Tc, Ru and I can be removed from the fuel material prior to subsequent operations, which will benefit the overall process by reducing the adverse effects of volatile and semi-volatile FPs.

Therefore, if considering high-temperature treatment as a head-end option, an off-gas treatment system is essential for the selective trapping of VFPs such as I, Tc and Cs.

When the spent oxide fuel after high-temperature pre-treatment is fed to the electroreduction (Step I in Figure 2.3), volatilisation of FPs is hardly expected, since the electroreduction is performed at a much lower temperature than the pre-treatment step. In the case where the spent oxide fuels are sent to the electroreduction step, it is possible that caesium and iodine volatilise to some degree considering that a small portion of the solvent LiCl vaporises at 650°C. At present, there are no reports indicating volatilisation of those fission product elements. Detailed investigation is expected in the future. Volatile higher oxides such as RuO_4 or Tc_2O_7 (typically observed at elevated temperatures during aqueous reprocessing) are not generated, since the spent oxide fuel is loaded at the cathode and kept in a reducing atmosphere during the electroreduction step.

A large part of the pyroprocessing for spent metal fuel (Steps II, IV, V and VI in Figure 2.3) are carried out at around 500°C under reducing atmosphere. Under these conditions, vapour pressure of most FPs (elemental or in the form of halides) is negligibly low. The vapour pressure of CsCl and CsI are higher than those of other fission product chlorides, but still in the order of 1 Pa at this temperature, which is comparable to that of solvent chlorides (LiCl and KCl). Visible vapourisation of CsCl or CsI has not been observed in the previous studies performed at around 500°C. Studies on the salt waste treatment (Step VII), where the FPs absorbed zeolite is heated to around 800°C to generate glass-bonded sodalite waste form, are carried out with careful attention to the relation between the process temperature and vapourisation of solvent chlorides adherent to the zeolite (see Section 2.4.4).

$ZrCl_4$ is known as one of the chlorides of higher volatility. During normal pyroprocessing operations, vapourisation of $ZrCl_4$ can be ignored, since it is thermodynamically stabilised by the complex ion ($ZrCl_6^{2-}$) formation in LiCl-KCl [47] and instantly reduced to metal in the presence of the actinide metals.

Cadmium has an exceptionally high vapour pressure (in the order of kPa) among the FPs existing as metals in pyroprocessing. The cadmium aerosol formed at higher temperature steps is condensed and accumulated at lower temperature steps of the process equipment. Besides the control of this VFP, the engineering design for confining cadmium vapour within each process equipment is one of the important technical issues to be solved, since a much larger amount of non-radioactive cadmium is introduced and used as the essential solvent in the pyroprocessing.

Some of the other steps (III and VIII) are performed in closed equipment at higher temperature (1 200-1 600°C) under reduced pressure to distil off the chlorides and cadmium accompanying the recovered actinides or the metal waste. All the FPs in the form of their halides are vaporised together with the solvents (LiCl, KCl, $CdCl_2$) and actinide chlorides. It has been demonstrated in the conditioning operation of the irradiated metal fuels [48] that the vaporised materials containing FP elements are condensed and collected at the lower temperature region of the equipment as designed. The condensed materials are returned back to the electrorefining step (Step II) without additional treatment.

2.4. Generation of off-gas from waste treatment processes

The previous sections detailed off-gas generation and treatment from reprocessing of UNF. However, in the case of reprocessing via dissolution in nitric acid, an aqueous HLW stream containing the majority of the FPs is produced and must be managed. The preferred method of HLW treatment is through immobilisation in glass at temperatures around 1 000°C, i.e. vitrification. The conditions found in the vitrification process are conducive to the release of volatile and semi-volatile species (see Chapter 1 for the definition of volatile and semi-volatile). The release of FPs during the high-temperature vitrification process depends on their chemical speciation. The composition of relevant compounds of volatile elements and their behaviour under elevated temperatures are listed in Table 2.2.

Table 2.2. Composition and relevant properties of volatile elements for the design of off-gas treatment systems

Element	Compound	Characterisation, sublimation and vapour pressure
Molybdenum	$Mo(VI)O_3$	T_m: 795°C, T_b: 1 155°C
Selenium	SeO_2	T_m: 340°C Volatilising ratio: 0.01% @ 300°C 1% at800°C [49] 16 hPa (70°C) Safety data sheet
Technetium	Tc_2O_7	T_m: 119.5°C [49], T_b: 310.8°C [50] Log p= $-7205/T+15.404$
	$CsTcO_4$ and other TcO_4^- compounds	T_m: 595°C [50, 51]
Caesium	Cs_2O	T_m: 490°C [52] 20°C: 0.35 mbar, 30°C: 0.72 mbar, 50°C: 2.8 mbar
		Cs volatilises also in the form of pertechnetate or molybdate
Ruthenium	Ru(NO)	Ru-compounds in nitric acid $RuNO(NO_3)x(OH)_{3-x}(H_2O)_2 \cdot yH_2O$ Autoxidation leads to RuO_4 (thermodynamically unstable) [53] Volatilising ratio: 10% at 300°C, decreasing at higher temperatures, 1% at 800°C [50] Ru loss to the off-gas: 20% [54]
	RuO_4	Gas phase compound
	RuO_2	Sublimation at 1 200°C
Iodine		Mainly released during fuel dissolution in nitric acid
Fluorine/chlorine	F, Cl	Unknown

Notes: T_m: melting point; T_b: boiling point; mbar: millibar.

A recent publication reviewed volatile species of technetium and rhenium during waste vitrification [55]. Besides the volatile/semi-volatile elements, the off-gas contains water vapour, nitrogen oxide (NO_x) and particles consisting of abraded glass from the beads and dried HLW. For this reason, other elements such as strontium can be found in the off-gas pipes/components.

The behaviour of these volatile elements in high-temperature vitrification processes used for nuclear waste treatment is discussed through three industrial examples: 1) the liquid-fed ceramic melter technology developed at Karlsruhe Institute of Technology in Germany; 2) the vitrification process using a hot or cold crucible developed at the CEA (France); and 3) the hot crucible vitrification process used at Sellafield (United Kingdom).

2.4.1. Behaviour of volatile elements in the German vitrification process

Description of the German vitrification process

Karlsruhe Institute of Technology developed a vitrification technology for high-level liquid wastes (HLLW) based on a liquid-fed ceramic melter technology with direct heating of the glass melt [56, 57]. Electrodes contacting the glass melt heat it up to temperatures between 1 100°C and 1 200°C. The process starts from melting prefabricated glass beads. After starting operation with water feeding, nitric HLLW solution is poured directly onto the glass melt. Under these conditions, the water and HNO_3 of the HLLW solution evaporates into the off-gas. Increasing the temperature transforms the FP nitrates into oxides at *ca.* 700°C. Finally, the FP and actinide oxides as well as process chemicals and the glass form a homogeneous phase, which is discharged batch-wise into steel canisters. Active application of this technology occurred first at the PAMELA plant at the EUROCHIMIC facility at Mol, Belgium [58], followed by the German Verglasungseinrichtung Karlsruhe (VEK) project, which was established to vitrify HLLW produced during the operation of the Karlsruhe Reprocessing Plant (WAK).

Due to the evaporation and the oxidation of the nitrates, the temperature at the surface of the melt drops during the feeding of the HLLW and forms a “cold cap”. This cold cap covers parts of the surface of the glass melt. The extent of the cold cap was optimised to retain VFPs in the melt and to minimise the discharge into the off-gas.

The behaviour of volatile elements and particulate contaminants in the off-gas of a directly fed ceramic melter was studied in many inactive test runs as well as in the two hot vitrification processes for HLLW in PAMELA and in the VEK.

Volatile distribution in the off-gas treatment system

The removal sequence for off-gas treatment was as follows: particulates, water vapour, nitrogen oxides, gaseous ruthenium and again particulates. The off-gas system consisted of the following components:

- Wet treatment components:
  - dust scrubber;
  - condenser;
  - jet scrubber;
  - NO_x absorber column.
- Dry components:
  - glass fibre filter as high efficiency mist eliminator;

- HEPA filter;
- iodine filter;
- cooler.

Finally, the off-gas was released via a stack.

Details of the off-gas system of the PAMELA plant are published in [60, 61]. The report concludes that "nearly 99.9% of the initial radioactivity could be fixed in the waste glass product. This high melter decontamination efficiency is obviously due to the good retention of volatile compounds like Cs by the cold cap conditions at the glass pool surface". A series of aerosol measurements showed the efficiencies of the off-gas treatment components, presented in Table 2.3.

Table 2.3. Decontamination factors obtained for the first operating low-enriched waste concentrate campaign at PAMELA

System	DF(α-activity)	DF(β-activity)	DF(Cs-137)
Melter	576	63.9	26.5
Wet off-gas treatment (dust scrubber, condenser, jet scrubber)	78.5	63.7	61.3
Wet off-gas treatment II (NO_x absorber)		25	
Glass fibre filter (high efficiency mist eliminator)		2 000	
HEPA filters (2)		$> 5.8\times10^{5}$	
Total DF from single DFs		$> 5.8\times10^{13}$	
Total DF feed to stack (direct measurement of filters before the stack)	1.6×10^{13}	6.0×10^{14}	6.0×10^{14}

Note: DF: decontamination factor.

The VEK vitrification process

The German VEK project has been established to vitrify approximately 55 m³ of HLLW with a total radioactivity inventory of 7.7×10^{17} Bq. In the WAK, UNF was reprocessed originating from pilot reactors as well as from commercial power plants. The average burnup of the mainly UO_2 UNF was below 36 GWd/MTIHM and the cooling time before reprocessing was relatively short [62].

Table 2.4 shows some of the main features of the VEK melter.

Table 2.4. Main features of the VEK melter

Parameter	Data
Design data	
Throughput capacity	9 L/h
Glass production rate	4.5 kg/h
Geometrical data	
Outside dimensions	∅ 1.5 m, height 1.7 m
Weight	8 metric tonnes
Volume of the melt	*ca.* 150 L
Glass pool surface	0.44 m^2
Heating system	
Glass pool heating	1 pair of air-cooled Inconel 690® electrodes
Installed electrical power	80 kVA (power electrodes)
Glass pouring system	Bottom drain

Notes: L/h: litres per hour; kg/h: kilogrammes per hour.
Source: Based on [63].

The waste load of the glass product was 16 wt.% ± 1.5 wt.% [64]. The off-gas system consisted of the proven components, such as dust scrubber and condenser located in the vitrification cell and jet scrubber, NO_x absorbers, glass and HEPA filters as well as an iodine filter. After passing the different filtration steps, the off-gas was cooled and exhausted. To minimise loss of volatile species to the off-gas, a high degree of cold cap coverage (80-90%) was required. This corresponded to a plenum temperature of 500-650°C. The pool coverage was adjusted by control of the feeding rate [63]. Details of the off-gas system is described by Roth et al. [67] and shown in Figure 2.4. The target concentrations of volatile nuclides were estimated as shown in Table 2.5.

Table 2.5. Target concentrations of volatile compounds to be vitrified in the VEK

Oxide	Target concentration of the HLW glass (wt.%)
$Mo(VI)O_3$	0.93
SeO_2	0.02
Tc_2O_7	0.24
Cs_2O	0.53
RuO_2	0.71
Iodine	Not detected
F, Cl	<< 0.01 wt.%

Source: Based on [58].

In the course of the HLLW processing, the melter emissions increasingly caused material deposits along the wall of the melter off-gas pipe, as shown in Figure 2.4. The properties of these deposits proved to be of a hard nature. As a result, the periodical cleaning with pressurised air blasters was not effective enough to prevent long-term plugging of the off-gas pipe. The somewhat sintered material reflected a relatively high off-gas temperature due to non-optimised cold cap conditions in the melter.

Figure 2.4. Schematic design of the off-gas pipes from the melter to the first wet off-gas treatment component

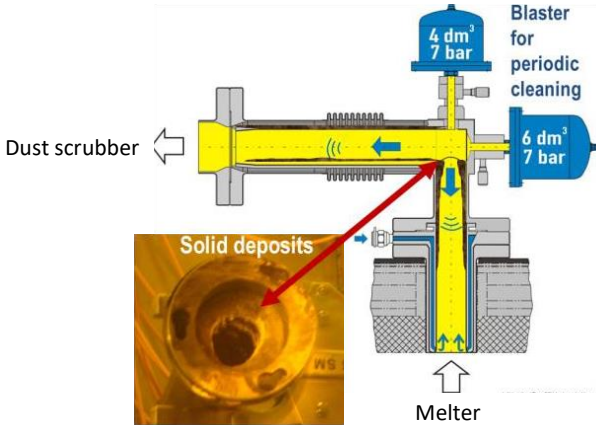

Source: [67].

Higher than anticipated temperature conditions in the VEK melter plenum entailed an increased volatility of elements like caesium and technetium. From balance calculations, the Cs retention of the melter did not reach the values known from the operation of the PAMELA plant and of inactive operation of the prototype test facility. However, the

emitted caesium was effectively retained in the off-gas treatment system, as there was no indication of increased radioactivity at the monitoring point at the stack [69].

2.4.2. Behaviour of volatile elements in the French vitrification process

The French vitrification processes used are a batch process, in a joule heated metal melter (JHMM), and a continuous process with two-step calcination and vitrification in a JHMM or in a cold crucible induction melter (CCIM). During the development of the French vitrification processes, the volatility of active isotopes has always been considered. The objective is to ensure that as much activity as possible from the waste is trapped in the confinement material, in particular thanks to recycling effluent from the dust scrubber.

The decontamination factors of French vitrification pilots and industrial lines at the Atelier de Vitrification de Marcoule (AVM) and the Atelier de Vitrification de La Hague (AVH) plants are reported in the following sections.

Pilots and vitrification processes

Initially, a batch vitrification technology was developed, known as PIVER, capable of the direct vitrification of 200 litres of fission product solution with 100 kg of glass, reaching a 25% loading factor. A joule inductor metallic melter directly connected to a condenser was used. The waste liquid was fed in with a vitrification slurry additive. This blend was successively dried, calcined and vitrified. Aerosols from the vitrification melter were trapped in an off-gas treatment, with more than 99% of them stopped in the first device, the condenser.

Based on the same principle, VULCAIN was a facility used to prepare about 2 kg of glass to study its long-term behaviour. These two facilities supplied the first volatility results, which strongly influenced the current off-gas treatment design.

With lessons learnt from the PIVER vitrification experience, the basic principles led to the choices and design of the French two-step industrial vitrification. Thus, in today's two-step process (Figure 2.5), a nitric acid solution containing the concentrated FP solution is sent to a rotary calciner which carries out evaporation, drying and calcination functions. A calcination additive is also added to the feed to reduce some of the nitrates and to limit ruthenium volatility. At the calciner outlet, the calcine falls directly into the melter along with the glass frit, which is fed in separately. The melter is fed continuously, and is batch poured. The glass is heated to 1 100°C in the JHMM and to 1 200°C for the CCIM.

Off-gas treatment equipment comprises a hot wet dust scrubber with tilted baffles, a water vapour condenser, an NO_x absorption column and a washing column. The most active gas washing solutions are recycled from the dust scrubber to the calciner.

Two melter technologies are implemented at the La Hague facility:

- The JHMM: like PIVER, a metal melter is heated by Joule effect using electric inductors. The heating system is outside the melting pot and the metal melter directly heats the glass by conduction and radiation.
- The CCIM: glass in the crucible is heated directly by eddy currents generated by the inductor surrounding the shell. The currents dissipate power by the Joule effect, which heats the calcine and glass frit to form the glass melt. The cooling of the vessel produces a solidified glass layer (the cold crucible) which acts as a protection for the melter inner wall against corrosion and high-temperature damage.

Figure 2.5. Full-scale vitrification pilot with CCIM or JHMM

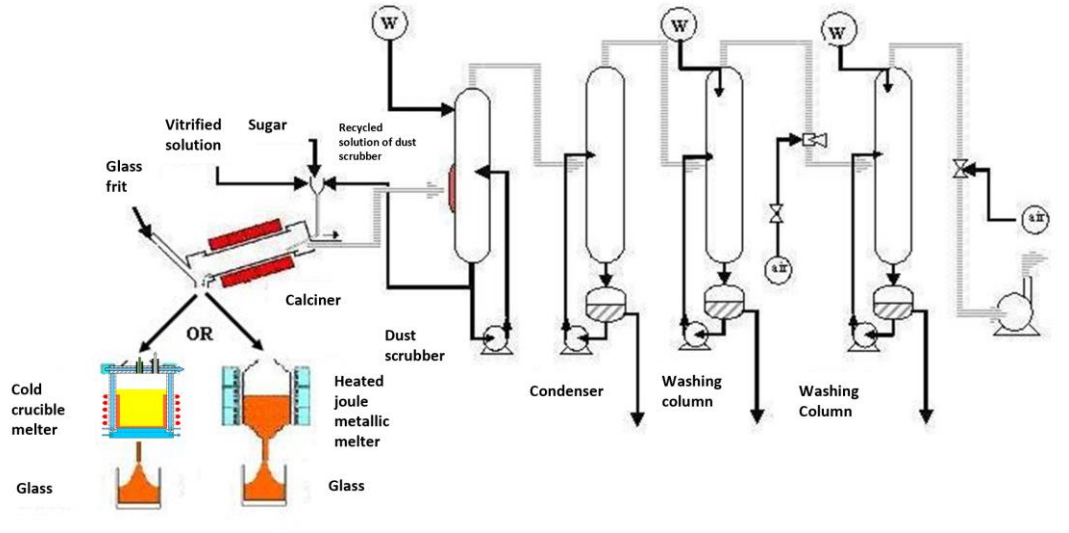

Source: [69].

Volatility results from various facilities are provided below:

- AVM: starting active operation in June 1978, AVM was the world's first vitrification facility to operate in line with a reprocessing plant. This facility was designed to have a nominal glass throughput capacity of 15 kg/h with an evaporative capacity of about 40 L/h.
- ATLAS: vitrification active pilot to study volatility with an evaporative capacity of 20 L/h.
- La Hague vitrification lines: based on the industrial experience gained in the Marcoule Vitrification Facility, the process was implemented on a larger scale in order to operate in line with the La Hague reprocessing plants. Both vitrification facilities are equipped with three vitrification lines having a nominal glass production capacity of 25 kg/h each and an evaporative capacity of 90 L/h (initially 60 L/h). In 2010, a cold crucible melter replaced the JHMM in one of the six vitrification lines at La Hague.
- PEV: an inactive vitrification pilot which was a full-scale replica of a La Hague vitrification line.

Behaviour of volatile elements

Volatility results are expressed as decontamination factors (DFs). For the batch process, only the DF at the melter outlet is given. For the two-step process, a DF can be found at the calciner outlet (DFcv) and another at the scrubber outlet (DF). The latter represents the element amount which is not in the glass and is, therefore, comparable to the batch process DF.

Four radionuclides were measured: Ru-106, Cs-137, Ce-144 and Sr-90. Table 2.6 presents the DFs.

Table 2.6. Batch process decontamination factors

Facility	Ru-106	Cs-137	Ce-144	Sr-90
VULCAIN	2-4	200-500	200-600	150
PIVER	10	1 000	2 000	700

Despite ruthenium volatility, the DFs are high. It is known that the majority of ruthenium volatilises between the end of drying and the beginning of calcination. Therefore, the melter heating has a high impact on this volatility. Moreover, the PIVER volatility was lower than that of VULCAIN. This is probably related to the smaller ratio of glass bath surface to glass mass in PIVER.

At the two-stage facilities, AVM and ATLAS, it was found that the volatilities for the four previously mentioned radionuclides were greater than in the batch process. Table 2.7 presents the volatility results of the AVM facility obtained over the first two campaigns.

Table 2.7. Decontamination factors of the AVM facility

	Ru-106	Cs-137	Ce-144	Sr-90
Calciner outlet (DFcv)	2.5-5	9-16	17-26	19-33
Scrubber outlet (DF)	6-14	75	55	500-1 000

For Cs and Ce, retention in the glass is between one and two orders of magnitude lower than PIVER. This difference is explained by continuous glass production. As calcine and glass frit were fed in at the hot glass melting surface, species volatility increased.

Like VULCAIN and PIVER, ruthenium volatility mainly came from calcination; hence, a study to reduce this volatility was conducted on ATLAS. Two solutions were found: the prior denitration of the liquid waste with formic acid or a sugar additive mixing with the liquid waste just before calcination. The sugar addition during calcination was retained for the La Hague facilities because its implementation in an industrial process is much easier.

At the ATLAS facility, ruthenium decontamination factors with sugar were equal to 20 in the calciner outlet (DFcv) and 100 in the scrubber outlet (DF). The impact is about one order of magnitude.

La Hague facilities and PEV

Virtually all the volatility results for the two-step process were obtained on the full-scale PEV pilot. This system provides statistical volatility data, obtained from an HLLW surrogate. This allowed comparing the two melter technologies, the JHMM and the CCIM. There are two major differences impacting volatility and unfavourable to the CCIM. The overall air bubbling rate and the melting temperature are higher in the CCIM: about three times more bubbling flow and 100°C more in the melting glass.

Figure 2.6 shows the decontamination factors for different elements from the frit or UOX solution. This factor characterises the release of these elements beyond the dust scrubber.

Figure 2.6. Comparison of decontamination factors for selected elements between the JHMM and the CCIM

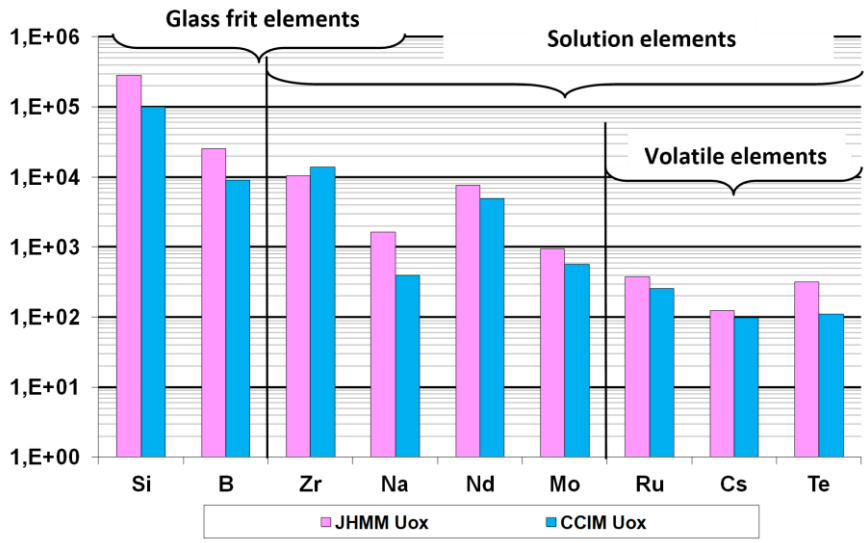

Notes: JHMM: Joule heated metal melter; CCIM: cold crucible induction melter.
Source: [69].

Despite differences between the JHHM and the CCIM, the DFs are in the same order of magnitude. This observation is valid for all the elements except sodium, which is more affected by the higher process temperature. However, its management is less problematic because this element is not a fission product.

In conclusion, the minimisation of volatility has always been an objective during vitrification process development. Two improvements have made its management possible: 1) the recycling of the scrubber solution; and 2) the sugar addition before the calcination.

In addition, although it enables glasses to be produced at higher temperatures, the cold crucible leads to only minor decreases to DFs.

2.4.3. Behaviour of volatile elements in the UK vitrification process

Vitrification in the United Kingdom

The early efforts in vitrification development in the United Kingdom focused on a single-stage batch process using induction heating [71]. Comparison with the French AVM concluded that the two-stage process had a higher throughput and could be more rapidly deployed. The decision was, therefore, taken to implement the French system, which by this time was the second-generation AVH.

Initially, two lines were constructed at the Waste Vitrification Plant (WVP) at Sellafield, and began operation in 1990, followed by a third line in 2002 to increase throughput. However, despite this increased capacity, there was a regulatory requirement to further reduce highly active liquor stored at Sellafield, so improvements in glass production rate and waste incorporation were necessary. To this end, a non-active vitrification test rig was built and began operation in 2004 [72].

Volatile elements in the UK vitrification process

As discussed in Section 2.4.2, sugar is used to control Ru volatility during the calcination process. Work was carried out on the vitrification test rig to optimise sugar additions as excessive sugar results in dusty calcine and, therefore, an increased burden on the dust scrubber. The correlation between sugar feed rate (as a function of grammes of sugar per kilogramme of total metal oxide within the highly active liquor) and ruthenium lost to the dust scrubber is shown in Figure 2.7 [72]. This allows the calciner conditions to be controlled to ensure as much ruthenium is immobilised in the glass as possible.

Figure 2.7. Variation of ruthenium concentration in the dust scrubber (g/L) as sugar concentration in the feed is varied (g[sugar]/kg[waste oxide])

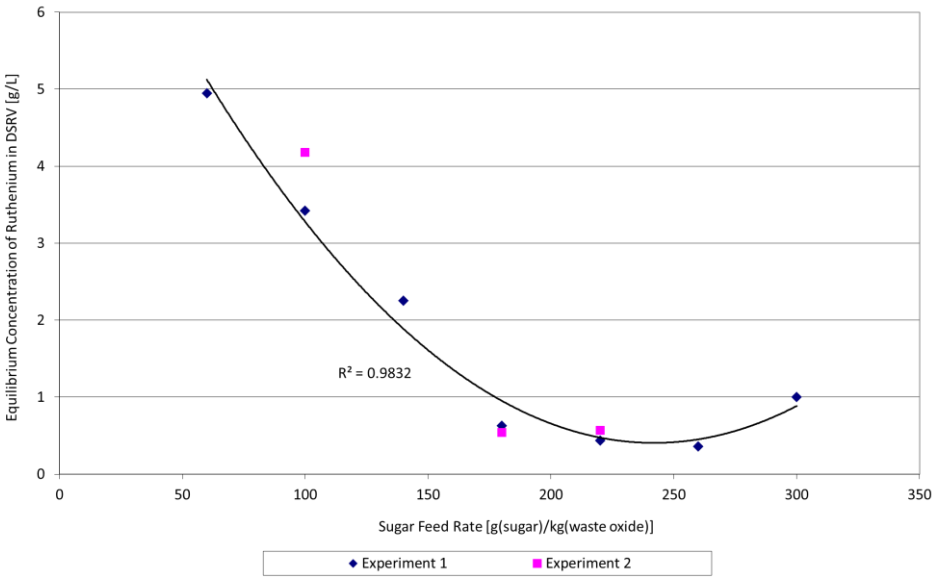

Notes: DSRV: Dust scrubber recycle vessel.
Source: Based on [72].

Molybdenum is an FP which gives little to no volatility concern for the majority of the fuel cycle but requires control measures in the vitrification process. It has a low solubility in standard borosilicate (known as MW) glass, and the oxide combines with alkali, alkali earth, chrome and rare earth elements to form partially crystalline, semi-volatile phases, termed "yellow phase" (see Figure 2.8) [73].

Figure 2.8. Typical "yellow phase" composition

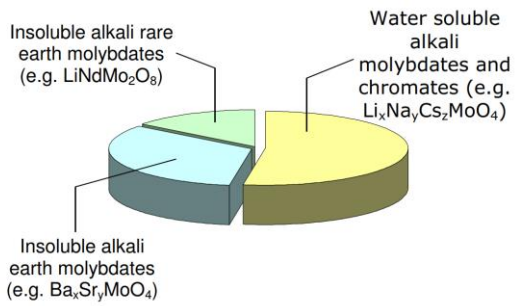

Source: [73].

The semi-volatile yellow phase has a low density, causing it to rise to the surface of the glass melt; it is corrosive to the Nicrofer melting vessel, and some of the alkali molybdates are water soluble. For these reasons, generation must be avoided. Traditionally this was managed by reducing waste loading in the glass to maintain Mo concentration in the glass-soluble region. To increase the glass-soluble Mo concentration, a new base glass has been developed. This was predominately created to aid clean out of HLLW storage tanks at Sellafield. The new base glass formulae include oxides of calcium, zinc and aluminium. The new base glass (known as Ca/Zn) preferentially forms glass-soluble calcium molybdate, over the glass insoluble but water soluble (and volatile) alkali molybdates.

Volatile technetium, in the form of caesium pertechnetate ($CsTcO_4$), presents major operational difficulties at WVP. The $CsTcO_4$ is volatilised under the high temperatures experienced in the melter. This volatile gas will travel along the off-gas system until it reaches a cooler section of pipework where it is condensed and crystallised. This usually occurs between the dust scrubber and the condenser [74]. The crystallised $CsTcO_4$ will then form a blockage requiring a plant outage to enable unblocking operations to be carried out.

2.4.4. Behaviour of volatile elements during the waste treatment of salt waste from the chloride-based pyrochemical process

Section 2.3.2 discussed the steps taken to separate the actinides, metal wastes and FPs in the chloride pyrochemical process. This section examines in greater detail the treatment carried out on the FP-bearing waste salt.

The electrorefining step (Section 2.3.2, Figure 2.3, Step II) produces a waste salt stream containing FPs (including, but not limited to, the volatile species Cs and I) and some residual actinides. The waste salt is treated further with an actinide removal stage followed by an FP removal stage allowing the salt to be recycled. The FP removal stage utilises zeolite columns as the FP absorbent, which can be combined with glass and converted into a ceramic. The total salt waste treatment process is schematically shown in Figure 2.9.

Argonne National Laboratory (ANL) and Idaho National Laboratory (INL) developed the monolithic ceramic waste form, glass-bonded sodalite using a pressureless consolidation method [76, 77]. In these studies, the chloride salt from the electrorefining step, which contains low concentration of FPs, was directly contacted with Zeolite-4A then blended with glass material.

Testing of the material was carried out [75] where the heating/pressing conditions were selected (Table 2.8) considering the conversion temperature of sodalite (770°C), the collapse temperature of sodalite (1 000°C) and the softening temperature of the borosilicate glass (820°C). Figure 2.10 illustrates the heating/pressing procedure of the fabrication tests. The reference condition in Table 2.8 was determined based on the experimental procedure reported by the ANL and the INL [76, 77].

Figure 2.9. Salt waste treatment process flow sheet, detailing Steps V, VI and VIII for the pyroprocessing of metallic/oxide fuels

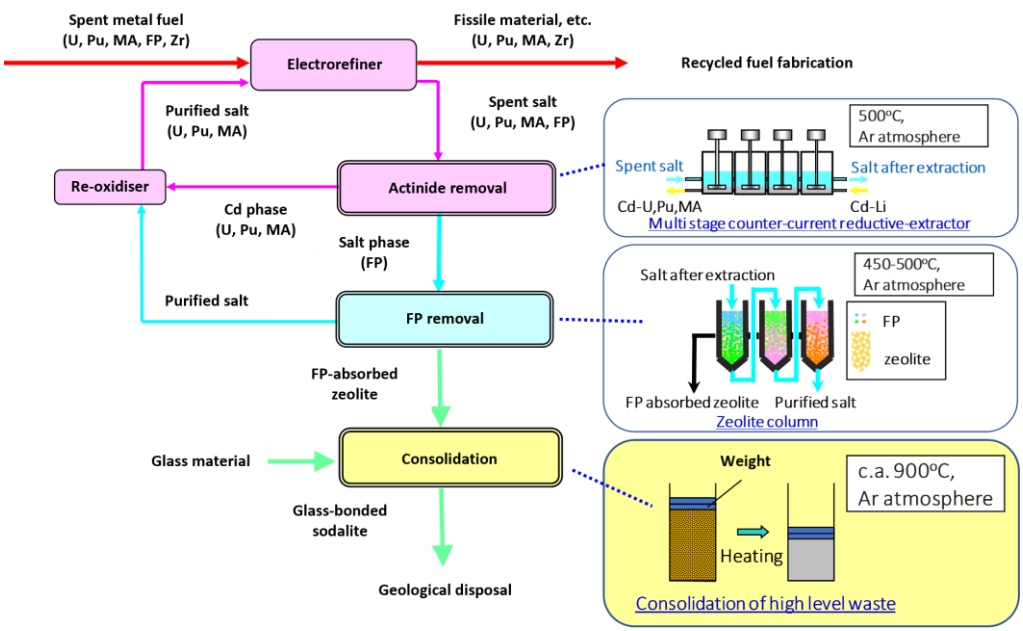

Note: FP: fission product.
Source: Based on [75].

Figure 2.10. Heating/pressing procedure of glass-bonded sodalite fabrication tests

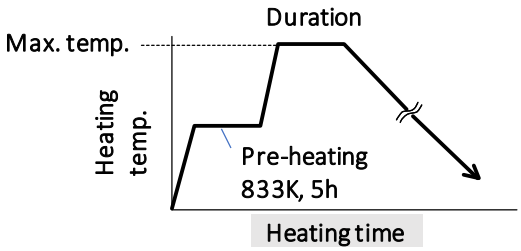

Source: Based on [75].

Table 2.8. Heating/pressing conditions surveyed in glass-bonded sodalite fabrication tests

Parameters	Test conditions	
	Reference condition	Parameter variation
1. Maximum temperature (max. temp.)	1 188 K	1 043, 1 093, 1 273 K
2. Duration of heating at max. temp.	5 h	10, 20 h
3. Glass ratio of initial material	25 wt.% (salt + zeolite : glass = 3 : 1)	13, 33 wt.%
4. Weight load	6.9×10^3 Pa	0.2, 3.6, 21×10^3 Pa

Note: K: kelvin; h: hour; wt.%: weight per cent; Pa: pascal.
Source: Based on [75].

The distribution of each element after the fabrication test under reference conditions determined by the chemical analysis is shown in Table 2.9 compared with the composition in the initial material.

Table 2.9. Distribution of elements after glass-bonded sodalite fabrication test carried out under reference condition

Element	Content in initial material (mg of element per 1 g of initial material)	Mass balance after fabrication (detected ratio in weight vs. amount of each element in initial material			
		In product		Volatilised (%)	Measured total (%)
		Stabilised (%)	Free salt (%)		
Li	9.3	99.7	0.2	0.1	101
K	24.4	99.6	0.1	0.3	92
Na	130	99.6	0.3	0.1	90
Cs	3.4	99.6	0.4	0.0	94
Sr	0.9	99.7	0.2	0.0	91
Nd	1.7	99.9	0.1	0.0	100
I	0.1	97.2	1.2	1.4	116
Cl	50	98.8	0.6	0.6	103

Source: Based on [75].

The volatilised ratios of Cs, Sr and Nd were very low. On the other hand, the vaporised ratio of iodine was higher than that of chlorine according to the difference in melting point of the corresponding halides (1 324°C for KI and 1 407°C for KCl) [78]. Most of the vaporised salt adhered to the top cover of the heating vessel and contained Na, K and Cl as the main components. The total amount of the free salt (water-soluble constituent in the fabricated waste form sample) was 0.74 mg per gramme of the product, and it included Na and Cl as the main components. It is noted that the water-soluble portion of Cs and I was slightly higher than the other elements.

Figure 2.11 shows the effect of the maximum temperature on the mass ratios of the volatilised salt, the free salt in the product and the apparent density of the product. Increasing the maximum temperature, the volatilised salt and the free salt content were increased remarkably beyond 820°C, suggesting decomposition of the sodalite structure. In the same way, effects of the heating/pressing conditions in Table 2.9 on the mass ratios of the volatilised salt, which should be closely related to the FP volatilisation, the free salt in the product and the apparent density of the product were evaluated [75]. The obtained results suggested that the maximum temperature should be kept at around 820°C for reduction of the volatilised salt ratio and that the pressure during fabrication should be as high as 2.1×10^4 Pa, whereas other parameters did not show any significant influence.

Figure 2.11. Effect of maximum temperature on ratio of volatilised/free salt and apparent density of fabricated glass-bonded sodalite

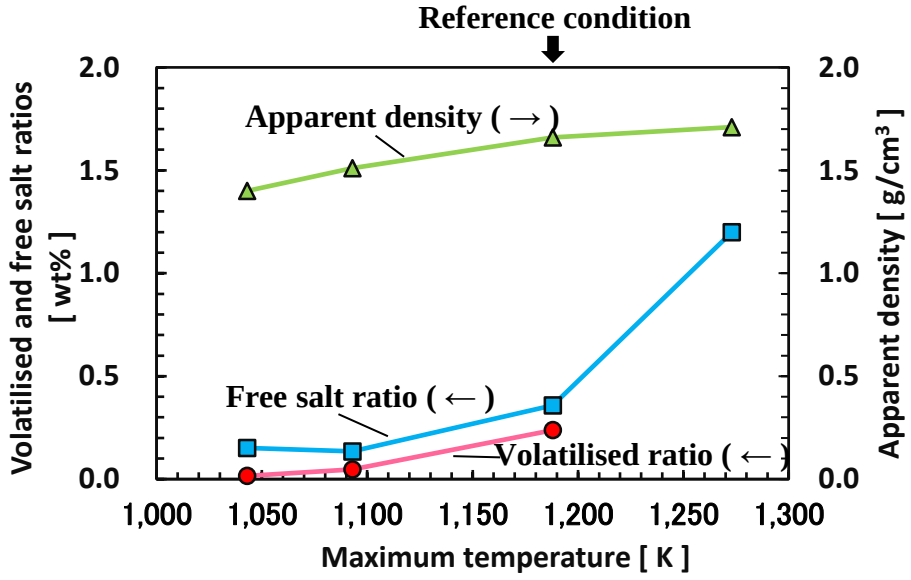

Source: Based on [75].

2.5. Summary

This chapter has considered the generation of volatile and semi-volatile species across a range of different processes that are either used already at the industrial scale or under development for future UNF reprocessing (and HLLW treatment). The head-end stage, including shearing and dissolution, is the major generator of VFP into the off-gas and would, if unabated, yield substantial aerial discharges. Specific measures for C-14 and I-129 abatement have been used in current commercial reprocessing facilities, but noble gases are currently discharged unabated. The majority of tritium remains in the process nitric acid and is ultimately discharged to sea with little abatement. High-temperature pre-treatment is a technique under investigation that offers an option for tritium management. Furthermore, it can volatilise a range of both volatile and semi-volatile species for abatement before the UNF is dissolved.

Pyrochemical processes in fluoride or chloride salts also release volatile and semi-volatile species that must be abated. In the molten salt reactor, on-line recycling and removal of volatile species is a specific requirement that bears similarities to the processes used in the fluoride volatility method and pyroprocessing. Lastly, this chapter has reviewed the VFP species generated during the HLLW treatment processes. In general, semi-volatiles become important to consider as the process temperatures involved mean that these compounds have appreciable vapour pressures. The vitrification processes used at an industrial scale have to consider Ru, $CsTcO_4$ and Mo.

3. Off-gas trapping

Off-gas treatment in a fuel reprocessing plant must address three main gaseous streams. The first is the off-gas from the head end, which includes the shear, the optional pre-treatment and the dissolver. This collectively is sometimes called the dissolver off-gas (DOG). The second is the vessel off-gas (VOG), which collects in-leakage to all of the process equipment and the instrument air used in bubbles, air sparge discharges, etc. This is sometimes split into sub-units, depending on facility design, but is generalised here. The third is the cell ventilation, which provides confinement to the process cell. Each of these has unique characteristics and processing challenges, although the elements or radionuclides to be captured may be found in one or more of these streams. For this reason, it is convenient to discuss capture technology for each of the targeted species in turn rather than by off-gas system.

3.1. Tritium

Tritium arises in used nuclear fuel primarily by tertiary fission of uranium, while a significant fraction is produced by neutron activation of lighter hydrogen isotopes. Historically, tritium is not captured or treated in used nuclear fuel processing facilities. Rather, it is released to the environment atmospherically or with wastewater discharges. However, the capture of tritium would likely be required in the United States to meet existing regulations [79], as well as potentially in next-generation reprocessing facilities internationally. Methods of confinement and/or recovery of tritium very much depend on the use of tritium pre-treatment, or its lack of use, before dissolution.

3.1.1. Tritium in aqueous spent nuclear fuel reprocessing

Without high-temperature pre-treatment (HTPT), the sheared fuel is fed directly to the hot nitric acid dissolution process. Tritium is retained in the aqueous dissolver solution as tritiated water and enters the dissolver off-gas stream as a small fraction of the water vapour rising from the solution. Most of the water vapour is returned to the process using a condenser, but nevertheless some water vapour escapes into the off-gas system. Tritium may be allowed to accumulate in the plant water systems until the concentration is such that the water vapour escaping the plant either balances the tritium entering with the used fuel or release limits are reached. To avoid exceeding release limits, the plant water may then be replaced and the contaminated water appropriately treated and disposed. Other techniques for tritium disposal, such as water feed and bleed, can be implemented, but all involve disposing of significant amounts of water that must be immobilised for decades if tritium abatement is required. Another option involves isotopic separation of the tritiated water from the bulk of the water, but inexpensive processes have yet to be developed [80].

3.1.2. Tritium management in dry systems

As discussed in Section 2.1, there are several tritium pre-treatment processes that can quantitatively remove the tritium from the used fuel. There are two processes for capturing the tritium: one is removal of HT in the gaseous state, the other is removal of HTO in the liquid or vapour state. The removal of HT employs hydrogen getters; these are normally non-oxidative processes. Getters typically consist of zirconium alloys and compounds. However, the selection of the appropriate getter depends greatly on the other constituents of the gas. The fact that most getters will not tolerate oxygen in the feed stream greatly limits the usefulness of getters for most effluent streams. The use of a heated catalytic

combiner ensures that all tritium released from the fuel is converted to water, which facilitates tritium confinement [81, 82]. Copper oxide is usually used as the catalyst [83, 84]. Experimental work has been undertaken in Japan on conversion of H_2 to H_2O using 99.9% purity CuO granule powder at various temperatures (Figure 3.1) [85].

Since the uranium oxides processed in the HTPT may act as a catalyst for oxidising tritium, there is some potential for eliminating a separate copper oxide catalyst.

Figure 3.1. H_2O converting ratio according to reaction temperatures and hydrogen concentrations

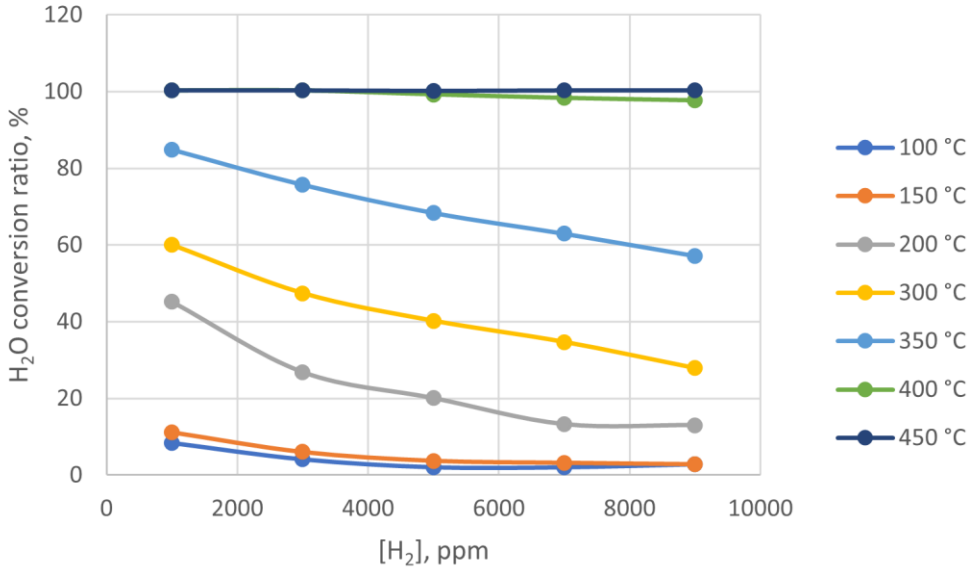

Source: Based on [85].

The off-gas from the standard pre-treatment process contains tritium in higher concentrations than the off-gas from the dissolver, but it also contains small quantities of iodine, carbon dioxide and the noble gases. Water may be removed from the off-gas stream by a variety of methods, such as condensation, absorption into hydrophilic liquids (e.g. anhydrous glycol) or adsorption on solids (e.g. molecular sieves). Decontamination factors may be improved with any of these processes by adding additional water vapour to the off-gas stream such that any fraction of water that passes the removal system contains a smaller fraction of tritium. This has the disadvantage of increasing the quantities of water requiring treatment, for example solidification in grout.

Tritium may be removed from the off-gas stream with desiccants or molecular sieves [86]. Anhydrous $CaSO_4$ has been reported as a possible desiccant. Molecular sieves exhibit high water capacities: 10-20% based on the dry weight of the sorbent. The 3Å molecular sieves are obtained by substituting potassium cations for the inherent sodium ions of the 4A structure, thus reducing the effective pore size to ~3 Å, with an excluding diameter >3 Å. This prevents larger molecules from being incorporated into the sieve, for example ethane.

The use of molecular sieves has many advantages, including efficient removal of water vapour from off-gas streams, removal to very low dew points at room temperature, ease of handling and the potential for regeneration. Type 3Å molecular sieves have been extensively tested for this application [87]. These tests have shown that the presence of iodine vapour does not have an adverse effect on the performance of the Type 3Å

molecular sieve for removing tritiated water, although iodine was co-captured on the molecular sieve. Simulated off-gas containing 0.0010 -0.0018 g I_2/g dry air and 0.006-0.008 g H_2O/g dry air was dried to a dew point between -40°C and -50°C. Iodine retention ranged from 0.2 mg/g to 0.4 mg/g of sieve pellets. Water loading was ~0.16 g/g of dry bed, which decreased to ~0.11 g/g of dry bed after 37 loading-regeneration cycles.

Heating of the iodine/water loaded Type 3Å molecular sieve showed that the iodine was preferentially released first, but it is anticipated that the desorbed species, i.e. iodine and water, will not be pure streams. This indicates either a need to separate the components during sieve regeneration or to verify that the disposal matrix is compatible with all components. Due to the long half-life of I-129, mixing implies that the waste form may require longer term isolation than if it contained the shorter half-life tritium alone. For this reason, where tritium beds are employed, they are preceded with AgZ or silver-functionalised silica aerogel beds to remove iodine to the extent possible.

Tritium capture with Type 3Å molecular sieves may be further complicated because it has been shown to also sorb carbon dioxide at temperatures significantly below room temperature [88]. There are variations in performance characteristics of the material obtained from different manufacturers, as evidenced by differences in the elution temperature for carbon dioxide. Competition from carbon dioxide sorption may be a significant factor if non-CO_2-free air is used in the temperature pre-treatment process. A potential flowsheet capable of effective management of both I-129 and H-3 from off-gas utilising iodine adsorption followed by a Type 3Å molecular sieve tritiated water trap has been suggested [89]. Any water sorbed on the iodine trap is desorbed by flowing dry air at an elevated temperature.

Options to solidify the recovered tritium for disposal include: regeneration of the Type 3Å molecular sieves with condensation of the water and addition of grout to the water; and direct addition of the Type 3Å molecular sieves to grout.

3.1.3. Tritium management in molten salt reactors

Tritium is formed in somewhat large quantities in molten salt reactors (MSRs), where lithium ions in the fuel salt may absorb neutrons from the fission reaction. The estimated production for a 1000 MW(e) Li, Be, Th, U/F MSR design is about 8.88×10^{13} Bq/day. Tritium may then diffuse through the fuel salt mixture, pipe walls, and heat exchanger walls into the steam generator and could possibly escape from the system with the steam or in the industrial process application.

The main strategies for mitigation include advanced materials for the piping and heat exchangers, inert gas sparging, additional coolant lines, and metal hydride addition or chemical removal.

US ORNL molten salt breeder reactors planned on using a tritium trapping NaF-$NaBF_4$ intermediate salt. In addition to its primary functions of isolating the highly radioactive primary circuit from the steam system and serving as an intermediate heat transfer fluid, the molten NaF-$NaBF_4$ mixture plays a major role in limiting the release of tritium from MSR system. Consequently, the majority of the tritium (>80%) is trapped or condensed out of the secondary circuit cover gas, and less than 0.2% of the total is released. The tritium addition experiments conducted in the Coolant Salt Technology Facility (CSTF) at the ORNL demonstrated the effectiveness of sodium fluoroborate for sequestering tritium [90]. However, further experimentation and research would be required to yield a better understanding of tritium behaviour in sodium fluoroborate, to better define basic parameters and to explain some of the observed phenomena as a result of conducting the experiments in the CSTF . The drawback of this strategy deals with undesirable physical

and chemical properties (highly corrosive and toxic). The fallback position of the ORNL is to employ double walled intermediate heat exchangers. It is known technology, but expensive and based on complex components.

Further exploration of the mitigation strategies with the most potential for near-term development is needed, considering:

- permeability values for Ni-based alloys (HN80MTY, EM721, Hastelloy N, etc.);
- additional development of permeation-resistant coatings, including W-Si and various carbides;
- ultrasonic degassing to facilitate the removal of tritium, reducing required total bubble volume for gas sparging;
- refinement of the geometric configuration of the intermediate heat exchangers, minimising tritium flux;
- discovery of reusable solvents for direct tritium removal from molten salt;
- the chemistry of sodium fluoroborate and the trapping process by which tritium is retained by the salt;
- solubility data for the dissolution of elemental hydrogen (tritium) in sodium fluoroborate;
- identification of the sink that required saturating before steady-state conditions could be established.

3.2. Iodine

The distribution of I-129 in gas and liquid process streams has been measured at the Karlsruhe reprocessing plant (WAK) [91] and predicted for the Barnwell Nuclear Fuel Plant (BNFP) [1]. These data indicate that about 94-99% of the I-129 is released to the DOG downstream of the two reflux condensers and the rest remains in the dissolver product solution and is distributed among the aqueous streams of the separation processes. While most of the iodine is released to the DOG, the VOG and other off-gas streams will also require treatment to recover the I-129 that is evolved from the process vessels by out-gassing to achieve the plant-wide iodine recovery requirements. The iodine remaining in the waste solutions may also be released over time from the process waste vessels or will be released during thermal treatment of wastes. No discernible decrease in the evolution rate of I-129 into the VOG from the HLW tanks was noted in the five years following the WAK plant shut down (average release: ~2 MBq per month). A comparable amount (on a Bq basis) of I-131 arising from the spontaneous fission of Cm-244 in the waste is also released [92]. This means that technology to abate I-129 needs to operate under a range of different gas compositions, flow rates and I-129 concentrations.

Several reviews on I-129 recovery technology have been published [93-97]. Studies in Japan [98] indicate that up to 10% of the iodine from the fuel may be bound as colloidal iodine (AgI, PbI_2) in the dissolver solution after dissolution. In THORP, after initial formation, the colloidal iodine was expected to be broken down during the high-temperature leaching phase of the discontinuous process. For a continuous process, a sparging step is proposed to mobilise more of this iodine compared to simple NO_x sparging. Downstream of the head end it was noted in the WAK VOG 85% of the iodine was bound to organic compounds [93]. Characterisation indicated that the primary compound was n-dodecyl iodide. Other short chain alkyl iodides, nitroalkanes and esters of nitric acid were also detected. While thermodynamically it appeared possible to remove these via silver

nitrate or with elemental silver, under the conditions at the WAK, only metallic silver was effective. Tests conducted at Karlsruhe indicate that residual radioactive iodine in the dissolver solution could be reduced to < 0.4% through the addition of carrier iodate, thermal treatment of the solution and reduction of the iodate by NO_2 in a stripping column [94]. The rate of iodine evolution from the spent fuel solutions is related to the HNO_2 concentration (the presence of HNO_2 promotes the formation of the volatile species I_2) [95].

Technologies have been developed for the recovery of airborne I-129 based on scrubbing with caustic or acidic solutions and chemisorption on silver-coated or impregnated adsorbents. These methods make no isotopic separation and thus trap the other isotopes of iodine. They will also recover the other halogen elements, i.e. chlorine, fluorine and bromine. Therefore, in sizing a recovery technology, it is necessary to take into account the halogens in the UNF (I-127, Cl-36 and Br-81) as well as any halogens introduced via the chemicals used for fuel dissolution.

Liquid scrubbing methods work by dissolving the gas stream. In the case of a caustic scrubber, a chemical reaction takes place, converting the volatile I_2 to a non-volatile (at the conditions operated) sodium iodide and sodium periodate by the reaction equation displayed below. In an acidic scrubbing system, I_2 is the dominant form, thus the risk of volatilisation remains. In THORP, the DOG caustic solution is treated to remove C-14 (see Section 3.3), which also co-precipitates I^-/IO_3^- (~3.5%). The rest is discharged to sea under the principle of isotopic dilution.

$$I_2 + 2NaOH \longrightarrow 2NaI + NaOI + H_2O$$

Commercially available inorganic sorbent materials include silver-exchanged faujasite (AgX), zeolite (AgZ), silver-impregnated silicon dioxide (e.g. AC-6120) and aluminium oxide. The chemical reactions of iodine with silver on a substrate are not well defined, but the consensus is that chemisorbed iodides and iodates are formed. The general process for iodine recovery utilising these sorbents usually involves preheating the gas to about 150°C and passing it through a packed bed of the adsorbent [1]. More details on the processing chemistry may be found in several reviews on iodine removal [1, 96-99].

The development of silver-exchanged AgX and AgZ was conducted primarily in the United States and has not advanced beyond laboratory tests for I-129 recovery. These materials are reported with iodine loadings ranging from 80-200 mg(I)/g of AgX or AgZ while maintaining decontamination factors in the range of 100-10 000 for elemental iodine [100]. While effective in removing iodine from gas streams, the AgX substrate decomposes in the presence of NO_x, and water vapour; therefore, a more acid-resistant substrate was desirable for use in the DOG application. In addition, AgX did not exhibit satisfactory thermal stability during regeneration.

The AgZ sorbent based on a Norton Zeolon 900 mordenite substrate has been developed specifically for application in DOG streams because of its high acid resistance. Elemental iodine loadings of 170 mg I_2 per gramme of Ag^0Z [101, 102] and typical methyl iodide loadings of 140-180 mg CH_3I per gramme of substrate [103, 104] have been obtained for tests on simulated DOG streams. The methyl iodide loading is important as it is a simulant for organic iodides present in the VOG. This is equivalent to 125-161 mg of I_2 per gramme of substrate. The loading capacity is optimised by pre-treating the AgZ with hydrogen to reduce the silver to the metallic state (Ag^0Z) [101-104]. By controlling the operational parameters in the presence of NO_x, CH_3I can be converted to elemental iodine and loadings of 200-230 mg I/g of substrate are reported using 10-16 mesh particles [104]. This represents ~100% of the theoretical utilisation of the silver assuming the formation of AgI.

After limited success in attempts to develop an alternate metal-exchanged zeolite to replace the costly silver form, studies were undertaken to find a method to regenerate the filter bed.

Extensive development and application of iodine adsorbents was conducted in Germany with AC-6120. In the WAK, the use of AC-6120 has been developed to the stage of prototype DOG application. The DOG passes through an NO_2 absorption column and HEPA filter before entering the iodide trap. Since 1975, adsorbent beds have been used to recover I-129 with DFs > 1 000 [105]. Some of the operating and design parameters include those used by Wilhelm and Furrer [106]; in the early filters, 26 kg of low impregnation AC-6120 (~7 wt.% Ag) was used at a flow rate of 148 m^3/h, residence time of 0.6-1.4 sec, an operating temperature of 130°C and up to 2 volume% of NO_x in the gas stream. Peak NO_x concentrations of up to 20% were possible. DFs during the first 120-day service life ranged from 1.0×10^4 to 2.0×10^4. A high impregnation AC-6120H material, which contained ~12 wt.% Ag, was not used in the initial iodine sorption filter at WAK due to limited availability at the time. The system was later modified to provide two filter drums in series. Up to 95% utilisation of the AC-6120 based on the formation of AgI was achieved in the primary filter drum and DFs over the period 1975-85 were > 10^4 [95].

AC-6120H (~12 wt.% Ag) has also been tested on a side stream of the WAK VOG [107]. In this test, the iodine filter was operated for nearly one year on a 10% side stream (35 m^3/h) from the main VOG stream and obtained a DF >50. The filter was operated at 140°C.

Recent data on currently available silver mordenite indicate iodine loadings of 6.5-8.3% (70-90 mg I_2 per gramme of AgZ). Recent deep bed studies at the INL indicate that iodine DFs of > 1 000 are easily achievable [108].

The impurities in the cold process chemicals can also result in additional halogen loadings on the capture processes, depending on the particular streams under consideration: for example, common impurities in nitric acid include Cl^- and F^- [109]. Data from several nitric acid chemical specification data sheets are presented in Table 3.1.

Table 3.1. The concentration of halogens in different grades of nitric acid

Vendor	Cl, % (ppm)	F, ppm
No 1 (bulk)	0.002 (20)	Not reported
No 2 (tanker quantities)	0.01 (100)	Not reported
No 3 (reagent grades)	(0.5)	Not reported
No 3 (reagent grades)	(0.08)	1

Notes: Cl: chlorine; F: fluorine; ppm: part per million.
Source: Based on [109].

Conventionally, radioactive iodine (^{129}I) in off-gas stream is removed using silver-exchanged zeolites (AgX and AgZ) [110, 111]. Although these materials show high removal efficiency for ^{129}I, zeolite-based sorbents cannot exclude the physical sorption of iodine [112]. Such physically adsorbed iodine has the potential to be dissolved in groundwater or can be released during the immobilisation of spent filters at elevated temperatures. In this regard, KAERI has been studying the development of new sorbents for ^{129}I removal. Bismuth is being employed to induce the chemisorption of iodine [113]. Preliminary studies at KAERI showed that the adsorption capacity of iodine on synthesised samples is approximately twice as high as that on commercial AgX, and this iodine was retained by forming BiI_3 or BiOI compounds that are thermally stable up to 300°C, which suggests that physical sorption of iodine can be successfully avoided [114]. Additional optimisation studies are in progress at KAERI to increase the capture efficiency of iodine.

3.3. Carbon-14

Carbon-14 arises in nuclear fuel primarily as an activation product of nitrogen-14 in the uranium dioxide fuel. The bulk of the C-14 found in the irradiated nuclear fuel is assumed to be evolved as CO_2 into the DOG during fuel dissolution. In the THORP facility, it is reported that ~98% of the C-14 in the fuel is released during dissolution [115]. However, information from former AREVA, now Orano indicates that only ~50% of the C-14 is released during dissolution [116]. The THORP dissolver is a batch design with a long residence time. The La Hague dissolver is a continuous "bucket wheel" design which probably has a shorter residence time. The implication is that C-14 release during dissolution is highly dependent on residence time.

If standard HTPT is used, then approximately 50% of the C-14 will be released prior to dissolution. Advanced tritium pre-treatment methods have been shown to release larger fractions (see Section 2.1).

A number of technologies have been developed for CO_2 removal. These include caustic scrubbing, molecular sieve adsorption, adsorbent bed fixation, and co-absorption/ concentration in conjunction with Kr-85 recovery, followed by fixation. Vienna et al. summarise the various carbon recovery options and the current level of development [117].

Carbon dioxide adsorption utilising a caustic solution in a packed column to form carbonates is a common industrial process which has been described in detail [118]. NO_x and iodine should be removed from the waste stream prior to entering the caustic scrubber column to avoid added waste volume and complications. A carbon decontamination factor of 10-100 is anticipated.

The double-alkali process is briefly described in the book edited by Goossen [112]. CO_2 is initially scrubbed from the off-gas stream by an aqueous NaOH stream to form Na_2CO_3. The resulting solution is then reacted with lime (CaOH) to produce a solid product. The overall reactions are:

$$CO_2 + H_2O \rightarrow H_2CO_3$$

$$H_2CO_3 + 2NaOH \rightarrow Na_2CO_3 + 2H_2O$$

$$Na_2CO_3 + Ca(OH)_2 \rightarrow 2NaOH + CaCO_3(s)$$

The first step is usually conducted in a packed tower with counter current flow. In studies with a stirred tank for the fixation of $^{14}CO_2$ using a lime slurry, Holladay [119] suggests that the reaction rate data are consistent with liquid-phase control, and a fast pseudo first-order chemical reaction. German studies indicated that the optimum NaOH concentration in the scrubbing column was between 1.5 and 1.7 M [111]. THORP uses a caustic scrub and then reaction with barium nitrate to precipitate barium carbonate which is grouted to produce a storable waste form. This has been successfully used since 1994 under fully radioactive conditions and while processing with a design throughput of 5 tU/day. The THORP plant has incorporated within the dissolver off-gas system a C-14 removal process as noted above to meet stack release limits. Testing in pilot-scale equipment confirmed literature data that while most of the C-14 is released as CO_2, a small fraction (1%) is present as CO. The tests confirmed that this quantity would still permit the caustic scrubber to achieve a C-14 DF of 70 [120]. Between 2012 and 2016, THORP liquid C-14 discharges were between 4.1 TBq/y and 5.5 TBq/y (authorised limit 21 TBq/y), and aerial C-14 discharges were between 0.34 TBq/y and 0.52 TBq/y (authorised limit 3.3 TBq/y) [120]. Total C-14 arising from the 1 200t(U)/y of fuel is 28.9 TBq/y.

A US Environmental Protection Agency study addressing C-14 control from light water reactor fuel reprocessing plants determined the design parameters for a scrubber column which would have a theoretical recovery of 90% and 99% for CO_2, from a 170 m^3/h air stream containing 315 ppm CO_2 by volume [121].

Another potential method for C-14 capture is packed bed adsorption. Packed bed adsorption is a common industrial method for CO_2 capture. Laboratory scale testing has shown CO_2 can be removed to detection levels using molecular sieve 4A. The molecular sieve can be desorbed by heating at 200°C. Flowsheets utilising molecular sieve have been proposed for full-scale processing [121, 122]. If implemented, the loaded molecular sieve desorption process would require coupling with caustic scrubbing and production of a waste form from the solid product.

3.4. Krypton

The noble gases released from spent fuel are primarily xenon and krypton. Five years of post-irradiation cooling is enough to allow all of the Xe radioisotopes to decay. Kr-85, which has a half-life of 10.7 years, remains in sufficient abundance to cause concern about exposure in vicinities of a reprocessing plant. Neither of the two largest reprocessing plants in recent years, THORP or La Hague, installed technology to abate Kr-85 when built. At the time of construction, the costs and complexity of installing Kr-85 abatement systems dwarfed the potential benefits due to the inert nature of krypton and low exposure doses.

Various methods of trapping the krypton contained in off-gases have been considered. Cryogenic distillation and selective absorption in solvents have been the subject of numerous studies. Adsorption on activated charcoal has the advantage of simplicity and is widely used in reactors in the delay line for the decay of short-lived isotopes, while Kr-85, for its part, is discharged in the atmosphere. By using two parallel beds operating cyclically in the adsorption/desorption mode it is, however, possible to trap Kr and Xe. At the same time, this method requires large volumes and fire hazards exist owing to the presence of oxidising agents. Furthermore, solid sorbents provide a promising and potentially more cost-effective alternative to cryogenic methods.

In the case of molten salt reactors, the subsequent management of VFPs is not easy. Whereas xenon and krypton in the Molten Salt Reactor Experiment off-gas stream were trapped on charcoal, treatment of VFPs and the separation from volatile fluorides of actinides could be partially similar to VFP management in the fluoride volatility method. However, there will be some differences between these two techniques as a result of the on-line reprocessing of fuel from the MSRE. The reduction in VFP concentration in the gaseous stream of the fluoride volatility method means that the selection of abatement technologies used to capture volatiles will be different.

3.4.1. Cryogenic distillation

Cryogenic distillation is a technology to recover rare gases that has been used commercially for many years. The cryogenic distillation process has been successfully used at the Idaho Chemical Processing Plant (ICPP) to recover Kr. This is a commercial technology, but it was not optimised for high-Kr recovery DFs. Further development work on the cryogenic process has been done in Belgium, France, Germany and Japan. Decontamination factors of 100-1 000 have been reported [111].

When applied to dissolver off-gas, the gases must be pre-treated to remove interfering constituents, thus ensuring system safety and operability. All gases that would condense at liquid nitrogen temperatures ($T_m(N_2)$ = -196°C) would have to be removed to prevent plugging of the equipment. These include NOx ($T_m(NO_2)$ = -9.3°C, $T_m(NO)$ = -164°C),

water vapour ($T_m(H_2O)$ = 0°C), and CO_2 ($T_m(CO_2)$ = -57°C). Oxygen must also be removed to avoid the formation and accumulation of ozone. Krypton ($T_m(Kr)$ = -157°C) and xenon ($T_m(Xe)$ = -112°C) are then removed from the off-gas stream in a stripping column by dissolution in liquid nitrogen. They are subsequently separated in purification columns, where the solvent (nitrogen) is first removed along with most of the impurities then the krypton is boiled off from the xenon. Other variants have been demonstrated in which the nitrogen is removed in a rectification column and the Kr/Xe product from this column is separated by distillation.

Pilot-scale cryogenic units for krypton recovery in the absence of oxygen have been tested with inactive Kr in simulated off-gas streams at the KfK (Germany), CEA (France) and SCK CEN (Belgium) nuclear research centres [2, 123]. Each unit handles gas flows of 20-50 m^3/h. There are many similarities:

- each system has provisions to remove H_2O, NO_x and CO_2;
- each system has a hydrogen recombiner to remove O_2;
- the pre-treated gas stream enters a cryogenic column at about -150°C.

Operating pressures, however, vary among the systems:

- REDUCTION, ADAMO, KRETA (Germany) – 5 bar;
- SCK/CEN (Belgium) – 8 bar;
- CEA process (France) – 14 bar.

The column pressure impacts Xe solubility and crystallisation. The French process uses liquid argon in place of liquid nitrogen as the solvent. The second columns (second and third in the French process) are operated at lower pressures and higher temperatures to boil off the solvent then separate the Kr and Xe by fractional distillation. The three processes provide recovery efficiencies for Kr ranging from 99.5% to 99.99%.

Research and development of Kr recovery and immobilisation have been conducted since 1972 at JAEA (Japan Atomic Energy Agency) (former Japan Nuclear Cycle Development Institute and Power Reactor and Nuclear Fuel Development Corporation), and a demonstration scale facility named the Krypton Recovery Development Facility (KRF) was constructed. This was attached to the Tokai Reprocessing Plant (TRP) and operated from 1988 to 2001 [124]. KRF can accept all of the off-gas from the shearing and dissolving process in the TRP, where 0.7 t of spent fuel can be treated per day at maximum throughput.

Figure 3.3 shows process flow of Kr recovery in KRF [125, 126]. First, I_2 is removed by adsorption with Ag-impregnated zeolite. At the next step, O_2 is reduced to H_2O by H_2 and H_2O is adsorbed with activated alumina and molecular sieve 4A. After removal of CO_2 by adsorption with molecular sieve 13X, Xe is separated by adsorption with silica gel at 108 K. The resultant Kr-containing gas is liquefied and distilled at 180°C to separate the remaining impurities such as N_2 and Ar.

In demonstration tests using process off-gas from the TRP, 8.6×10^{15} Bq of Kr-85 were recovered in a yield of more than 95% with a purity of more than 95%. The separated Kr was stored in a high-pressure gas cylinder for use in immobilisation tests.

Figure 3.2. Krypton recovery process in the Krypton Recovery Development Facility

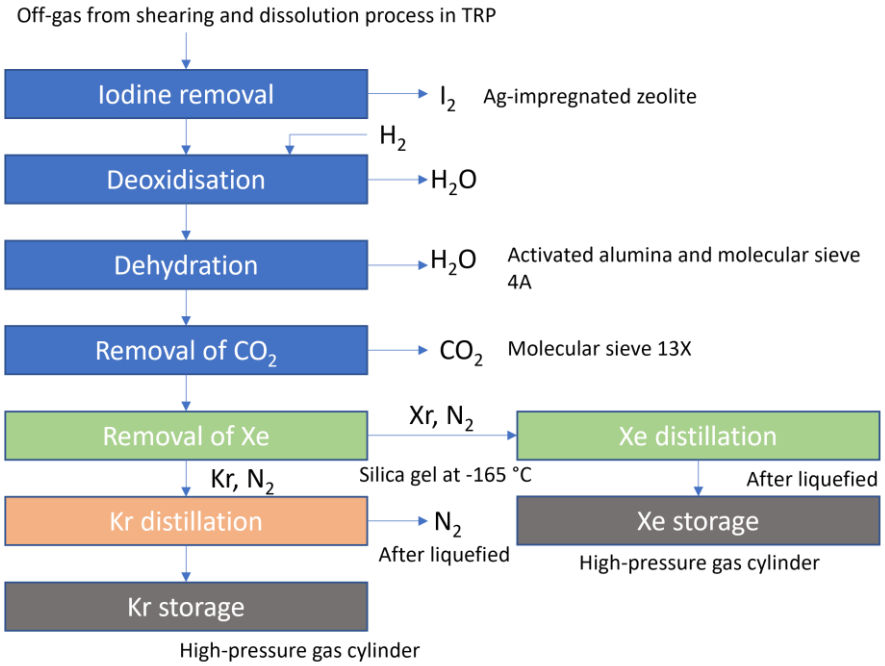

Note: TRP: Tokai Reprocessing Plant.
Source: Based on [127].

For Kr immobilisation, the ion-implantation method [126] was selected because it is a simple and reliable process and is operated in a depressurised condition [135 128-130]. It contains a target electrode at ~1 500-3 000 DC volts in the centre of the chamber and a substance electrode impressed to ~200-350 DC volts constituting the chamber wall. When Kr gas is introduced into the chamber, Kr ions (Kr^+) are formed in the glow discharge plasma and are accelerated and collide on the target electrode. Then some atoms of the target electrode are emitted and form a deposit in the substrate electrode encapsulating Kr atoms. Thus, Kr-implanted alloy is formed on the substance electrode. A combination of nickel and yttrium was chosen as material of the target electrode from the viewpoint of sputtering efficiency and immobilisation rate. Kr gas pressure was controlled to about 10 Pa with continuous introduction of Kr by measuring the pressure.

Three continuous immobilisation tests were performed with radioactive Kr recovered in KRF. About 0.3 m^3 (std.) of Kr was immobilised per one immobilising chamber by 1 100-hour operation, which corresponds to 3 tU as spent fuel. Totally, about 17% of stored Kr was immobilised. For a practical use, it is necessary to scale up the immobilising chamber.

Thermal stability of the Kr-implanted alloy was also examined using the chamber. The obtained Kr release rate at 200°C gave the estimation of Kr release ratio less than 0.1% of the immobilised Kr during 100 y. After 100 y, Kr-85 becomes 1/1 000 of the initial amount by radioactive decay. In conclusion, Kr-implanted alloy thus prepared has suitable gas retention properties for long-term storage.

A xenon purification process was also developed to recover and utilise Xe, as it is a valuable gas [127]. Purification of Xe by pressure swing adsorption using a Ca-type zeolite X was found to achieve Kr-85 concentrations in the Xe product of less than 0.1 Bq/cm^3 from a simulated Xe/Kr-85 mixture.

A cryogenic system designed to recover Kr-85 for beneficial use was operated at ICPP for a number of years [111, 131]. The system is designed to treat a DOG flow up to 34-51 m^3/h (20-30 standard cubic feet per minute). The DOG is pre-treated for removal of H_2, NOx, N_2O, CO_2 and H_2O; however, unlike the other cryogenic processes described above, O_2 is not removed. The system comprises a pre-treatment step, a primary distillation and a batch fractionating column.

Two subsystems are used to pre-treat the feed gas. The first is a rhodium catalytic converter to decompose the nitrous oxide and the second is a silica gel drier to remove water and nitrogen dioxide. The pre-treated gas is cooled to about -160°C in a cold trap where residual water, carbon dioxide and nitrogen oxides are frozen out. The gas stream now contains less than 2% residual contaminants and enters the primary distillation column.

Entering at mid-height to the primary distillation column, the gas stream is scrubbed by liquid N_2 at -190°C. The system is operated at ~2 atm pressure. The higher boiling constituents in the feed gas (O_2, Xe, Kr and Ar) are condensed and absorbed in the liquid N_2 and the waste gas (primarily N_2) is discharged at the top of the column. The waste gas has an additional use prior to stack discharge to cool the batch distillation condenser and purge and cool the regenerator columns. The down flowing liquid, which collects at the bottom of the primary column (N_2 and O_2 rich in Kr and Xe), is transferred several times a day to the batch fractionating column. After each transfer, the N_2 and O_2 are distilled off, but the rare gas components are accumulated in the still until there is a sufficient quantity for fractional distillation of Kr and Xe (generally six to seven transfers).

Fractional distillation is performed at a pressure of about 2.7 atm. The initial fraction containing primarily the residual oxygen is recycled to the feed gas compressor to prevent the loss of the small amount of rare gases in this fraction. The krypton fraction comes off next, followed by the Xe; the rare gas product streams are diverted into intermediate storage vessels for subsequent bottling in pressurised cylinders.

While the ICPP process was not specifically designed for effluent control, performance data presented by Bendixsen and German [132] indicate that during operation in 1974, average recovery efficiencies for krypton and xenon were 97% and an estimated >98%, respectively. However, due to process start up and upsets, the overall efficiencies for Kr and Xe were only 52% and 63%, respectively; thus pointing out the importance of continuous operation, reliable process equipment and highly trained operations staff.

3.4.2. Solid sorbents

Both activated carbon and zeolites have been studied to recover krypton from the DOG stream. One possible system uses a bed of synthetic silver mordenite (AgZ) at ambient temperatures to recover Xe. The "Xe-free" gas is then chilled and passed onto a second bed of hydrogen mordenite (HZ) operated at -80°C that absorbs the Kr. The Kr is recovered and concentrated on a third HZ column via temperature swing on the second column to ~60°C. The Kr is recovered from this third column again via a temperature swing to a cold trap [133]. The Xe bed is regenerated at 200-250°C. Laboratory tests have shown DFs of 400 for Kr and 4 000 for Xe [134].

It has been reported that AgZ has the highest Kr adsorption capacity, but other less expensive zeolites for Kr recovery and non-cryogenic operating temperatures have also been investigated [135]. It was found that hydrogen mordenite HZ has a capacity in the order of 10^{-9} moles Kr per gm HZ at ambient temperatures.

Munakata et al. have also examined the use of AgZ and HZ to recover Xe and Kr from a simulated dissolver off-gas stream [136]. They point out that this approach should have lower operating costs than cryogenic distillation and will avoid the possible fire hazard resulting from the accumulation of ozone in the cryogenic systems. It also has the advantage of avoiding the possible explosive reactions and fire risks associated with NOx reactions and activated carbons that have also been studied for the recovery of Kr/Xe. Loadings of 1×10^{-6} mol Kr/g AgZ and 2×10^{-7} mol Kr/g HZ were reported at a partial pressure of ~5 Pa. Xe loadings are estimated to be 2×10^{-4} mol Xe/g AgZ and 1.5×10^{-5} mol Xe/g HZ were reported at a partial pressure of ~55 Pa. Both loadings are at 0°C. Thus, processing of 1 MTIHM would require a minimum bed size of ~500 L of AgZ at a packed density of 0.662 g/cm^3. At these conditions, the bed would absorb ~0.3 mol of Kr (~5% total Kr) in addition to the 67.4 mol of Xe.

More recently, the INL has tested AgZ and HZ loaded onto a polyacrylonitrile (PAN) binder for the separation of Kr and Xe from simulated dissolver off-gas streams [137, 138]. For the HZ, a hydrogen mordenite powder was incorporated into a macroporous polymer binder (PAN) and formed into spherical beads. This engineered form HZ-PAN sorbent retained the surface area and microporosity of the mordenite powder. The HZ-PAN was evaluated for krypton adsorption capacity utilising thermal swing operations. These tests achieved a capacity of 1.0×10^{-4} mol Kr/g HZ-PAN at a temperature of -82°C. Adsorption/desorption cycling of the sorbent was also performed, with results indicating no decrease in krypton capacity. For the AgZ, sodium mordenite powder was incorporated into a PAN binder, formed into spherical beads and converted to a 9 wt.% silver form composite sorbent. The engineered form AgZ-PAN sorbent retained the surface area of the sodium mordenite powder. The sorbent was evaluated for Xe adsorption with capacities measured as high as 3.0×10^{-5} mol Xe/g AgZ-PAN at ambient temperature and 4.6×10^{-4} mol Xe/g AgZ-PAN at -53°C. The selectivity of xenon/krypton was 22.4 for a feed gas of 1 020 µL/L xenon and 150 µL/L krypton in a balance of air at -53°C. Adsorption/desorption thermal cycling of the sorbent was also performed, with results indicating sorbent performance was not significantly impacted.

Work is also underway on the development of high surface area metal organic frameworks (MOF) for removal of Xe and Kr at near room temperature. This includes nickel dioxobenzenedicarboxylic acid (NiDOBDC) [139] and a partially fluorinated MOF with copper (FMOF-Cu) [140], which have shown good Xe and Kr capacities [141]. Results for the NiDOBDC MOF showed a Xe adsorption capacity of 4.2×10^{-3} mol Xe/g at 100 kPa and 25°C and a Kr capacity of 3.6×10^{-4} mol Kr/g under similar experimental conditions. Silver nanoparticle-loaded NiDOBDC (Ag@NiDOBDC) had an improved Xe capacity (5.3×10^{-3} mol Xe/g) and a selectivity of Xe/Kr ≈ 7 [142].

Two-column testing of the NiDOBDC (Xe capture) and FMOF-Cu for Kr recovery has been demonstrated at the Pacific Northwest National Laboratory (PNNL) for a mixture of 400 ppm Xe, 40 ppm Kr in dry air [143]. Similar experiments using FMOF-Cu instead of NiDOBDC resulted in capacities 3.7 times higher for Kr than from a mixture containing Xe and Kr.

Absorption of Kr and Xe on zeolites was also studied at the CEA (France) to trap Kr-85 from the off-gas of spent nuclear fuel reprocessing plants. Dynamic breakthrough curves were measured with the commercial chabazite AW-500 in a fixed-bed column at different temperatures for the Kr/N_2 and Xe/N_2 binary systems [144] (Figure 3.3). The affinity of AW-500 is higher for Xe, but Kr can be efficiently adsorbed and removed from the off-gas.

Figure 3.3. Breakthrough curves of Kr and Xe in N_2 at -20°C on AW-500

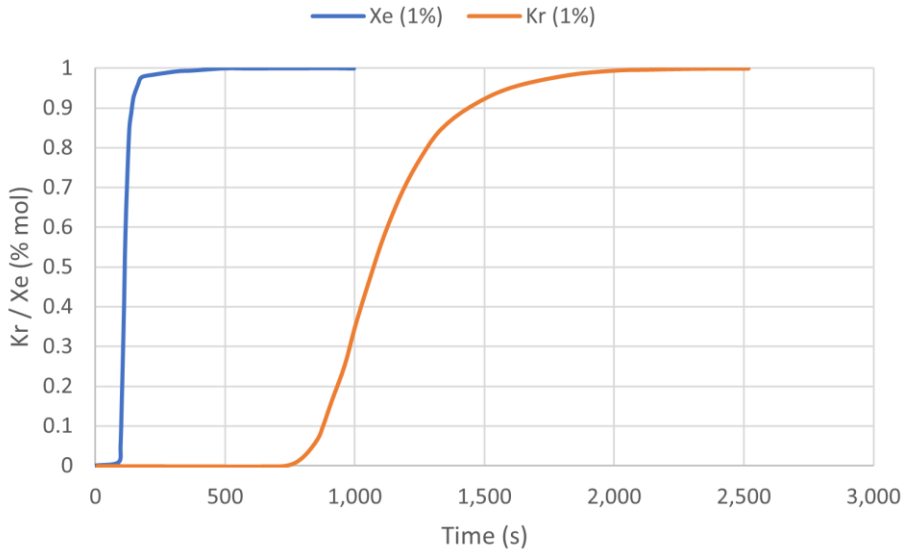

Source: Based on [144].

The potential interaction of other species (NO, NO_2, O_2, CO_2) with Kr and Xe was also checked. Almost no impact of NO, NO_2 or O_2 was observed on Kr adsorption, while a slight decrease of Kr and Xe adsorption (-15% and -10% respectively) has been noticed with 0.1 mol% of CO_2.

Kr and Xe adsorption was modelled by Bertrand et al. [144] using the dynamic simulation software ProSim DAC. The experimental data (breakthrough curves) obtained for the ternary system 0.1% Kr/0.1% Xe/N_2 were compared to the calculated values, showing a very good agreement. A Kr capture process by pressure or temperature swing adsorption on the zeolite AW-500 could be designed based on this first model.

The CEA has recently studied silver-loaded zeolites for the capture and the concentration of radioactive xenon from the air. Deliere et al. [145] showed that Ag@ZSM-5 made of silver nanoparticles supported on a silver-exchange zeolite exhibits outstanding performances in terms of adsorption capacity and Xe/Kr selectivity (Xe capacity ~ 3.5 x 10^{-4} mol.g^{-1} and $S_{Xe/Kr}$ > 100). While O_2, Ar and Kr are almost not retained by the sorbent, CO_2 is retained for a few minutes. In contrast, Xe capacity is about one order of magnitude greater than values reported on any other specific sorbent in the literature under similar conditions. This trend was recently confirmed by Monpezat et al., who compared performances of different sorbents (MOF, active carbon, Ag-loaded zeolites) towards Xe adsorption. They confirmed that Ag-loaded zeolites (Ag@ZSM-5, Ag@ETS-10) show Xe capacity and Xe/Kr selectivities that surpass all other materials [146]. Based on molecular simulation, the enhanced adsorption of xenon was attributed to the presence of silver nanoparticles located at the external surface of zeolite crystallites [147] (Figure 3.4). Once integrated into specific devices, such as packed columns of fixed beds, this promising sorbent can be envisioned to separate and capture Xe in a temperature swing adsorption process.

Figure 3.4. Xe, CO_2, Kr, O_2 and Ar breakthrough curves on Ag@ZSM-5 at 25°C for standard air containing 520 ppm Xe and 60 ppm Kr

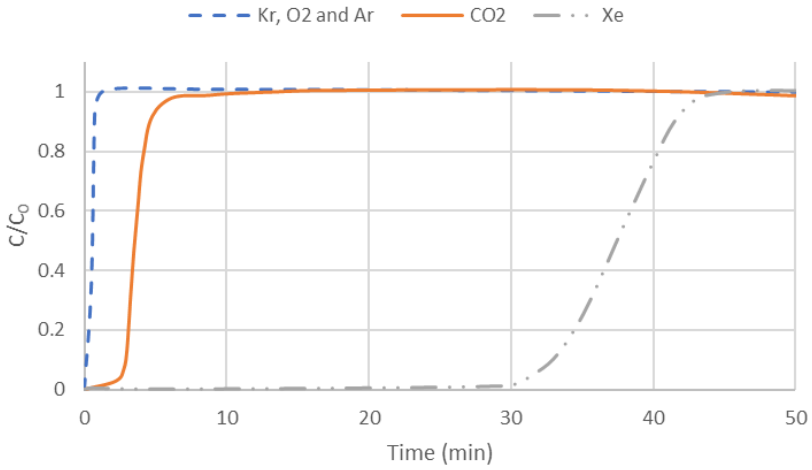

Source: Based on [145].

3.5. Semi-volatile components and particulates

In addition to the gaseous species, "semi-volatile" species are released to the off-gas stream. These include oxides of ruthenium, caesium, technetium, tellurium and antimony. Of these, the most studied are ruthenium and caesium, which also typically require the highest recovery factors. The amount released is highly dependent on the processing conditions. For example, under normal pre-treatment conditions, only very limited fractions of krypton, C-14 and iodine are released. However, work in Korea and the United States has recently shown that, under high temperatures, O_2 and O_3 oxidising conditions, virtually all of the H-3, C-14, Kr-85, I-129, Tc-99, ruthenium and caesium are released to the off-gas and significant fractions of the tellurium, rhodium and molybdenum are also volatilised. In the dissolution process, where the fuel is dissolved in boiling nitric acid, ruthenium is volatilised in two forms: ruthenium tetroxide (RuO_4) and ruthenium nitrosyl nitrate (a compound with the general formula $RuNO(NO_3)_4(OH)_2.4(H_2O)_2$) [148]. The distribution of volatile ruthenium between the nitrosyl nitrate and tetroxide forms is not well known.

3.5.1. Ruthenium

Yttria filter has been suggested as a trapping agent for gaseous oxides of ruthenium [149] (Figure 3.8). The ruthenium compound formed on yttria filter under air conditions at over 900°C was determined as $Y_2Ru_2O_7$ with a pyrochlore structure. The filter is expected to offer stable material in which the volatility of ruthenium can be effectively suppressed because of its incorporation into a lattice of high stability over 900°C in air. The X-Ray fluorescence result of ruthenium trapped on an yttria filter under air condition showed that the concentration of ruthenium on the back and front faces of the filter decreased linearly with increasing superficial air velocity, and the back face concentration of filter was lower than the front face concentration by about 30-45%. The Thermogravimetric analysis (TGA) result of ruthenium trapped on an yttria filter indicates that there is a weight loss of 5.8 wt.% up to 1 400°C, which is believed to be due to the fact that the thermally stable $Y_2Ru_2O_7$ phase was formed on the yttria filter.

Figure 3.5. Scanning electron micrograph of yttria fibres before (left), after trapping at 950°C (middle) and after trapping at 1 100°C (right) ruthenium oxides

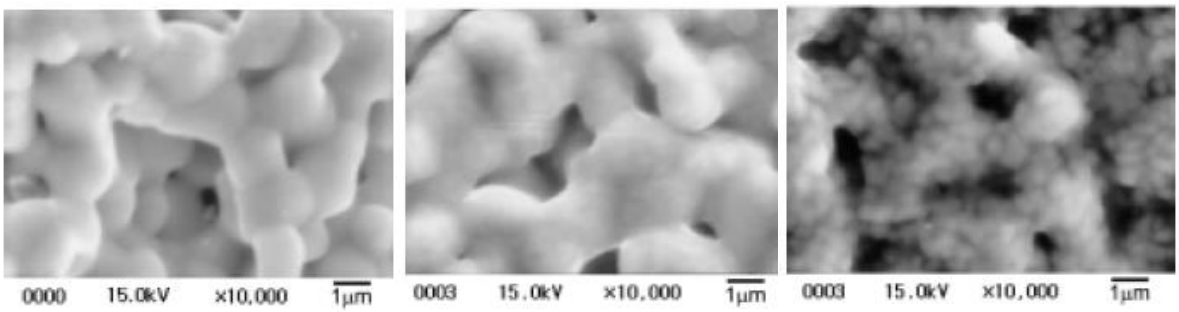

Source: [149].

Tests have also been conducted using silica gel to evaluate trapping of RuO_4 from dry gas streams. Initial tests showed that RuO_4 deposited on the test equipment. This deposition was minimal at ambient temperature, but was observed to be rapid and complete at around 150°C. It was found that RuO_4 retention from a dry air stream by silica gel at 40°C provided visual indication of the ruthenium penetration into the bed (Figure 3.6) [150]. RuO_4 retention on silica gel was found to be reversible, with RuO_4 diffusing from the Ru-bearing silica gel during storage [151].

Figure 3.6. Silica gel bed after exposure to RuO_4 (gas flowed from left to right)

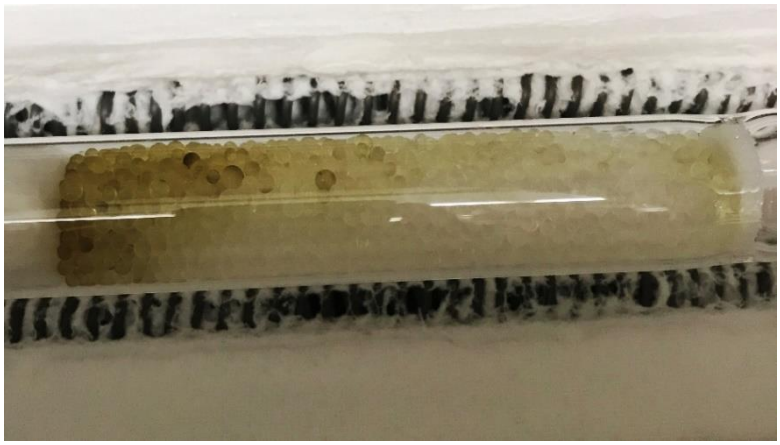

Source: [150].

Deposition of RuO_4 onto metal surfaces was characterised across a temperature range of 50-250°C. At a bed temperature of 150°C, penetration of the RuO_4 into a bed of steel wool varied with the packing density of the metal, ranging from 3.8 cm to 15.3 cm, and was less than the penetration into a silica gel bed. Increasing the bed temperature to 250°C decreased the penetration into the bed to less than 1.8 cm. The deposition zone did not increase in length, as additional RuO_4 was delivered to the sorbent bed, indicating that the depth of the deposition layer on the metal sorbent will continuously increase until the bed is removed from service. Use of stainless steel mesh located in front of the steel wool and at various depths within the steel wool packing provided samples for evaluating the deposition per unit surface area (Figure 3.7) [151]. Analysis of the RuO_4 concentration in the bed effluent resulted in estimated decontamination factors in excess of 10^6 for sorbent beds composed of steel wool [150, 152].

Figure 3.7. Ruthenium deposition on stainless steel mesh (left) and close-up view of section where the coating was chipped (right)

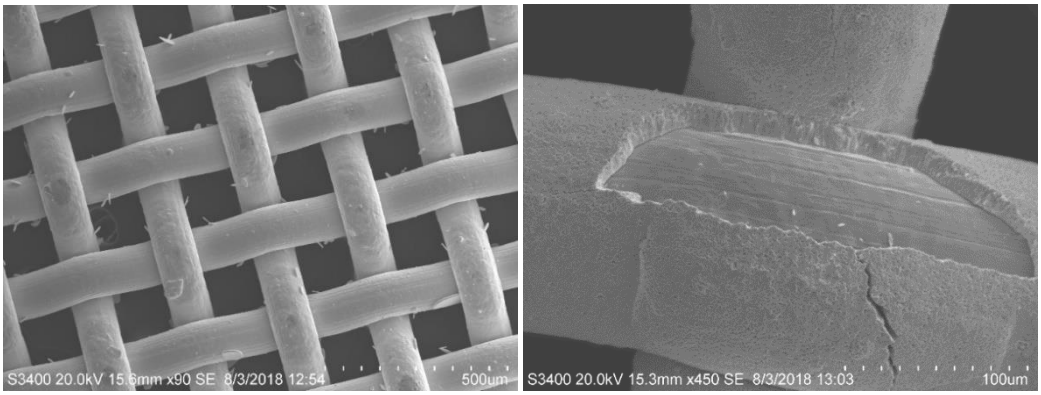

Source: [150].

3.5.2. Caesium

Experiments have been performed in Korea to determine the trapping characteristics and the minimum reaction temperature of gaseous caesium generated from different caesium compounds with fly ash filters [153] (Figure 3.8). The fly ash filters are used to capture the caesium given off by the high-temperature pre-treatment step used in their pyrochemical process (see Section 2.3.2). The trapping results of gaseous caesium generated from caesium silicate, CsI and CsOH by fly ash filters indicated that pollucite ($CsAlSi_2O_6$) and Cs-nepheline ($CsAlSiO_4$) were mainly formed [154]. The minimum reaction temperature between fly ash filter and gaseous caesium generated from caesium silicate, CsI and CsOH was determined at about 600°C.

The disk-type fly ash filters have shown good performance for the capture of gaseous Cs in hot cell experiments [155, 156]. Additionally, five types of granule filters, including a ball, tube and sponge structure-type filters, have been tested [157].

Figure 3.8. Photographs of fly ash filters before (left) and after (right) trapping gaseous caesium

Source: [158].

Fly ash filters fabricated with raw materials from power plants contain some impurities such as Fe_2O_3, CaO, K_2O and MgO. These impurities make it difficult to maintain uniform quality of the filter media. Therefore, a new filter using kaolinite as the raw material has been developed for capturing Cs [159]. This kaolinite-based silica-alumina (SA) filter consists of only silicon and aluminium oxide. Feasibility tests have shown that Cs

compounds chemically reacted to produce a thermally stable form of $CsAlSiO_4$ at 900-1 000°C.

3.5.3. Technetium

In the current PUREX process, nearly all of the Tc is retained in the dissolver liquor (>99.99%), either dissolved in the liquor (80-90%) or as insoluble residues (10-20%) [160], and only causes volatility concerns in the high-temperature vitrification process (see Section 2.4). However, the implementation of high-temperature pre-treatment options will result in volatile Tc entering the off-gas system. The PNNL carried out a thorough review of Tc immobilisation options [161], that is summarised here.

Tc behaviour in aqueous reprocessing, in the form of pertechnetate, is relatively well understood. However, there are considerable knowledge gaps with regards to:

- speciation, specifically non-pertechnetate species;
- removal from process streams: again specifically non-pertechnetates, and from off-gas scrub solutions;
- disposition – incorporation in glass is carried out internationally, other methods are less well understood.

Tc in off-gas systems can be captured in submerged bed scrubbers or wet electrostatic precipitators. Methods for separation of pertechnetate from alkali waste solutions include ion exchange, solvent extraction, electrochemical reduction and precipitation. These options are only effective for pertechnetates, so non-pertechnetates must be converted for these separation methods to be viable.

3.6. Summary

Trapping off-gases requires consideration of a couple of key factors. First, the physical and chemical behaviour of the radionuclide to be trapped, the other species within the off-gas stream and the order of the abatement techniques within an off-gas system. It is also important when developing a capture method to consider the final waste form, which will be discussed in Chapter 4. Overall, it is no surprise that in order to achieve high DFs, different approaches are required for each radionuclide of interest.

A general trend in technology development for most radionuclides is to move away from the use of liquid scrubbing to solid abatement methods. This reduces effluent produced and can be exploited to enable facile conversion into a final waste form. Two of the greatest challenges currently faced in the off-gas capture area are the capture of Kr-85 and H-3. However, the challenge revolves more around the economic recovery of material and not the technical feasibility of Kr-85 or H-3 abatement. For tritium recovery to become more viable, it is likely to necessitate an additional head-end step, which itself requires further development. There is promise that solid sorbents may enable more economic recovery of Kr-85, which would substantially reduce the aerial discharge. As techniques such as pyroprocessing and high-temperature pre-treatment are further developed, technical options for removing semi-volatiles from the off-gas stream become more significant and work has progressed in that area.

4. Waste produced by off-gas treatment

In abating radionuclides from off-gas streams, secondary wastes are generated. Each of the different volatiles and semi-volatiles pose an environmental hazard over vastly different timescales and have different dose consequences. The waste management approach must therefore be considered on a case-by-case basis and is coupled to the selection of abatement technology.

4.1. I-129

Iodine management has received special attention since the development of nuclear industry [162]. For a detailed review of I-129 capture and immobilisation options see reference [163]. The isotope is thought to be one of the main contributors to the dose released in the biosphere by a disposal site [164]. This can be explained by poor retention properties of geological formations generally considered for disposal sites. As a consequence, a waste form should have a fractional degradation rate lower than 10^{-5} y^{-1} so as to not significantly affect dose to an exposed individual.

A number of different waste forms have been proposed, including: glasses, ceramic composites, cement and inorganic materials such as sodalite or Synroc. There are three considerations when coming up with a suitable waste form: 1) the iodine capture material used; 2) the method of converting the secondary waste to the final form; and 3) the final waste form itself. The examples given below are results from recent promising efforts by the CEA in France, KAERI in Korea and the NNL in the United Kingdom that highlight aspects of those three considerations. The story of apatities is one of understanding and controlling chemistry over a long time period. Silver phosphate glasses show how small modifications can be used to manipulate the properties of the waste form. Throughout each section, it is important to consider how this will practically be achieved in commercial facility. This is further emphasised by considering the use of hot isostatic press (HIP) as a practical way of creating a waste form.

4.1.1. Silver phosphate glasses: Modifying properties to assist waste form synthesis

These glasses belong to the AgI-Ag_2O-P_2O_5 ternary system and can incorporate large quantities of silver iodide (> 20 mol.%). They were already proposed as potential conditioning matrices for iodine by Japanese teams in the late 1990s [165, 166]. Their properties can be influenced by their silver iodide content as well as by their Ag_2O/P_2O_5 molar ratio which defines the length of phosphate chains. The idea here was to improve their properties by modifying their composition with cross-linking reagents able to create new chemical bonds between phosphate chains [167]. Alumina and bismuth oxide, Bi_2O_3, have also been compared for this role [167, 168]. For a given composition (mol.%), $79.4AgPO_3$–$1.6X_2O_3$–19AgI (X=Al or Bi), it was found that these glasses could be easily obtained at 650°C. The lower temperature formation of glass is of benefit in minimising gaseous iodine losses during waste processing. However, in the case of the alumina-bearing glass, a phase separation was also observed. No more than 0.4-0.5 mol% of aluminium can be incorporated into the glass without the formation of $Al(PO_3)_3$ crystals. Such a difference between alumina and Bi_2O_3 was ascribed to the larger polarisability of Bi^{3+} ions, which are more able than Al^{3+} ions to accommodate the network distortion induced by the incorporation of AgI in large amounts. Current studies aim at elucidating the link between

structural modifications generated in silver phosphate glasses thanks to the addition of several oxides and their chemical durability.

Korean efforts have focused on using glasses to immobilise spent iodine filters. There was promise in the use of bismuth glass with a composition of Bi_2O_3(40-50%)-SiO_2(20-25%)-B_2O_3(30-40%), which could be loaded with up to 30 wt.% of spent iodine filters. However, recent work has moved on to using silver phosphate glass waste forms [169]. By using a melt-quenching method, silver phosphate glasses can be made at 450°C. It was found that silver iodide could be incorporated into the AgI-Ag_2O-P_2O_5 glasses up to 50 mol% without significant crystallisation. The corresponding leach rate was found to be about 2×10^{-4} g/m^2·d (PCT-A test). It was noted that improvements will be required to reduce the iodine loss during the immobilisation process.

4.1.2. Apatites: Control and understanding of long-term chemistry to reduce leach rate

Lead-bearing iodoapatites

Taking inspiration from nature, apatites have appeared as good candidates for iodine conditioning [170]. Not only do they have incorporated I-129 in their crystalline structure [170], but they also show a good stability in neutral to alkaline media (generally the conditions found for potential disposal sites) [171]. It had been shown that the lead-bearing apatite $Pb_{10}(VO_4)_{4.8}(PO_4)_{1.2}I_2$ has a forward rate (i.e. congruent dissolution) around $3x10^{-3}$ g.m^{-2}.d^{-1} at 90°C in pure water and that such a value is maintained over a pH range between 5.2 and 8.2 [171]. However, a point that was still unclear was the existence (or not) of a decrease of this rate with time. Actually, it is well known that the efficiency of confinement for HLW glasses (e.g. alumino-borosilicate glasses) over 1 million years relies on the existence of a gel layer which allows a severe drop of the dissolution rate with time. As a matter of fact, up to four or five orders of magnitude exist between elemental releases corresponding to the first stages of alteration (i.e. forward rate) and those associated to the ones observed in the presence of a dense gel layer. Consequently, it is crucial that such a behaviour could be evidenced for any matrix designed for the conditioning of iodine given the half-life of I-129. Figure 4.1 shows the normalised mass losses for iodine and lead in pure water at 90°C as well as the evolution of pH [172].

Figure 4.1. Normalised mass loss for lead and iodine (on the left) and leaching rate on the basis of iodine release (on the right) of a lead-bearing apatite, $Pb_{10}(VO_4)_{4.8}(PO_4)_{1.2}I_2$, altered in pure water at 90°C (S/V = 30 cm^{-1})

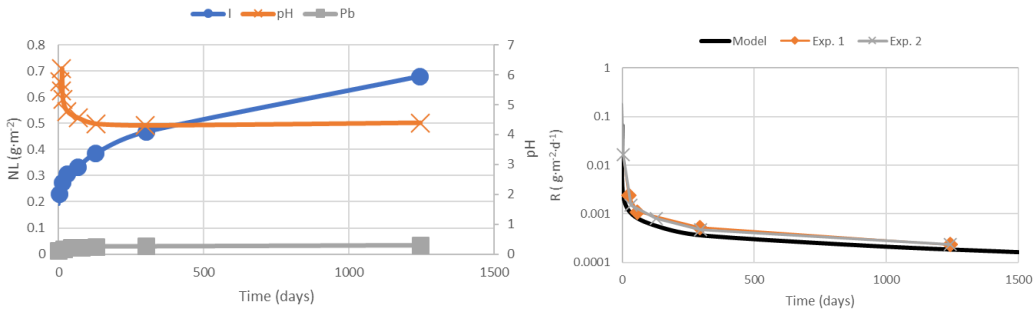

Source: Based on [172].

In this system, iodine was the only possible tracer for the alteration and the behaviour of the material was subsequently extrapolated from its release. Even after four years, the dissolution rate was found to decrease and the experiment was finally stopped at this duration. The final measurement gave a dissolution rate of $2x10^{-4}$ $g.m^{-2}.d^{-1}$. X-Ray diffraction characterisation of the altered powder revealed the formation of a phase of which the diffractogram was very close to that of hydroxyl-vanadinite, $Pb_{10}(VO_4)_6(OH)_2$. The combination of these results together with the evolution of the pH value during the test led to proposing a pseudomorphic transformation of the lead-bearing iodoapatite into a lead-bearing hydroxyl-apatite (on the basis of an ionic exchange $I^- \leftrightarrow OH^-$) to explain the long-term behaviour of such a matrix. This mechanism is supported by diffusion across the tunnels of the apatitic structure. A diffusion coefficient of $4.5x10^{-23}$ $m^2.s^{-1}$ could be calculated from these results.

The question of the shaping of iodine-bearing apatites, which have a poor thermal stability, was also addressed. The emergence of non-conventional sintering techniques like spark plasma sintering has partially overcome this difficulty. Lead-bearing apatites have been the first to benefit from these technical evolutions [173]. In the case of spark plasma sintering reacting at 400°C under 40 MPa (reagent mixture of $Pb_3(VO_4)_{1.6}(PO_4)_{0.4}$ and PbI_2 with a molar ratio of 3:1), samples with homogeneous composition and density were obtained; their relative density exceeds 96% in every case. Even if the final microstructure could be difficult to control [174], such a process could be an opportunity for this kind of material.

4.1.3. Calcium-bearing iodoapatites

The idea beneath the development of such an apatite is that it can incorporate iodine under its iodate form, IO_3^- [175]. As iodate is expected to be less mobile in a geological environment than the iodide form, I^- [176, 177], it could provide a means for decreasing the overall impact of iodine. Another point is that clay-equilibrated groundwater is enriched in calcium, which could provide a means for reaching saturated conditions in the quickest way (in the context of the French geological disposal site). Such trends were confirmed for stoichiometric calcium-bearing iodoapatite, for which the formula can be written as $Ca_{10}(PO_4)_6(IO_3)_{0.92}(OH)_{1.08}$ [178]. The normalised mass loss is shown in Figure 4.2. A residual rate (i.e. after a transitional initial regime corresponding to a congruent dissolution) of 10^{-4} $g.m^{-2}.d^{-1}$ was obtained on the basis of iodine release at 50°C in an initially deionised water. This rate fell by one order of magnitude in a clay-equilibrated groundwater. Here also, like for lead-bearing iodoapatite, the drop of dissolution rate between the initial regime and near-saturated conditions was explained by a diffusive process between IO_3^- ions coming from the solid and OH^- ions coming from the solution, leading to the formation of $Ca_{10}(PO_4)_6(OH)_2$ as a protective layer at the surface of the conditioning matrix.

The shaping of such apatites is still challenging, as no obvious technique has allowed a dense monolith (density >92% of the theoretical density) to be obtained without the generation of iodine-bearing by-products. However, cementation from various calcium phosphates and sodium iodate could be an interesting method for its synthesis, as it prevents the formation of unsuitable secondary phases and leads to a preliminary mechanical blocking [179].

Figure 4.2: Normalised mass loss on the basis of iodine release of $Ca_{10}(PO_4)_6(IO_3)_{0.92}(OH)_{1.08}$ altered in pure water (●) and in clay-equilibrated water (■) at 50°C (S/V = 80 cm^{-1})

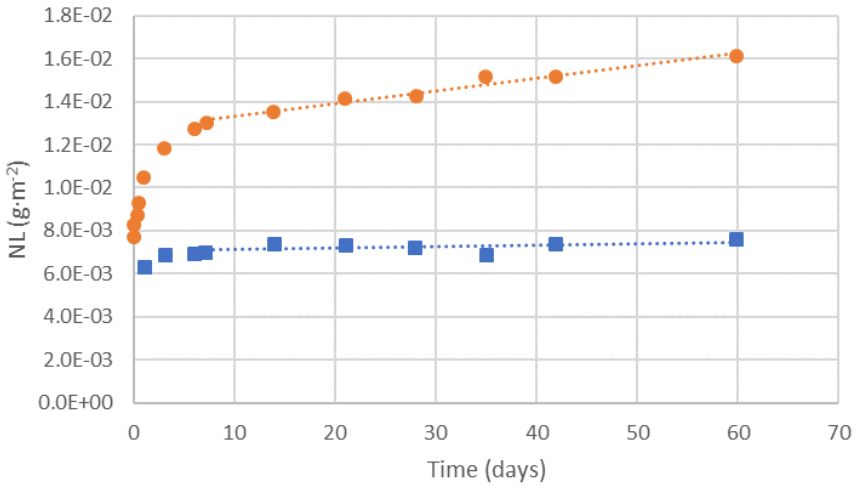

Source: Based on [178].

As can be seen from the above results, several matrices are now convincing materials for iodine conditioning as their chemical durability is of the order of magnitude of alumino-borosilicate glasses designed for the conditioning of HLW (which are not suitable materials for iodine due to volatilisation issues during the production process). Some of them particularly fit to a disposal site environment made of clay with an increased resistance to leaching. However, further studies are needed to get a complete overview of their performance, as they are not all at the same development stage. Their shaping to get a dense monolith is also a point that should be addressed in the future, as technologies which could allow this problem to be overcome are potentially not yet mature at an industrial scale for nuclear facilities.

4.1.4. Hot isostatic press: A process-led approach to creating suitable waste forms

Initial findings indicated that the iodine leach rate of iodosodalite [$Na_4(AlSiO_4)_3I$] was approximately an order of magnitude lower than for iodovanadinite [$Pb_5(VO_4)_3I$] in a pH 11 leachate. The leach data for iodovanadinite suggested an incongruent process possibly involving ion exchange. Leach data for sodalite, by contrast, was consistent with a congruent process [180]. The sodalite tested in these experiments was produced by a combination of hydrothermal synthesis and "HIPping" (hot isostatic pressing), which would not be readily transferable to a practical waste form production process.

The work also demonstrated that AgI could be physically encapsulated in both borosilicate glass and TiO_2 matrices. Although the waste form principle was confirmed, the effectiveness of this method as a waste form remains unconfirmed by the leach tests. This was because the leach data suggested that iodine losses were being limited by the intrinsic insolubility of AgI. It is emphasised that AgI will be unstable under typical disposal conditions due to reduction and anion exchange with the high levels of chloride ions in groundwater.

Given the superior performance of the sodalite phase, attention turned to how this phase could be produced by more practical methods. Sheppard et al. demonstrated that AgI could be occluded into an Ag exchanged zeolite and subsequently converted to sodalite by HIP

[181]. This process would require precipitation of AgI from a caustic off-gas scrubber liquor, and an effective method by which the AgI and zeolite can be mixed.

Ideally, an iodine waste form should be made by a combined capture and immobilisation method, in which iodine is captured directly from the off-gas and the resulting capture substrate can be converted directly to a waste form by HIP. To investigate the potential for this, a range of options for capturing iodine from vapour into silver-impregnated aluminosilicate substrates was studied [182]. This work indicated that a mixed cation iodide sodalite [$Na_3Ag(AlSiO_4)_3I$] could not be formed despite the similar ionic radii of Na^+ and Ag^+. It is suggested that this is due to the relative level of ionicity and covalency in the Na_4I and Ag_4I clusters in the sodalite structure. The work also confirmed that Ag sodalite formed from Ag exchanged zeolite via iodine capture from vapour.

Given the high Ag levels in the Ag sodalite phase, it was important to investigate various redox aspects [183]. This showed that interaction zones of the order of tens of µm formed between the Ag sodalite waste form and Cu and Ni HIP cans. More significantly, leach tests indicated that the Ag sodalite was susceptible to destabilisation by reducing conditions, meaning that significant care would be required when selecting a disposal environment.

4.2. C-14

While there are a number of potential options for immobilisation of C-14 wastes, such as bitumen, polymers and ceramics, cement has seen the greatest use so far in industry. It has the distinct advantage of being a well-established straightforward technique that operates at low temperatures.

Cement as a route to immobilising C-14 waste forms has already seen large-scale commercial use. In THORP, caustic scrubbing followed by precipitation as $BaCO_3$ has, for many years, demonstrated successful operation of the cementation process. $BaCO_3$ is combined with grout and compacted in steel drums.

Calcium, barium and strontium carbonates are all suitable to be embedded in concrete, with calcium carbonate found to be slightly improved compared with others. The high alkalinity of Portland cement reduces the solubility of carbonates [184].

4.3. Kr-85

Whether captured by inorganic materials such as zeolites and sodalite or by metal organic frameworks, Kr-85 would require storage for around 100 years to allow decay to the stable product, Rb-85 [119]. Work carried out in the 1970s and 1980s used stainless steel canisters to store Kr-85 saturated zeolites, HIPed cans containing zeolites and others with compressed gas. However, it was found that there were examples of canisters showing corrosion attack on the inside [185, 186]. The cause is currently thought to be corrosion caused by rubidium, although a literature review appears to highlight contradictions [187]. This is an area that will require further investigation, as the mechanism is currently unknown.

4.4. H-3

The shorter half-life of tritium enables a different approach to the waste form than for longer lived C-14 or I-129, since it only is required to prevent release of H-3 for around 100 years. It has been recommended that cement be used to immobilise tritium [119]. However, the mobility of water is likely to be too high within cement, thus requiring

additional barriers to prevent H-3 discharge. Plastic or steel high integrity containers are likely to be required for disposal of the cement waste forms as these are certifiable for more than 100 years. If these are used, grout is no longer required. It may be possible to use absorbents such as vermiculite or clay. Vienna et al. suggested that cemented H-3 water contained within a high integrity container be used, since grouting is well-developed as a method of stabilising a variety of waste forms [117]. It was identified that development of an efficient process for large volume, low concentration H-3 streams was required to reduce treatment cost.

4.5. Semi-volatiles

4.5.1. Cs waste forms generated from pyrochemical off-gas treatment

Immobilisation methods to fabricate waste forms for disposing used filters, used in a high-temperature, pre-treatment off-gas system, are under investigation at KAERI. Typically, most of the Cs ends up in vitrified HLW, with smaller quantities being immobilised from the treatment of liquid effluent. This section summarises immobilisation technologies for two kinds of Cs-trapped filters (fly ash and kaolinite-based SA filters) developed by the addition of glass frits.

It has been identified that pollucite ($CsAlSi_2O_6$) is a feasible final waste form for the long-term disposal of ^{137}Cs-containing waste [157]. The specific structure of pollucite means it tightly holds Cs ions, such that the hydrochemical and thermal properties are excellent. Therefore, KAERI has developed a simple immobilisation process to fabricate glass-ceramic waste forms for Cs-trapped filters [157]. Two types of Cs-trapped filters, FA and SA filters, and two types of glass frit (SiO_2: 60-75%, B_2O_3: 0-23%, Al_2O_3: 2-9%, CaO: 4-11%, Na_2O: 11-15%) were used in the temperature range of 950-1 150°C. The results of structural characterisation of the fabricated waste forms showed that the major phase of Cs was pollucite with a crystal size of 1-20 μm. This result implies that the pollucite structure was maintained in Cs-FA/SA filters during thermal processing and that glass-ceramic waste forms were fabricated. The PCT leach test revealed that the chemical resistance of these glass-ceramic waste forms showed a leach rate of 10^{-2} g/m^2·d (PCT test) and 7×10^{-5} g/m^2·d (MCC-1 test).

4.5.2. Tc-99

Immobilisation options for separated Tc-99 streams fall into two categories: 1) multi-contaminant waste forms (i.e. where Tc is not the only waste to be immobilised); or 2) Tc-specific immobilisation waste forms. Multi-contaminant waste forms include glass (borosilicate or aluminophosphate), grouts (such as a combination of fly ash, blast furnace slag and Portland cement), geopolymers, phosphate bonded ceramics, aluminosilicates and Synroc.

Tc-specific waste forms which have been investigated are iron-technetium oxides, metal alloys, Tc oxides, framework aluminosilicate minerals, titanates, apatites, layered double hydroxides and sulphur-based aerogels. However, it must be noted that these waste forms are not well developed.

4.6. Summary

The trapping of off-gases is intimately coupled to the final disposal route. The preferred method is to capture and contain over diluting and dispersing and this is typically achieved by converting the abated material into a final waste product. Each radioisotope that needs to be considered brings along a unique set of challenges.

The management of I-129 is particularly challenging due to the long half-life and high mobility in a geological repository. This explains why most development work has focused in this area. Compared to iodine, the technical options for immobilising the secondary wastes containing H-3 and C-14 are more mature, revolving around cementation. Nevertheless, there remains room to improve waste volumes and performance even with the mature technologies. There are some uncertainties around corrosion of the waste container for the Kr-85 technical option which will need to be resolved to boost confidence in the ability to store the captured noble gas. As the semi-volatiles in a classic reprocessing system typically end up in either HLW glass or discharged, waste form development of capture media for these species is relatively immature.

5. Advanced materials for volatile fission products capture

5.1. Introduction

This chapter focuses on the applications of advanced materials, specifically nanomaterials, for the capture of volatile fission products. These represent potential "next generation" technologies with some significant benefits. Using a bottom-up synthetic approach to selectively capture targeted species, rather than top-down modification, allows for greater control over material properties. However, these options are currently in their infancy, with many challenges to overcome in order to progress these materials up the TRL scale. Applications in this chapter are mainly focused on iodine capture, but some work on noble gases is also considered. Initially, the adsorption process using silver zeolites for iodine capture is discussed before extending the overview to MOFs and nanocomposites.

5.2. Silver zeolites for iodine adsorption: Limitations of current technology

The use of zeolite-type sorbents for the capture of iodine has been a topic of extensive development, the reasons for which were outlined in Chapter 3. To explain the need for exploring nanomaterials, it is first important to understand the problems associated with the use of the current generation of solid sorbents. First, iodine diffusion inside zeolites has been found to be slow and is likely to limit adsorption. There are also concerns over the chemical stability of silver-exchanged zeolites. For example, silver-exchanged faujasite (AgX) decomposes in the presence of NO_x and water vapour and AgX also does not exhibit satisfactory thermal stability during regeneration. In addition, the fibrous nature of mordenite may present an inhalation hazard. One of the problems with alumina and silver impregnation is the high quantity of AgI that can be absorbed. This is counterintuitive, but these materials capture iodine by forming AgI along grain boundaries. This interconnected network leads to a higher leach rate of these materials, which is an issue when considering the final disposal waste form.

To better design capture materials, the iodine capture mechanisms are useful to understand. As an example, the zeolite mordenite is one of the leading materials for iodine capture (MOR, Figure 5.1), but mechanistic performance remained largely unexplored until recently [188]. Two products are formed by the reaction of I_2 with silver-exchanged zeolites: AgI and $AgIO_3$. The precise reactions that take place depend on temperature, the oxidation state of the silver and the zeolite. For example, Ag_2O (Ag^+) can react with I_2 to form AgI and O_2. Furthermore, Ag(0) metal can also react with I_2 to form AgI. There are three phases of AgI to consider: 1) a β-phase below 147°C; 2) an α-phase above 147°C; and 3) a metastable γ-phase that can co-exist at high temperatures. The α-phase AgI was found to be localised within the pores, while the metastable γ-phase was found to be localised on the surface of the zeolite structure in the form of a larger nanoparticle. It was proposed that the Ag^+ and iodine was mobile within the structure, leading to the observation of surface particles. This has importance when it comes to disposal and leach performance. Interestingly, if a hydrogen pre-treatment step in the creation of the silver-impregnated zeolite was not used, the silver iodide clusters remained within the pores. Typically, hydrogen pre-treatment generates Ag^0, which has been shown to increase the iodine capacity in some situations, but can be detrimental when the pre-treatment is carried on for too long. This is thought to lead to large Ag nanoclusters forming, reducing pore volume and surface area of Ag to react with iodine.

Figure 5.1. Mordenite structure and α-, β-, and γ-AgI polymorphs

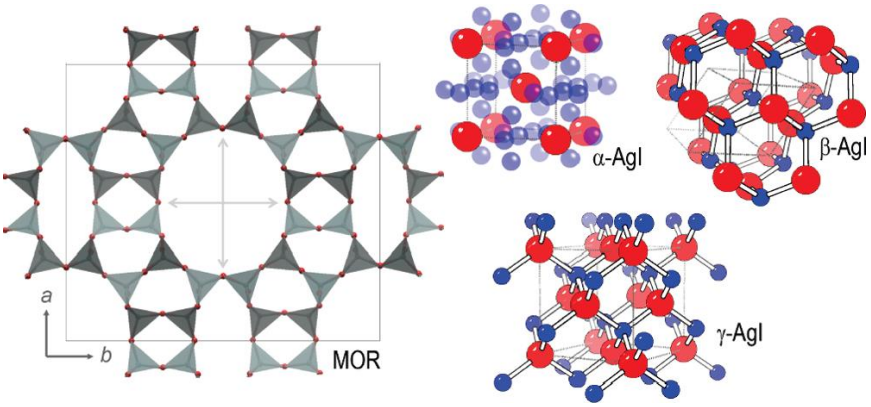

Notes: Red: I; blue: Ag. The MOR framework defines one-dimensional channels (12-rings, 6.5 x 7.0 A2) parallel to the c-axis, which contain exchangeable cations and water molecules (omitted for clarity).
Source: [189].

Figure 5.2. A schematic of iodine capture by silver-containing mordenite

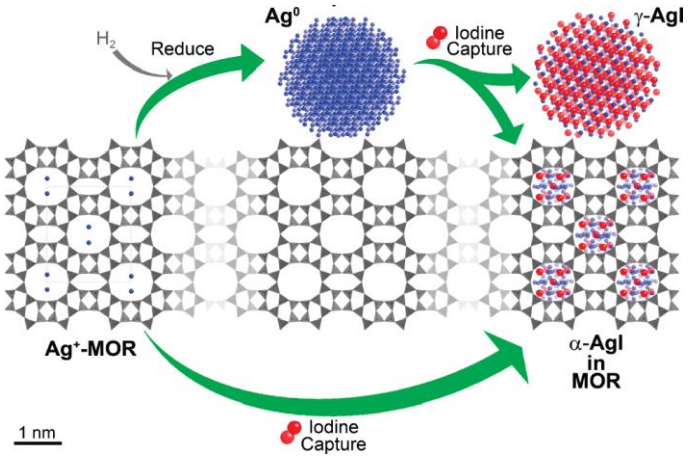

Note: While pre-reducing the silver MOR yields in a mixture of γ-AgI nanoparticles and sub-nanometer α-AgI, direct iodine uptake by silver-exchanged MOR produces exclusively sub-nanometer α-AgI.
Source: [189].

5.3. Metal organic frameworks

Mechanistic studies of VFP capture by nanoporous materials enables better design of molecules and materials for commercialisation. This has led to the exploration of MOFs for fission gas capture in reprocessing [190]. This section uses the examples of Kr and I capture to highlight the benefits of using these materials.

Two well-known MOFs (MOF-5 [191] and the nickel salt of 2,5-dihydroxyterephthalic acid NiDOBDC [192]; see Figures 5.3 and 5.4) were synthesised and studied for xenon capture and separation. The results indicate that NiDOBDC adsorbs significantly more xenon than MOF-5 and is more selective for xenon over krypton than activated carbon. More recently, MOFs have been used that can selectively remove Xe from Kr, while also remaining resistant to radiation [193]. Known as SIFSIX-3, it remains stable up to doses of 50 kGy. According to the authors, this means that 1 g of the material can separate Kr-85

from approximately 2 674 g of spent nuclear fuel (130 TBq/Mg case) without any crystal structure damage, if the Kr-85 is retained for a total of 1 hour.

Figure 5.3. MOF-5 structure shown as ZnO4 tetrahedra (blue polyhedra) joined by benzene dicarboxylate linkers (H, white, O, red and C, green) to give an extended 3D cubic framework with interconnected pores of 8 Å aperture width and 12 Å pore (yellow sphere) diameter

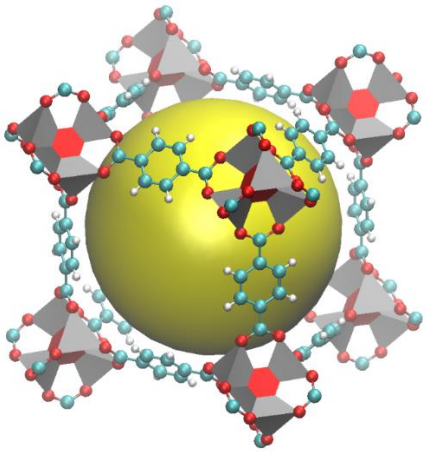

Note: Yellow sphere represents the largest sphere that can occupy the pores without coming within the van der Waals size of the framework.
Source: Based on [191]. Courtesy of Jonathan Austin, National Nuclear Laboratory, United Kingdom, 2020.

Figure 5.4. Honeycomb network structure of NiDOBDC (nickel salt of 2,5-dihydroxyterephthalic acid)

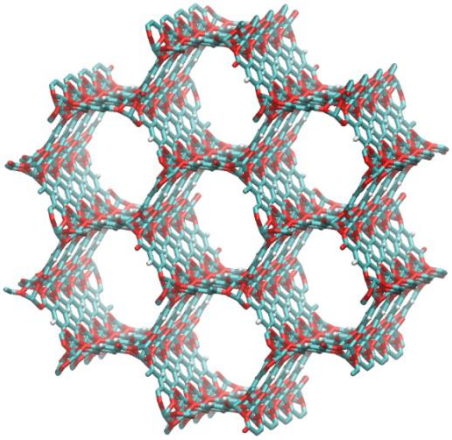

Source: Based on [192]. Courtesy of Jonathan Austin, National Nuclear Laboratory, United Kingdom, 2020.

The combination of advanced computing and synthesis/characterisation with related gases have opened this avenue in nanoporous materials to nuclear applications. For example, studies of ZIF-8 (an MOF with small zeolite-like pore openings on the order of I_2 gas molecule size; see Figure 5.6) showed the framework had structural durability for high weight loadings and high gas retention. The Zeolitic imidazolate framework (ZIF) structure is similar to classical aluminosilicate zeolites but with the advantage of greater tunability

of pore size and control of topology which has been explored in more detail since then [194].

Figure 5.5. 3D view of ZIF-8

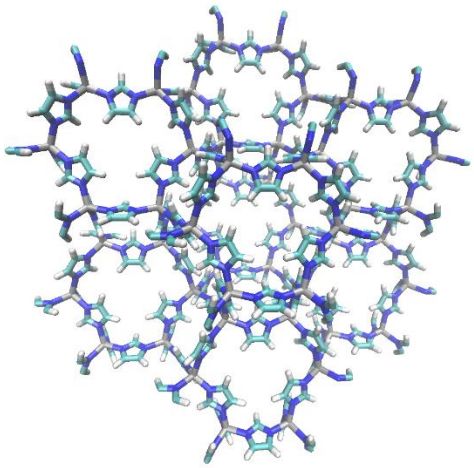

Source: Jonathan Austin, National Nuclear Laboratory, United Kingdom, 2020.

Furthermore, recent studies have shown that mechanical pressure amorphises the I_2-ZIF-8 MOF to where the I_2 remains captured but is held inside the material longer as compared to crystalline MOF, thereby making a one-step capture-interim storage material for the iodine [195].

The ability to bring successful nanoporous material research from the chemical and petrochemical industries to nuclear fuel cycle applications may further succeed in the area of mixed-matrix membranes for increased gas permeability. For example, MOFs with large pore sizes have been incorporated into polymer membranes for O_2/N_2 separations (Figure 5.7) [196]. It is, therefore, a natural extension to explore applications to the capture of fission gases.

Figure 5.6. Structure of MIL-101 (Chromium(III) Terephtalate Metal Organic Framework)

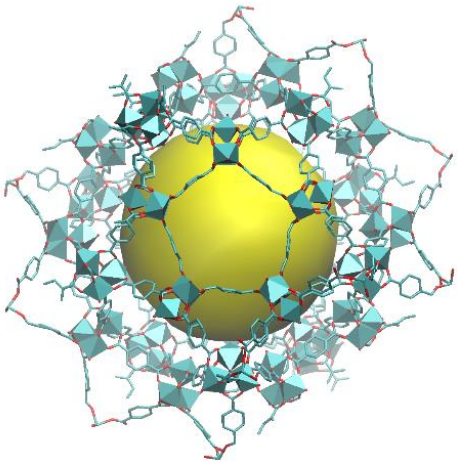

Note: Water-stable MIL-101 microcrystals adhere well to polysulfone.
Source: Based on [196]. Courtesy of Jonathan Austin, National Nuclear Laboratory, United Kingdom, 2020.

Generally speaking, MOFs have been found to have high sorption capacities and are tuneable to different volatile elements. However, the long-term fate of the organic structure in a high heat/radiation field is only now becoming the focus of recent studies. In this regard, researchers at Sandia National Laboratories have developed a new generation of high-performance radionuclide adsorbent materials for nuclear waste reprocessing and disposal. A suite of inorganic nanocomposite materials (SNL-NCP) has been prepared to effectively entrap various radionuclides including gaseous ^{129}I (Figure 5.8) and anionic ^{99}Tc [197]. Importantly, after the sorption of radionuclides, these materials can be easily converted into nanostructured waste forms, which are expected to have unprecedented flexibility to accommodate a wide range of radionuclides with high waste loadings and low leaching rates.

Figure 5.7. Iodine sorption onto SNL-NCP and other related materials under variable relative humidity

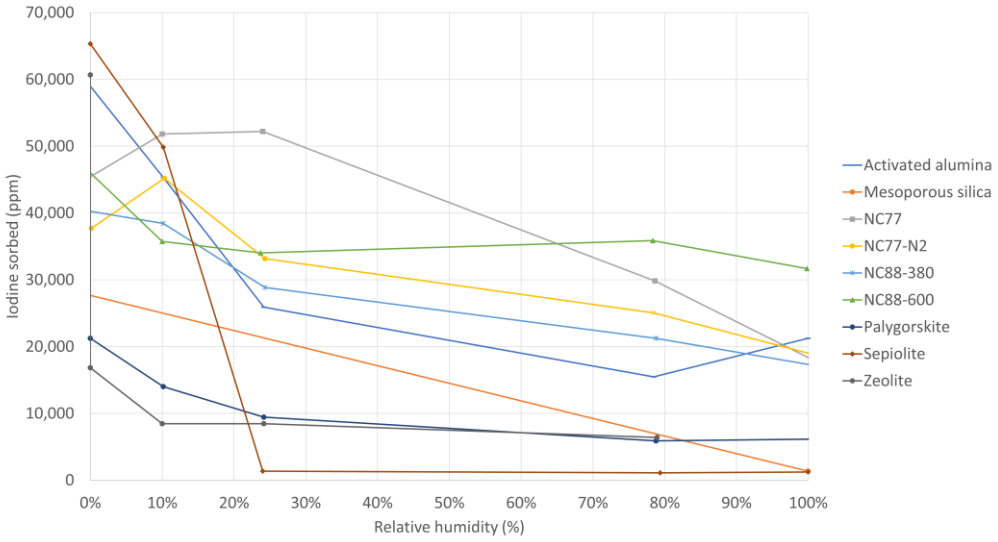

Source: [197].

5.4. Nanocomposites for iodine adsorption

In the field of adsorption, storage and confinement of volatile radioactive iodine, several processes to capture molecular iodine rely on the use of selective silver-based adsorbents, for example silver-exchange zeolite or silver nitrate adsorbed onto ceramic support. Most of these materials exhibit a low adsorption capacity due to the micron size of the iodine host structure: indeed, iodine penetrates only in the surface of the sorbent due to diffusion limitation. This drawback leads to the generation of a significant volume of radioactive wastes. In this context, the use of nanoparticles of sorbent able to entrap iodine, with increased surface to volume ratio of the sorbent, will increase the iodine extraction capacity. However, while nanoparticles are unsuitable for an industrial abatement process, nanocomposites are more promising. These consist of nanoparticles of iodine selective sorbent on a ceramic support, powder, beads or membrane. This support can also be shown to be a precursor of the containment matrix. These nanocomposites exhibit fast kinetics due to their high porosity, coming from the support, compared to, for example, zeolite-like materials; and high capacity coming from the nano size of the sorbent inserted into the support.

As an example, Hofmann's clathrate nanoparticles inserted onto silica-based support are an efficient material to entrap iodine from gaseous phases [198]. These co-ordination solid networks exhibit a general formula M'(L)[M''$(CN)_4$], where M'=Ni(II) or Co(II); L=pyrazine (pz), bipyridine or azopyridine; and M''=Ni(II), Pd(II) or Pt(II). As a first step of this study, different bulk Hofmann-type structures were evaluated [199]. It was shown that for $Ni^{II}(pz)[Ni^{II}(CN)_4]$, molecular iodine was inserted into the network cage of the structure with about one I_2 molecule per unit cell. This high capacity, about 3 mmol of I per gramme of solid, comes from the slight adaptation of the lattice structure. After the study of bulk materials, mesoporous silica-based support, pure silica (SBA15), then mesoporous glass beads were functionalised with nanoparticles of $Ni^{II}(pz)[Ni^{II}(CN)_4]$ [200]. The synthesis route was a classic step-by-step precipitation method, i.e. $Ni^{II}(pz)[Ni^{II}(CN)_4]$ nanoparticles were covalently anchored to the pores surface of the supports by an initial grafting of a diamido function followed by a step-by-step impregnation method with salt precursor of the Hofmann-type structure. Small spherical nanoparticles, 2-3 nm, into the porosity of the supports were observed and characterised. Entrapment tests showed that these functionalised materials had a high affinity to molecular iodine with a capacity of capture up to 1.7 mmol of iodine per gramme of support [201]. This capacity is, of course, lower than for bulk materials due the presence of silica phase, but the sorption capacity calculated by $mmol.g^{-1}$ of clathrate nanoparticles is higher than that corresponding to the bulk one. This nanocomposite is thus a promising material efficient for iodine capture.

5.5. Summary

While macro-scale porous materials, such as zeolites, are straightforward to use, there are some drawbacks to overcome. While mechanistic work might allow for these top-down type materials to be improved, a bottom-up design approach, using nanomaterials, may yield improved results. This can improve properties such as higher capacity, better material diffusion, selectivity and co-contaminant resistance. However, these materials will need to be demonstrated in industrial conditions, shown to be resistant to radiation damage, keep control of costs and have a well-defined route to a suitable waste form. For these materials to be used, they need to be moved up the TRL scale from small-scale laboratory experiments to larger scale demonstrations.

6. Summary and future perspective

This report brings together the life cycle story of key volatile species that are released in the reprocessing of UNF, from their generation to ultimate disposal. Only once that entire picture is understood can decisions be taken on the best methods for managing VFPs, which is a major challenge that has been the subject of a substantial body of research and technology development over the last few decades. The scope of this report, therefore, has been limited to providing an overview of the challenges caused by volatile fission products, the main abatement technologies used or investigated, and their consequent immobilisation into suitable waste forms. For more detailed information, the reader is directed towards the wider body of literature cited in the references.

While it is correct that most off-gases are released in the head-end section of a reprocessing plant, it is too simplistic to concentrate attention there, especially if aiming for a near-zero discharge process. For example, the speciation of iodine in the separations plant can cause additional challenges, especially if other areas of the reprocessing plant are less well protected with abatement systems than the dissolver. Therefore, consideration of volatile release from a whole system approach is key to VFP management.

It is not just abatement technology that can help manage the treatment of VFPs. Changing the process itself can potentially be useful. High-temperature pre-treatment provides not only a promising route to enabling tritium control, but also a method of releasing volatile and semi-volatile species prior to dissolution and dispersion throughout the rest of a reprocessing plant. However, complexity, cost and engineering challenges are not to be underestimated for this head-end process. These limitations need to be fully understood before committing to the inclusion of HTPT to an already expensive part of the facility, at least for a light water reactor reprocessing plant. For pyroprocessing, a head-end treatment step is almost a necessity, driven by the need to condition some fuel types prior to dissolution in the salt.

Chapter 5 presented nanomaterials as one of the ways to increase the control of volatiles. These materials can be synthesised with great control over their physical structure, leading to greater levels of selectivity. In addition, a move away from relying on liquid effluents to manage volatiles means that volatile species can be readily converted into final waste forms without the additional need to treat the effluent. Further to what was presented in Chapter 5, advances in on-plant monitoring coupled to the use of modelling and simulation, forming what is known as “digital twins”, will help future operators better manage their plant to minimise off-gas generation. It is also key to integrate the development of abatement and final waste form technologies to ultimately minimise the steps required to convert waste into a waste form ready for storage and disposal. Reducing the number of different plants or plant stages will reduce the footprint of a reprocessing site, which reduces the upfront capital expense. There are further broad ambitions for advanced fuel cycles that have been presented, which apply to the treatment of VFPs (Table 6.1).

Table 6.1. Volatile fission product requirements for advanced fuel cycles

Strategic objective	Fuel cycle requirement	Potential implications for reprocessing plant flowsheets
Process safety	– Safer processes	
Waste management and environmental impact	– Reduced impact of fuel cycle on GDF (geological disposal facility) footprint (radiotoxicity and heat loading) – Reduced waste generation and lower environmental impact	– Reduced number and volumes of aqueous waste streams – Target "near-zero" emissions – Capture of volatile species (H-3, C-14, Kr-85 and I-129) – New waste forms
Economic	– Reduced capital costs through smaller plant footprint – Greater flexibility of process	– Intensified processing – Fewer waste streams – Process light water reactor, MOX and fast reactor fuels – Feed variations (carbide, nitride and metal fuels as well as oxides) – Higher burnup – Short cooled fast reactor**,** very long cooled light water reactor fuels – depends on scenario

Source: Selected from Table 1 in [202].

This report has focused on technologies, but it is impossible to separate the implementation of a technology from the regulations which govern aerial discharges. National approaches to environmental regulation differ, but often are based on applying the BAT[1] and ALARA[2] principles to guide decision-making on whether to abate a radionuclide and to what level. To further guide new plant development, regulatory bodies may state a maximum dose to the critical group (e.g. 150 µSv/y) as is the approach in the United Kingdom. Furthermore, there is a preference for concentrate and contain over dilute and disperse, coupled with a requirement for a continuous reduction in discharges [203]. In contrast, in the United States, the regulatory environment is specific for some species, such as I-129 and Kr-85 [204]. However, looking at current regulations gives a picture of the world today, rather than what may actually apply to an advanced reprocessing system of the future. It is therefore not certain what the environmental standards will be and consequently the levels of performance that new or emerging technologies will have to meet.

Looking back on the history of nuclear programmes for perspective, what was once good practice at the time of a plant's design can be quickly eclipsed by improving environmental standards. The impact of changes over time has meant that there are examples of reprocessing plants that were retrofitted with abatement systems to reduce discharges to

[1] BAT is a term defined in the OSPAR Convention and European Council Directive 96/61/EC on Integrated Pollution Prevention and Control (IPPC).

[2] ALARA is a principle to minimise safety risks to operators and to the general public as much as possible. It is not as simple as a cost-benefit analysis, as the safety improvement under consideration is weighted to be favourable compared to other factors such as cost.

meet those increasing standards. The Enhanced Actinide Removal Plant was one such plant, built to treat effluent to remove long-lived actinides. Considering Pu-239/240, this led to approximately a fourfold reduction in discharge despite an increase in reprocessing activity [205]. In hindsight, any additional plant added to a process after design of the reprocessing plant is suboptimal. Efficiencies are lost relative to considering incorporating those abatement facilities during the original design and build. Therefore, when developing new technologies today, the focus should be on providing options for the abatement of volatile and semi-volatile species to meet a wider variety of future scenarios, e.g. from a business-as-usual scenario to a "net zero" emissions scenario. The challenging ambition of aiming for net zero, as articulated by the NEA, helps to guide researchers towards developing technologies of the future [206].

Finally, the treatment of volatile fission products should be considered in the context of the wider reprocessing plant and associated waste treatment. The better this can be modelled and understood prior to design, the more optimised the facility can be to deliver reduced costs and reduced discharges relative to the plants of today. By developing improved technologies for the treatment of VFPs that reduce environmental impacts and waste generation, credible options for spent fuel recycling in future closed fuel cycles are enhanced. Such abatement technologies support both aqueous reprocessing and pyrochemical processing of spent fuels for either generation III+ thermal reactors or the deployment of generation IV reactors and their associated fuel cycles.

7. References

[1] Hebel, W. and G. Cottone (1981), "Management modes for Iodine-129", Harwood Academic Publishers for the Commission of the European Communities, New York, NY.

[2] Hebel, W. and G. Cottone (1982), "Methods of Krypton-85 management", Harwood Academic Publishers for the Commission of the European Communities, New York, NY.

[3] IAEA (2004), "Management of waste containing tritium and Carbon-14", *IAEA Technical Report Series*, No. 421, International Atomic Energy Agency, Vienna.

[4] Jubin, R.T., D.M. Strachan, G. IIas, B.B. Spencer and N.R. Soelberg (2014), "Radioactive semivolatiles in nuclear fuel reprocessing", INL-EXT-14-33122, Idaho National Lab., Idaho Falls, ID.

[5] IAEA (2014), "Treatment of radioactive gaseous waste," IAEA-TECDOC-1744, International Atomic Energy Agency, Vienna.

[6] Jubin, R.T., N.R. Soelberg, D.M. Strachan and G. IIas (2012), "Fuel age impacts on gaseous fission product capture during separations", US Department of Energy.

[7] Soelberg, N.R., T.G. Garn, M.R. Greenhalgh, J.D. Law, R. Jubin, D.M. Strachan and P.K. Thallapally (2013), "Radioactive iodine and krypton control for nuclear fuel reprocessing facilities", *Science and Technology of Nuclear Installations, Special Issue: Nuclear Fuel Reprocessing Technologies and Commercialization*, https://doi.org/10.1155/2013/702496.

[8] DEFRA (2002), "UK Strategy for Radioactive Discharges 2001-2020", Department for Environment, Food and Rural Affairs, London.

[9] Spencer, B.B., G.D. Del Cul, E.C. Bradley, R.T. Jubin, T.D. Hylton, and E.D. Collins (2008), "Design, fabrication, and testing of a laboratory-scale voloxidation system for removal of tritium and other volatile fission products from used nuclear fuel", American Nuclear Society 2008 Annual Meeting, Anaheim, California, 8-12 June.

[10] KAERI (2007), "Hot experiment on fission gas release behaviour from voloxidation process using spent fuel", Korea Atomic Energy Research Institute.

[11] Kim, W.K., S.S. Kim and G.I. Park (2004), "Experiment on the improvement of OREOX process for fabrication of dry recycling nuclear fuel pellets", Korea Atomic Energy Research Institute.

[12] Ko, W.I., H. Kim and M.S. Yang (2004), "Advantages of irradiated DUPIC fuels from the perspective of environmental impact", *Nuclear Technology*, Vol. 138/2.

[13] KAERI (2008), "Evaluation of the effects of advanced voloxidation process on pyroprocessing. 1. Radiation and decay heat analysis of the advanced voloxidation process", Korea Atomic Energy Research Institute.

[14] NEA (2012), "Spent nuclear fuel reprocessing flowsheet", OECD Publishing, Paris.

[15] Collins, E.D., G.D. Del Cul, R.D. Hunt, J.A. Johnson and B.B. Spencer, B (2013), *Advanced Dry Head-End Reprocessing of Light Water Reactor Spent Nuclear Fuel*, US 8,574,523 B2.

[16] Del Cul, G.D., B.B. Spencer, R.D. Hunt, R.T. Jubin and E.D. Collins (2012), "Advanced head-end for the treatment of used LWR fuel", in *Actinide and Fission Product Partitioning and Transmutation: Eleventh Information Exchange Meeting, San Francisco, California, 1-4 November 2010*, Nuclear Energy Agency, OECD Publishing, Paris, www.oecd-nea.org/jcms/pl_14696/actinide-and-fission-product-partitioning-and-transmutation

[17] Grimes, W.R., D.C. Hampson, D.J. Larkin, J.O. Skolrud and R.W. Benjamin (1982), "An evaluation of retention and disposal options for tritium in fuel reprocessing", ORNL/TM-8261, Oak Ridge National Laboratory, Oak Ridge, TN.

[18] Spencer, B.B. (1982), "Voloxidation", in: *Annual Information Meeting of the Fuel Recycle Division*, Oak Ridge National Laboratory, Oak Ridge, TN, 22-23 June.

[19] Bruffey, S.H., B.B. Spencer, D.M. Strachan, R.T. Jubin, N. Soelberg and B.J. Riley (2015), *A Literature Survey to Identify Potentially Problematic Volatile Iodine-bearing Species Present in Off-gas Streams*, US Department of Energy, Oak Ridge, TN, https://doi.org/10.2172/1235202.

[20] Jonke, A.A. (1965), "Reprocessing of nuclear reactor fuels by processes based on volatilization, fractional distillation, and selective desorption", *Atomic Energy Review*, Vol. 3/3, International Atomic Energy Agency, Vienna.

[21] Schmets, J.J. (1970), *Atomic Energy Review*, Vol. 8/3, International Atomic Energy Agency, Vienna.

[22] Uhlíř, J., M. Mareček, J. Škarohlíd, F. Lisy and R. Bican (2011), "Development of FBR fuel reprocessing by fluoride volatility method", *Proceedings of ICAPP 2011*, Nice, France.

[23] Shatalov, V.V., M.B. Seregin, V.F. Kharin and L.A. Ponomarev (2001), "Gas-fluoride technology for processing spent oxide fuel", *Atomic Energy*, Vol. 90, pp. 224-234, https://doi.org/10.1023/A:1011376412282.

[24] Rosenthal, M.W., P.N. Haubenreich, H.E. McCoy and L.E. McNeese (1971), "Recent progress in molten-salt reactor development", *Atomic Energy Review*, Vol. 9/601.

[25] Novikov, V.M., V.V. Ignatiev, V.I. Fedulov and V.N. Cherednikov (1990), "Molten salt nuclear energy systems: Perspectives and problems", Energoatomizdat, Moscow.

[26] Yu. P. Korchagin (1981), "The kinetic study of uranium removal from molten fluorides by gas phase fluorination technique", *Collection Book "Uranium Chemistry"*, Nauka, Moscow, pp. 360-363 (in Russian).

[27] Haubenreich, P.N. and J.R. Engel (1970), "Experience with the molten-salt reactor experiment", *Nuclear Applications & Technology*, Vol. 8, pp. 118-136.

[28] Sakamura, Y., M. Iizuka and T. Inoue (2009), "Development of oxide reduction process to bridge oxide fuel cycle and metal fuel cycle", *Proceedings of GLOBAL 2009*, Paris.

[29] Koyama, T., M. Iizuka, Y. Shoji, R. Fujita, H. Tanaka, T. Kobayashi and M. Tokiwai (1997), "An experimental study of molten salt electrorefining of uranium using solid iron cathode and liquid cadmium cathode for development of pyrometallurgical reprocessing", *Journal of Nuclear Science and Technology*, Vol. 44, pp. 384-393.

[30] Uozumi, K., M. Iizuka, T. Kato, T. Inoue, O. Shirai, T. Iwai and Y. Arai (2004), "Electrochemical behaviours of uranium and plutonium at simultaneous recoveries into liquid cadmium cathodes", *Journal of Nuclear Materials*, Vol. 325, pp. 34-43.

[31] Murakami, T., A. Rodrigues, M. Iizuka, L. Aldave de las Heras and J.-P. Glatz (2018), "Electrorefining of metallic fuel with burn-up of ~7 at% in a LiCl-KCl melt", *Journal of Nuclear Science and Technology*, Vol. 55, pp. 1 291-1 298.

[32] Sakamura, Y., T. Inoue, T.S. Storvick and L.F. Grantham (1995), "Development of pyropartitioning process: Separation of transuranium elements from rare earth elements in molten chlorides solution: Electrorefining experiments and estimation by using the thermodynamic properties", *Proceedings of GLOBAL '95*, Versailles, France.

[33] Sakamura, Y., T. Hijikata, K. Kinoshita, T. Inoue, T.S. Storvick, C.L. Krueger, J.J. Roy, D.L. Grimmett, S.P. Fusselman and R.L. Gay (1998), "Measurement of standard potential of actinides

(U, Np, Pu, Am) in LiCl-KCl eutectic salt and separation of actinides from rare earths by electrorefining", *Journal of Alloys and Compounds*, Vol. 592, pp. 271-273.

[34] Sakamura, Y., O. Shirai, T. Iwai and Y. Suzuki (2001), "Distribution behaviour of plutonium and americium in LiCl-KCl eutectic/liquid cadmium systems", *Journal of Alloys and Compounds*, Vol. 321, pp. 76-83.

[35] Hayashi, H., M. Takano, H. Otobe and T. Koyama (2013), "Syntheses and thermal analyses of curium trichloride", *Journal of Radioanalytical and Nuclear Chemistry*, Vol. 297, pp. 139-144.

[36] Johnson, I., M.G. Chasanov and R.M. Yonco (1965), "Pu-Cd system: Thermodynamics and partial phase diagram", *Transactions of the Metallurgical Society AIME*, Vol. 233, 1408.

[37] Iizuka, M., K. Kinoshita, Y. Sakamura, T. Ogata and T. Koyama (2013), "Performance of pyroprocess equipment of semi-industrial design and material balance in repeated engineering-scale fuel cycle tests using simulated oxide/metal fuels", *Nuclear Technology*, Vol. 184, pp. 107-120.

[38] Westphal, B.R., J.C. Price, D. Vaden and R.W. Benedict (2007), "Engineering-scale distillation of cadmium for actinide recovery", *Journal of Alloys and Compounds*, Vols. 444-445, pp. 561-564.

[39] Nakamura, K., T. Ogata. T. Kato, K. Nakajima and Y. Arai (2009), "Fabrication of metal fuel slug for an irradiation test in JOYO", *Proceedings of GLOBAL 2009*, paper 9 163, Paris.

[40] Iizuka, M., M. Akagi and T. Omori (2013), "Development of treatment process for anode residue from molten salt electrorefining of spent metallic fast reactor fuel", *Nuclear Technology*, Vol. 181, pp. 507-525.

[41] Kinoshita, K. and T. Tsukada (2008), "Counter-current test in LiCl-KCl and liquid Cd system for pyropartitioning and pyro-reprocessing", *Proceedings of the 10th OECD/NEA Information Exchange Meeting on Actinides and Fission Product Partitioning and Transmutation*, Mito, Japan, OECD Publishing, Paris, www.oecd-nea.org/science/reports/2010/nea6420-actinide10th.html.

[42] Uozumi, K., T. Hijikata, T. Tsukada, T. Koyama, T. Terai and A. Suzuki (2014), "Measurement of molten chloride salt flow and demonstration of simulated fission product removal using a zeolite column apparatus for spent salt treatment in pyroprocessing", *Nuclear Technology*, Vol. 188, pp. 83-96.

[43] Koyama, T., C. Matsubara and T. Sawa (1997), "Waste form development for immobilization of radioactive halide salt generated from pyrometallurgical reprocessing", *Proceedings of GLOBAL'97*, Yokohama, Japan.

[44] Koyama, T. and M. Iizuka (2015), "Pyrochemical fuel cycle technologies for processing of spent nuclear fuels: Developments in Japan", Chapter 18 in: Taylor, R. (ed.), *Reprocessing and Recycling of Spent Nuclear Fuel*, Woodhead Publishing Series in Energy: No. 79, Woodhead Publishing, London.

[45] Westphal, B.R., K.J. Bateman, C.D. Morgan, J.F. Berg, P.J. Crane, D.G. Cummings, J.J. Giglio, M.W. Huntley, R.P. Lind and D.A. Sell (2008), "Effect of process variables during the head-end treatment of spent oxide fuel", *Nuclear Technology*, Vol. 162, pp. 153-157.

[46] Park, J.J., J.M. Shin, C.J. Park, J.W. Lee, G.I. Park, K.C. Song and J.I. Chun (2008), "Radioactivity analysis of the advanced voloxidation process", International Pyroprocessing Research Conference (IPRC) 2008, Jeju Island, Korea.

[47] Lee, J.W., W.K. Kim, J.W. Lee, G.I. Park, M.S. Yang and K.C. Song (2007), "Remote fabrication of DUPIC fuel pellets in a hot cell under quality assurance program", *Journal of Nuclear Science and Technology*, Vol. 44, pp. 597-606.

[48] Westphal, B.R., R.D. Mariani, D. Vaden, S.R. Sherman. S.X. Li and D.D. Keiser (2000), "Recent advances during the treatment of spent EBR-II fuel", *Proceedings of the Embedded Topical Meeting on DOE Spent Nuclear Fuel and Fissile Material Management*, San Diego, CA.

[49] Igarashi, H., K. Kato and T. Takahashi (1992), "Effect of temperature on the entrainment of ruthenium, technetium and selenium in continuous calcination of simulated high-level liquid waste", *Journal of Nuclear Science and Technology*, Vol. 29, pp. 576-581.

[50] Langowski, M.H., J.G. Darab and P.A. Smith (1996), "Volatility literature of chlorine, iodine, caesium, strontium, technetium, and rhenium: Technetium and rhenium volatility testing", PNNL-11052, Pacific Northwest National Laboratory, Richland, WA.

[51] German, K.E. and V.F. Peretrukhin (1995), "Study of the sublimation and vaporization of alkali metal pertechnetats, $MTcO_4$ (M = K, Cs)", Institute of Physical Chemistry, Russian Academy of Sciences, Moscow.

[52] CRC (1997), *Handbook of Chemistry and Physics, 77th Edition*, CRCPress.

[53] Fletcher, J.M., P.L. Jenkins, F.S. Martin, A.R. Powell and R. Todd (1955), "Nitrato and nitro complexes of nitrosylruthenium", *Journal of Inorganic Chemistry*, Vol. 1, p. 378.

[54] IAEA (1982), "Control of semivolatile radionuclides in gaseous effluents at nuclear facilities", Technical Reports Series No. 220, International Atomic Energy Agency, Vienna.

[55] Sakai, A., H. Koikegami, S. Weisenburger, G. Roth, N. Kanehira and S. Komamine (2017), "Comparison of advanced melting process for HLW vitrification, Joule-heated ceramic-lined melter (JHCM) and cold-crucible induction melter (CCIM)", presented at the 25th International Conference on Nuclear Engineering, Volume 7: Fuel Cycle, Decontamination and Decommissioning, Radiation Protection, Shielding, and Waste Management: Mitigation Strategies for Beyond Design Basis Events, Shanghai, China.

[56] Weisenburger, S. (1979), "Non-radioactive operation experience with a Joule heated ceramic melter for vitrification of high-level liquid waste", in: McCarthy, G.J. [Hrsg.], *Scientific Basis for Nuclear Waste Management*, Springer, Boston, MA, https://doi.org/10.1007/978-1-4615-9107-8_6.

[57] Weisenburger, S., W. Gruenewald and H. Koschorke (1979), "Vitrification of high-level radioactive waste in a continuous liquid-fed ceramic melter", in: *Ceramics in Nuclear Waste Management*, Proceedings of an International Symposium held in Cincinnati, OH, pp. 86-92.

[58] DWK (1981), "PAMELA, eine Anlage für radioaktiven Abfall", *Physikalische Blätter*, Vol. 37, p. 375.

[59] Baumgärtner, F., R. v. Ammon, E. Henrich, E. Hutter, G. Koch and W. Weinländer (1978), "Stand der Technik bei der Behandlung des Auflöserabgases einer Wiederaufarbeitungsanlage und Wege der Verfahrensoptimierung", presented at the Sammlung der Vorträge anläßlich des 2. Statusberichtes des Projektes Wiederaufbereitung und Abfallbehandlung, Karlsruhe.

[60] IAEA (1988), "Design and operation of off-gas cleaning systems at high level liquid waste conditioning facilities", *Technical Reports Series*, No. 291, International Atomic Energy Agency, Vienna.

[61] Heimerl, W. (1979), "Solidification of HLW solutions with the PAMELA process", presented at the International Symposium on Ceramics in Nuclear Waste Management, Cincinnati, OH.

[62] Eitz, A.W., H. Ramdohr and W. Schüller (1970), "Die Wiederaufarbeitungsanlage Karlsruhe: Zielsetzung und Einführung in die Konzeption der Anlage", *Atomwirtschaft*, Vol. 15, pp. 74-76.

[63] Grünewald, W., G. Roth, W. Tobi, and K. Weiss (2000), "Cold demonstration of the VEK vitrification technology in a full-scale mock-up facility", presented at the WM2000 Conference, Tucson, AZ.

[64] Fleisch, J., W. Grünewald, G. Roth, F.J. Schmitz, W. Tobie and M. Weishaupt (2011), "Successful hot operation of the German vitrification plant VEK: Results and experiences", presented at the WM2011 Conference, Phoenix, AZ.

[65] Roth, G., S. Weisenburger, J. Fleisch and M. Weishaupt (2005), "Process technique and safety features of the German VEK vitrification plant currently under commissioning", in: *Proceedings of GLOBAL 2005*, Tsukuba, Japan.

[66] Fleisch, J., H. Kuttruf, W. Lumpp and S. Weisenburger (2000), "Vitrification facility Karlsruhe (VEK) – Steps from planning to realization", presented at the WM2000 Conference, Tucson, AZ.

[67] Lausch, J., F.-J. Schmitz and M. Weishaupt (2010), "Safeguarding a vitrification facility at the dismantled WAK pilot reprocessing plant", in: *Symposium on International Safeguards: Preparing for Future Verification Challenges*, Vienna.

[68] Grünewald, W., G. Roth, W. Tobie, J. Fleisch, F.J. Schmitz and M. Weishaupt (2012), "Hot operation performance of the German vitrification plant VEK", presented at the GLOBAL 2011: Toward and Over the Fukushima Daiichi Accident, Makuhari Messe, Chiba, Japan.

[69] Stumpf, T. and H. Geckeis (eds.) (2011), *Annual Report 2010: Institute for Nuclear Waste Disposal*, KIT Scientific Reports, No. 7600, KIT Scientific Publishing, Karlshure, Germany, https://publikationen.bibliothek.kit.edu/1000024303.

[70] Gruber, P., E. Tronche, A. Ledoux, V. Labe, J.-F. Hollebecque, J. Lacombe, C. Ladirat and S. Naline (2011), "Limited increase of particle entrainment in the off-gas system of a cold crucible induction melter compared with a Joule-heated metal melter for HLLW vitrification – 11465", WM2011 Conference, Phoenix, AZ.

[71] Harrison, M.T. (2014), "Vitrification of high level waste in the UK", *Procedia Materials Science*, No. 7.

[72] Bradshaw, K. and N. Gribble (2007), "UK full-scale non-active vitrification development and implementation of research findings onto the waste vitrification plant", WM2007 Conference, Tucson, AZ.

[73] Short, R. (2014), "Phase separation and crystallisation in UK HLW vitrified products", *Procedia Materials Science*, No. 7.

[74] Paterson, H.C., M. Cowley and C.J. Steele (2015), "$CsTcO_4$ blockages in waste vitrification and the use of rhenium as a non-radioactive surrogate", *Chemistry in Energy Conference*, Edinburgh.

[75] Uozumi, K., K. Fujihata and T. Tsukada (2018), "Parameter surveys on glass-bonded sodalite synthesis conditions from spent salt generated in pyroprocess", *Nuclear Technology*, Vol. 203, pp. 261-271.

[76] Battisti, T.J., K.M. Goff, K.J. Bateman, M.F. Simpson and J.P. Lind (2002), "Ceramic waste form production and development at ANL-West", *Proceedings of the 5th Topical Meeting, DOE Spent Nuclear Fuel and Fissile Materials Management*, Charleston, SC.

[77] Bateman, K.J. and D.D. Capson (2004), "A finite difference model used to predict the consolidation of a ceramic waste form produced from the electrometallurgical treatment of spent nuclear fuel", ANL-NT-209.

[78] Koyama, T. and M. Iizuka (2015), "Pyrochemical fuel cycle technologies for processing of spent nuclear fuels: Developments in Japan", Chapter 18 in: Taylor, R. (ed.), *Reprocessing and Recycling of Spent Nuclear Fuel*, Woodhead Publishing Series in Energy: No. 79, Woodhead Publishing, London.

[79] Jubin, R.T., D.M. Strachan and N.R. Soelberg (2013), "Iodine pathways and off-gas stream characteristics for aqueous reprocessing plants: A literature survey and assessment", FCRD-SWF-2013-000308, Oak Ridge National Laboratory, Oak Ridge, TN.

[80] Geniesse, D.J. and G.E. Stegen (2009), *2009 Evaluation of Tritium Removal and Mitigation Technologies for Wastewater Treatment*, United States Department of Energy, Richland, WA.

[81] Oak Ridge National Laboratory and Bechtel National Inc. (1978), "Hot experimental facility interim design report", ORNL/AFRP-78/6, Vol. III, Union Carbide Corp., Oak Ridge National Laboratory, Oak Ridge, TN.

[82] McKay, H.A.C. (1979), "Tritium immobilization", *European Applied Research Reports, Nuclear Science*, Vol 1, pp. 599-711.

[83] Benedict, M., T. Pigford and H. Levi (1981), *Nuclear Chemical Engineering*, 2nd ed., McGraw-Hill, New York, NY.

[84] Uchiyama, G., M. Kitamura, K. Yamazaki, S. Sugikawa, M. Maeda and T. Tsujino (1991), *Development of Voloxidation Process for Tritium Control in Reprocessing*, JAERI-M91-199, Japan Atomic Energy Research Institute, https://jopss.jaea.go.jp/pdfdata/JAERI-M-91-199.pdf.

[85] Jung, In-ha, Joung-Ick Chun, Jin-Myung Shin and Jang-Jin Park (2007), "Trapping of tritium in off-gas dry-processes", *Transactions of the Korean Nuclear Society Spring Meeting*, Jeju, Korea.

[86] University of Rochester (2005), "Technologies for mitigating tritium releases to the environment", *LLE Review*, Vol. 103, www.lle.rochester.edu/media/publications/lle_review/documents/v103/103_05Technol.pdf.

[87] Holland, W.D. (1979), "Drying of iodine-containing air using linde type 3A molecular sieves", ORNL/TM-7045, Union Carbide Corp., Oak Ridge National Laboratory, Oak Ridge, TN.

[88] Rivera, D.A., M.K. Alam, L. Martin and J.R. Brown (2003), "Characterization of water and CO_2 adsorption by stores 3A desiccant samples using thermal gravimetric analysis and fourier transform infrared spectroscopy", SAND2003-0398, Sandia National Laboratories, Albuquerque, NM.

[89] Spencer, B.B., S.H. Bruffey, J.F. Walker, K.K. Anderson and R.T. Jubin (2013), "Iodine and water co-adsorption and desorption on deep beds of 3A-molecular sieve and silver mordenite", FCRD-SWF-2013-000329, Oak Ridge National Laboratory, Oak Ridge, TN.

[90] US Atomic Energy Commission (1972), "An evaluation of the molten salt breeder reactor", WASH-1222 report, Federal Council on Science and Technology Goals R&D Study.

[91] Herrmann, F.J., V. Motoi, B. Herrmann, D. Fang, L. Finsterwalder and K.D. Kuhn (1993), A. van Schoor, Ch. Beyer, "Minimizing of iodine-129 release at the Karlsruhe reprocessing plant WAK", *Proceedings of the 22nd DOE/NRC Nuclear Air Cleaning Conference*, Vol. 1, CONF-9020823, pp. 75-90.

[92] Herrmann, F.J., B. Herrmann and K.D. Kuhn (1997), "Control of radio-iodine at the German reprocessing plant WAK during operation and after shutdown", *Proceedings of the 24th DOE/NRC Nuclear Air Cleaning and Treatment Conference*, CONF-960715, pp. 618-627.

[93] Herrmann, F.J., V. Motoi, B. Herrmann and A. van Schoor (1991), "Retention and measurement of iodine-129 and of organoiodine in the off-gas streams of the Karlsruhe reprocessing plant WAK", *Proceedings of the 21st DOE/NRC Nuclear Air Cleaning Conference*, Vol. 1, CONF-900813, pp. 222-233.

[94] Furrer, J., R. Kaempffer, A. Linek and K. Jannakos (1993), "Iodine stripping from nitric acid solutions in IATEMA", *Proceedings of the 22nd DOE/NRC Nuclear Air Cleaning Conference*, Vol. 1, CONF-9020823, pp. 91-99.

[95] Sakurai, T., K. Komatsu and A. Takahashi (1997), "Behavior of iodine in the dissolution of spent nuclear fuels", *Proceedings of the 24th DOE/NRC Nuclear Air Cleaning and Treatment Conference*, Portland, OR.

[96] IAEA (1987), "Treatment, conditioning and disposal of iodine-129", *IAEA Technical Report Series*, No. 276, International Atomic Energy Agency, Vienna.

[97] Goossen, W.R.A., G.G. Eichholz and D.W. Tedder (1991), "Treatment of gaseous effluents at nuclear facilities", *Radioactive Waste Management Handbook Volume 2*, Harwood Academic Publishers, Chur.

[98] Sakurai, T., A. Takahashi and N. Ishikawa (1994), "A study on the expulsion of iodine from spent-fuel solutions", *Proceedings of the 23rd DOE/NRC Nuclear Air Cleaning and Treatment Conference*, CONF-940738, pp. 321-332.

[99] Jubin, R.T. (1988), "Airborne waste management technology applicable for use in reprocessing plants for control of iodine and other off-gas constituents", ORNL/TM-10477, Oak Ridge National Laboratory, Oak Ridge, TN.

[100] Thomas, T.R., B.A. Staples, L.P. Murphy and J.T. Nichols (1977), "Airborne elemental iodine loading capacities of metal zeolites and a method for recycling silver zeolite", ICP-1119.

[101] Staples, B.A., L.P. Murphy and T.R. Thomas (1976), "Airborne elemental iodine loading capacities of metal zeolites and a dry method for recycling silver zeolite", *Proceedings of 14th ERDA Air Cleaning Conference*, Vol. 1, CONF-760822, p. 363.

[102] Thomas, T.R., B.A. Staples and L.P. Murphy (1978), "The development of Ag^0Z for bulk 129I removal from nuclear fuel reprocessing plants and PbX for 129I storage", *Proceedings of the 15th DOE Nuclear Air Cleaning Conference*, Vol. 1, CONF-780819, p. 394.

[103] Jubin, R.T. (1983), "Organic iodine removal from simulated dissolver off-gas systems using partially exchanged silver mordenite", *Proceedings of the 17th DOE Nuclear Air Cleaning Conference*, CONF-820833, pp. 183-197.

[104] Scheele, R.D., L.L. Burger and C.L. Matsuzaki (1983), "Methyl iodide sorption by reduced silver mordenite", PNL-4489, United States Department of Energy.

[105] Furrer, J., J.G. Wilhelm and K. Jannakos (1978), "Aerosol and iodine removal system for the dissolver off-gas in a large fuel reprocessing plant", *Proceedings of the 15th DOE Nuclear Air Cleaning Conference*, Vol. 1, CONF-780819, p. 494.

[106] Wilhelm, J.G. and J. Furrer (1976), "Head-end iodine removal from a reprocessing plant with a solid sorbent", *Proceedings of the 14th ERDA Air Cleaning Conference*, CONF-760822, p. 447.

[107] Herrmann, F.J., V. Motoi, H. Fies, B. Stojanik, J. Furrer and R. Kaempffer (1989), "Testing an iodine filter for the vessel off-gas of the German industrial-scale reprocessing plant", *Proceedings of the 20th DOE/NRC Nuclear Air Cleaning Conference*, Vol. 1, CONF-880822, pp. 234-245.

[108] Soelberg, N.R. and T.L. Watson (2014), "Phase 2 methyl iodide deep-bed adsorption tests", FCRD-SWF-2014-000273, Idaho National Laboratory, Idaho Falls, ID.

[109] Jubin, R.T. and D. Strachan (2015), *Assessments and Options for Removal and Immobilization of Volatile Radionuclides from the Processing of Used Nuclear Fuel*, Oak Ridge National Laboratory, Oak Ridge, TN.

[110] Choi, B.S., G. Il Park, J.H. Kim, J.W. Lee and S.K. Ryu (2001) "Adsorption equilibrium and dynamics of methyl iodide in a silver ion-exchanged zeolite column at high temperatures", *Adsorption*, Vol. 7/2, pp. 91-103.

[111] Haefner, D.R. and T.J. Tranter (2007), "Methods of gas phase capture of iodine from fuel reprocessing off-gas: A literature survey", INL/EXT-07-12299, Idaho National Laboratory, Idaho Falls, ID.

[112] Goossen, W.R.A., G.G. Eichholz and D.W. Tedder (eds.) (1991), "Treatment of gaseous effluents at nuclear facilities", *Radioactive Waste Management Handbook*, Vol. 2, Harwood Academic Publishers, Chur.

[113] Taylor, P. (1990), "A review of methods for immobilizing iodine-129 arising from a nuclear fuel cycle plant, with emphasis on waste-form chemistry", AECL-10163, Atomic Energy of Canada Limited, https://inis.iaea.org/collection/NCLCollectionStore/_Public/23/002/23002552.pdf.

[114] Yang, J.H., Y.J. Cho, J.M. Shin and M.S. Yim (2015), "Bismuth-embedded SBA-15 mesoporous silica for radioactive iodine capture and stable storage", *Journal of Nuclear Materials*, Vol. 465, pp. 556-564, https://doi.org/10.1016/j.jnucmat.2015.06.043.

[115] Willis, W., C. Phillips, R. Carter, S. Baker, W. Bowen and M. Grygiel (2013), "Task order 9: Improving the estimates of waste from recycling", Task 5 – Final Report, Energy Solutions.

[116] AREVA Federal Services LLC (2013), Task Order 9: Improving the estimates of waste from recycling, sub-task 5: Final technical report, RPT-3007827-000, AREVA Federal Services LLC.

[117] Vienna, J.D. et al. (2015), *Closed Fuel Cycle Waste Treatment Strategy*, FCRD-MRWFD-2015-000674, Pacific Northwest National Laboratory, Richland, WA.

[118] Bray, G.R., C.L. Miller, T.D. Nguyen and J.W. Rieke (1977), *Assessment of Carbon-14 Control Technology and Costs for the LWR Fuel Cycle*, EPA 520/4-77-013, United States Environmental Protection Agency, Office of Radiation Programs, https://nepis.epa.gov/Exe/ZyPDF.cgi?Dockey=9100BW8L.PDF.

[119] Holladay, D.W. (1978), "Experiments with a lime slurry in a stirred tank for the fixation of carbon-14 contaminated CO_2 from simulated HTGR fuel reprocessing off-gas", ORNL/TM-5757, Oak Ridge National Laboratory, Oak Ridge, TN.

[120] Hudson, P.I.C., P. Buckley and W.W. Miller (1994), "The development and design of the off-gas treatment system for the thermal oxide reprocessing plant (THORP) at Sellafield", *Proceedings of the 23rd DOE/NRC Nuclear Air Cleaning and Treatment Conference*, CONF-940738, p. 333.

[121] Brown, R.A., J.D. Christian and T.R. Thomas (1983), *Airborne Radionuclide Waste Management Reference Document*, ENICO-1133, Exxon Nuclear Idaho Company, Idaho Falls, ID.

[122] US DOE (1979), *Technology for Commercial Radioactive Waste Management*, DOE/ET-0028, United States Department of Energy, Washington, DC.

[123] IAEA (1980), "Separation, storage and disposal of krypton-85", *Technical Report Series*, No. 199, International Atomic Energy Agency, Vienna.

[124] Hayashi, S., H. Shoji, T. Kurihara, N. Kawashima, T. Osawa, H. Yamato and T. Aizawa (2002), "Development of krypton recovery and storage technology", *JNC Technical Review*, No. 17, p. 43 (in Japanese).

[125] Samoto, H., N. Kimura, T. Ohtani, E. Sugai and S. Hayashi (2009), "Study on immobilization technology of radioactive krypton gas by ion implantation and sputtering process", *Proceedings of GLOBAL 2009*.

[126] Whitmell, D.S. (1987), *Immobilization of Krypton in a Metal Matrix*, EUR 11253, European Communities.

[127] Tomiku, Y., K. Okimoto, H. Shoji and S. Hayashi (2002), "Development of refining technology of Xe tecovered from reprocessing plant off gas for commercial use", *JNC Technical Review*, No. 15, p. 113 (in Japanese).

[128] Hayashi, S., S. Kamiya, S. Ikeda and Y. Nakanishi (1997), "Study on immobilization technology of krypton gas by ion implantation and sputtering process", *Proceedings of GLOBAL '97*.

[129] Hayashi, S., S. Kamiya, H. Nakamichi, S. Ikeda and Y. Nakanishi (1997), "Development of immobilization technology for krypton gas by ion implantation and sputtering process", *PNC Technical Review*, No. 101, p. 103 (in Japanese).

[130] Sano, Y., E. Seki, Y. Kobayashi, S. Nakahigashi, S. Hayashi and Y. Nakanishi (1991), "Rare gas storage using ion sputtering and implantation process", *Proceedings of the 14th Symposium on Ion Sources and Ion-Assisted Technology*, Tokyo.

[131] Bendixsen, C.L. and G.L. Offutt (1969), "Rare gas recovery facility at the Idaho Chemical Processing Plant", IN-1221, presented at the ANS Meeting 30 November-4 December, San Francisco, CA.

[132] Bendixsen, C.L. and F.O. German (1975), *1974 Operation of the ICPP Rare Gas Recovery Facility*, ICP-1157, United States Energy Research and Development Administration, Idaho Falls, ID.

[133] Trevorrow, L.E., G.F. Vandergrift, V.M. Kolba and M.J. Steindler (1993), *Compatibility of Technologies with Regulations in the Waste Management of H-3, I-129, C-14, and Kr-85. Part I. Initial Information Base*, ANL-83-57, Argonne National Laboratory, Argonne, IL.

[134] Pence, D.T. (1981), "Critical review of noble gas recovery and treatment systems", *Nuclear Safety*, Vol. 22/6.

[135] Monson, P.R. (1981), "Krypton retention on solid adsorbents", 16th DOE Nuclear Air Cleaning Conference, San Diego, CA, pp. 1 387-1 400.

[136] Munakata, K., S. Kanjo, S. Yamatsuki, A. Koga and D. Ianovski (2003), "Adsorption of noble gases on silver-mordenite", *Journal of Nuclear Science and Technology*, Vol. 40/9, pp. 695-697.

[137] Greenhalgh, M.R., T.G. Garn and J.D. Law (2014), "Development of a hydrogen mordenite sorbent for the capture of krypton from used nuclear fuel reprocessing off-gas streams", *Journal of Nuclear Science and Technology*, Vol. 51/4.

[138] Garn, T.G., M.R. Greenhalgh and J.D. Law (2016), "Development and evaluation of a silver mordenite composite sorbent for the partitioning of xenon from krypton in gas compositions", *Journal of Nuclear Science and Technology*, Vol. 53/10, pp. 1 484-1 488.

[139] Thallapally, P.K. and D.M. Stachan (2012), *Initial Proof-of-principle for Near Room Temperature Xe and Kr Separation from Air with MOFs*, FCRD-SWF-2012-00131, PNNL-21452, United States Department of Energy, www.pnnl.gov/main/publications/external/technical_reports/PNNL-21452.pdf.

[140] Fernandez, C.A., J. Liu, K. Thallapally and D.M. Strachan (2012), "Switching Kr/Xe selectivity with temperature in a metal organic framework", *Journal of the American Chemical Society*, Vol. 134/22, pp. 9 046-9 049, https://doi.org/10.1021/ja302071t.

[141] Banerjee, D., A.J. Cairns, J. Liu, R.K. Motkuri, S.K. Nune, C.A. Fernandez. R. Krishna, D.M. Strachan and P.K. Thallapally (2015), "Potential of metal-organic frameworks for separation of xenon and krypton", *Accounts of Chemical Research*, Vol. 48/2, pp. 211-219.

[142] Liu, J., D.M. Strachan and P.K. Thallapally (2014), "Enhanced noble gas adsorption in Ag@MOF-74Ni", *Chemical Communications*, Vol. 50, pp. 466-468.

[143] Liu, J., C.A. Fernandez, P.F. Martin, D.M. Strachan and P.K. Thallapally (2014), "A two-column method for the separation of Kr and Xe from process off-gases", *Industrial & Engineering Chemistry Research*, Vol. 53, pp. 12 893-12 899.

[144] Bertrand, M., P. Pochon, N. Cedat, O. Baudoin and R. Sardeing (2018), "Modelling and thermodynamic study of krypton separation by dynamic fixed-bed adsorption on zeolite", *30th ESAT 2018 Conference (European Symposium on Applied Thermodynamics)*, Prague.

[145] Deliere, L., B. Coasne, S. Topin, C. Gréau, C. Moulin and D. Farrusseng (2016), "Breakthrough in xenon capture and purification using adsorbent-supported silver nanoparticles", *Chemistry: A European Journal*, Vol. 22/28, pp. 9 660-9 666, https://doi.org/10.1002/chem.201601351.

[146] Monpezat, A., S. Topin, L. Deliere, D. Farrusseng and B. Coasne (2019), "Evaluation methods of adsorbents for air purification and gas separation at low concentration: Case studies on xenon and krypton", *Industrial & Engineering Chemistry Research*, Vol. 58/11, pp. 4 560-4 571.

[147] Deliere, L., S. Topin, B. Coasne, J.P. Fontaine, S.D. Vitor, C.D. Auwer, P.L. Solari, C. Daniel, Y. Schuurman and D. Farrusseng (2014), "Role of silver nanoparticles in enhanced xenon adsorption using silver-loaded zeolites", *The Journal of Physical Chemistry C*, Vol. 118/43, pp. 25 032-25 040.

[148] Aly, H.F., N. EL-Said and A.T. Kassem (2016), "Separation and speciation of ruthenium from nitrate medium by Ira-410 anion exchangers kinetic, thermodynamics and reaction mechanism", *European Journal of Applied Sciences*, Vol. 8/1, pp. 28-40.

[149] Shin, J. and J. Park (2003), "Trapping characteristics of volatile ruthenium oxides by Y2O3 filter", *Korean Journal of Chemical Engineering*, Vol. 20, pp. 145-150, https://doi.org/10.1007/BF02697200.

[150] Spencer, B.B., M.L. Parks and S.H. Bruffey (2018), "Initial assessment of ruthenium removal systems for tritium pre-treatment off-gas", ORNL/SPR-2017/576, NTRD-MRWFD-2018-000200, Oak Ridge National Laboratory, Oak Ridge, TN.

[151] Spencer, B.B. and S.H. Bruffey (2018), "Initial series of ruthenium adsorption optimization studies", ORNL/SPR-2018/913, NTRD-MRWFD-2018-000197, Oak Ridge National Laboratory, Oak Ridge, TN.

[152] Spencer, B.B. and S.H. Bruffey (2019), "Characterization of ruthenium tetroxide capture from dry gas streams by silica gel and metal surfaces", *ANS Global and Top Fuel 2019*, Seattle, WA.

[153] KAERI (2005), *Trapping Technology for Gaseous Fission Products from Voloxidation Process*, KAERI/TR-3047/2005, Korea Atomic Energy Research Institute.

[154] Yang, Jae Hwan, Hwan-Seo Park and Yung-Zun Cho (2017), "Immobilization of Cs-trapping ceramic filters within glass-ceramic waste forms", *Annals of Nuclear Energy*, Vol. 110, pp. 1 121-1 126, www.sciencedirect.com/science/article/pii/S0306454917302633.

[155] Westphal, B.R., J.J. Park, J.M. Shin, G.I. Park, K.J. Bateman and D.L. Wahlquist Westphal (2008), "Selective trapping of volatile fission products with an off-gas treatment system", *Separation Science and Technology*, Vol. 43/9, pp. 2 695-2 708, https://doi.org/10.1080/01496390802122139.

[156] Shin, J.M., J.J. Park, K.C. Song and J.H. Kim (2009), "Trapping behavior of gaseous cesium by fly ash filters", *Applied Radiation and Isotopes*, Vol. 67/7-8, pp. 1 534-1 539.

[157] Park, J.J., J.M. Shin, J.H. Yang, Y.H. Baek, J.W. Yoo and G.I. Park (2013), *Fly-ash Granule Filter for Trapping Gaseous Cesium*, KAERI/TR-5277/2013, Korea Atomic Energy Research Institute.

[158] Park, J.J., J.M. Shin, M.S. Yang, K.S. Chun and H.S. Park (2001), *Trapping Characteristics for Gaseous Ceasium Generated from Different Cesium Compounds by Fly Ash Filters*, IAEA-SM-357/71, DUPIC Fuel Development Team, Korea Atomic Energy Research Institute.

[159] Yang, J.H., J.H. Yang, J.Y. Yoon, J.H. Lee and Y.-Z. Cho (2017), "A kaolinite-based filter to capture gaseous cesium compounds in off-gas released during the pyroprocessing head-end process", *Annals of Nuclear Energy*, Vol. 103, pp. 29-35.

[160] IAEA (2008), *Spent Fuel Reprocessing Options*, IAEA-TECDOC-1587, International Atomic Energy Agency, Vienna, www.iaea.org/publications/8143/spent-fuel-reprocessing-options.

[161] Westsik, J.H. Jr., K.J. Cantrell, R.J. Serne and N.P. Qafoku (2014), *Technetium Immobilization Forms: Literature Survey*, PNNL-23329, United States Department of Energy, Oak Ridge, TN, www.pnnl.gov/main/publications/external/technical_reports/PNNL-23329.pdf.

[162] Wilhelm, J.G. and H. Schuettelkopf (1973), "Control of iodine in the nuclear industry", *IAEA Technical Reports Series*, No. 148, pp. 47-56, International Atomic Energy Agency, Vienna.

[163] Riley, B.J., J.D. Vienna, D.M. Strachen, J.S. McCloy J.L. Jerden (2016), "Materials and processes for the effective capture and immobilisation of radioiodine: A review", *Journal of Nuclear Materials*, Vol. 470, pp. 307-326.

[164] ANDRA (2005), *Evaluation de la faisabilité du stockage géologique en formation argileuse*, Agence Nationale pour la gestion des Déchets Radioactifs, p. 211, Châtenay-Malabry, France.

[165] Fujihara, H., T. Murase, T. Nisli, K. Noshita, T. Yoshida and M. Matsuda (1999), "Low temperature vitrification of radioiodine using AgI-Ag_2O-P_2O_5 glass system", *MRS Proceedings*, Vol. 556, p. 375.

[166] Sakuragi, T., T. Nishimura, Y. Nasu, H. Asano, K. Hoshino and K. Iino (2008), "Immobilization of radioactive iodine using AgI vitrification technique for the TRU wastes disposal: Evaluation of leaching and surface properties", *MRS Proceedings*, Vol. 1107, p. 279.

[167] Lemesle, T., F.O. Méar, L. Campayo, O. Pinet, B. Revel and L. Montagne (2014), "Immobilization of radioactive iodine in silver aluminophosphate glasses", *Journal of Hazardous Materials*, Vol. 264, pp. 117-126.

[168] Lemesle, T., L. Montagne, F.O. Méar, B. Revel, L. Campayo and O. Pinet (2015), "Bismuth silver phosphate glasses as alternative matrices for the conditioning of radioactive iodine", *Physics and Chemistry of Glasses: European Journal of Glass Science and Technology B*, Vol. 56/2, pp. 71-75.

[169] Park, J.J., J.M. Shin, C.J. Park, J.W. Lee, G.I. Park, K.C. Song and J.I. Chun (2008), "Radioactivity analysis of the advanced voloxidation process", *International Pyroprocessing Research Conference (IPRC) 2008*, Jeju Island, Korea.

[170] Nichols, R.H. Jr., C.M. Hohenberg, K. Kehm, Y. Kim and K. Marti (1994), "I-Xe studies of the Acapulco Meteorite: Absolute I-Xe ages of individual phosphate grains and the Bjurböle Standard", *Geochemica et Cosmochimica Acta*, Vol. 58/11, pp. 2 553-2 561.

[171] Guy, C., F. Audubert, J.E. Lartigue, C. Latrille, T. Advorcat and C. Fillet (2002), "New conditionings for separated long-lived radionuclides", *Comptes Rendus Physique*, Vol. 3/7-8, pp. 827-837.

[172] Campayo, L., F. Audubert, J. Lartigue, E. Courtois-Manara, S. Le Gallet, F. Bernard, S. Rossignol (2014), "French studies on the development of potential conditioning matrices for iodine 129", *MRS Proceedings*, Vol. 1744, pp. 15-20, https://doi.org/10.1557/opl.2015.309.

[173] Le Gallet, S., L. Campayo, E. Courtois, S. Hoffmann, Y. Grin, F. Bernard and F. Bart (2010), "Spark plasma sintering of iodine-bearing apatite", *Journal of Nuclear Materials*, Vol. 400/3, pp. 251-256.

[174] Campayo, L., S. Le Gallet, D. Perret, E. Courtois, C. Cau Dit Coumes, Y. Grin and F. Bernard (2015), "Relevance of the choice of spark plasma sintering parameters in obtaining a suitable microstructure for iodine-bearing apatite designed for the conditioning of I-129", *Journal of Nuclear Materials*, Vol. 457, pp. 63-71.

[175] Campayo, L., A. Grandjean, A. Coulon, R. Delorme, D. Vantelon and D. Laurencin (2011), "Incorporation of iodates into hydroxyapatites: A new approach for the confinement of radioactive iodine", *Journal of Materials Chemistry*, Vol. 21/44, pp. 17 609-17 611.

[176] Fuhrmann, M., S. Bajt and M.A.A. Schoonen (1998), "Sorption of iodine on minerals investigated by X-ray absorption near edge structure (XANES) and ^{125}I tracer sorption experiments", *Applied Geochemistry*, Vol. 13/2, pp. 127-141.

[177] Fukui, M., Y. Fujikawa and N. Satta (1996), "Factors affecting interaction of radioiodide and iodate species with soil", *Journal of Environmental Radioactivity*, Vol. 31/2, pp. 199-216.

[178] Coulon, A., A. Grandjean, D. Laurencin, P. Jollivet, S. Rossignol and L. Campayo (2017), "Durability testing of an iodate-substituted hydroxyapatite designed for the conditioning of ^{129}I", *Journal of Nuclear Materials*, Vol. 484, pp. 324-331.

[179] Coulon, A., D. Laurencin, A. Grandjean, C. Cau Dit Coumes, S. Rossignol and L. Campayo (2014), "Immobilization of iodine into a hydroxyapatite structure prepared by cementation", *Journal of Materials Chemistry A*, Vol. 2, pp. 20 923-20 932.

[180] Maddrell, E., A. Gandy and M. Stennett (2014), "The durability of iodide sodalite", *Journal of Nuclear Materials*, Vol. 449/1-3, pp. 168-172.

[181] Sheppard, G.P., J.A. Hriljac, E.R. Maddrell and N.C. Hyatt (2006), "Silver zeolites: Iodide occlusion and conversion to sodalite – A potential I-129 waste form?", *Materials Research Society Symposium Proceedings*, Vol. 932, pp. 775-782.

[182] Maddrell, E.R., E.R. Vance and D.J. Gregg (2015), "Capture of iodine from the vapour phase and immobilisation as sodalite", *Journal of Nuclear Materials*, Vol. 467, pp. 271-279.

[183] Maddrell, E.R., E.R. Vance, C. Grant, Z. Aly, A. Stopic, T. Palmer, J. Harrison and D.J. Gregg (2019), "Silver iodide sodalite – Wasteform/HIP canister interactions and aqueous durability," *Journal of Nuclear Materials*, Vol. 517, pp. 71-79.

[184] IAEA (2004), *Management of Waste Containing Tritium and Carbon-14*, International Atomic Energy Agency, Vienna.

[185] Jubin, R.T. and S. Bruffey (2016), *Analysis of Selected Legacy ^{85}Kr Samples*, FCRD-MRWFD-2016-000047, United States Department of Energy, Oak Ridge, TN, https://info.ornl.gov/sites/publications/files/Pub68896.pdf.

[186] Bruffey, S.H. and R.T. Jubin (2017), "Analysis of krypton-85 legacy waste forms: Part I", *Nuclear Technology*, Vol. 200/2, pp. 159-169, https://doi.org/10.1080/00295450.2017.1369802.

[187] Asmussen, R.M. and J.J. Neeway (2020), "The sporadic history of rubidium and its role in corrosion of steel related to nuclear material storage", *Journal of Nuclear Materials*, Vol. 530, https://doi.org/10.1016/j.jnucmat.2019.151914.

[188] Huve, J., A. Ryzhikov, H. Nouali, V. Lalia, G. Auge and T.J. Daou (2018), "Porous sorbents for the capture of radioactive iodine compounds: A review", *RSC Advances*, Vol. 8, pp. 29 248-29 273, https://doi.org/10.1039/C8RA04775H.

[189] Chapman, K.W., P.J. Chupas and T.M. Nenoff (2010), "Radioactive iodine capture in silver-containing mordenites through nanoscale silver iodide formation", *Journal of the American Chemistry Society*, Vol. 132/26, pp. 8 897-8 899.

[190] Nanonuclear (2012), "Collaborative report on the workshop", Nanonuclear 2012, Gaithersburg, MD.

[191] Eddaoudi, M. (2002), "Systematic design of pore size and functionality in isoreticular MOFs and their application in methane storage", *Science*, Vol. 295/5554, pp. 469-472.

[192] Thallapally, P.K., J.W. Grate and R.K. Motkuri (2012), "Facile xenon capture and release at room temperature using a metal-organic framework: A comparison with activated charcoal", *Chemical Communications*, Vol. 48, pp. 347-349.

[193] Elsaidi, S.K., M.H. Mohamed, A.S. Helal, M. Galanek, T. Pham, S. Suepaul, B. Space, D. Hopkinson, P.K. Thallapally and J. Li (2020), "Radiation-resistant metal-organic framework enables efficient separation of krypton fission gas from spent nuclear fuel", *Nature Communications*, Vol. 11/3103, https://doi.org/10.1038/s41467-020-16647-1.

[194] Miensah, E.D., M.M. Khan, J. Yu Chen, X.M.Zhang, P. Wang, Z.X. Zhang, Y. Jiao, Y. Liu and Y. Yang (2020), "Zeolitic imidazolate frameworks and their derived materials for sequestration of radionuclides in the environment: A review", *Critical Reviews in Environmental Science and Technology*, Vol. 50/18, pp. 1 874-1 934.

[195] Mahdi, E.M., A.K. Chaudhuria and J.C. Tan (2016), "Capture and immobilisation of iodine (I_2) utilising polymer-based ZIF-8 nanocomposite membranes", *Molecular Systems Design and Engineering*, Vol. 1, pp. 122-131.

[196] Jeazet, H.B.T., C. Staudt and C. Janiak (2012), "A method for increasing permeability in O_2/N_2 separation with mixed-matrix membranes made of water-stable MIL-101 and polysulfone", *Chemical Communications*, Vol. 48, pp. 2 140-2 142.

[197] Wang, Y., H. Gao, A. Miller and P. Pohl (2012), *A New Generation of Adsorbent Materials for Entrapping and Immobilizing Highly Mobile Radionuclides: Municipal and Industrial Waste Disposal*, Dr. Xiao-Ying Yu (ed.), Sandia National Laboratories.

[198] Grandjean, A., Y. Barré, A. Tokarev, J. Causse, Y. Guari, J. Larionova, G. Massasso and J. Long (2014), *Use of a Hofmann Clathrate Material for Extracting Molecular Iodine*, WO2014037353 A1.

[199] Massasso, G. et al. (2015), "Molecular iodine adsorption within Hofmann-type structures $M(L)[M'(CN)_4]$ (M = Ni, Co; M′ = Ni, Pd, Pt): Impact of their composition", *Dalton Transaction*, Vol. 44, pp. 19 357-19 369.

[200] Massasso, G. et al. (2014), "Iodine capture by Hofmann-type clathrate $Ni^{II}(pz)[Ni^{II}(CN)_4]$", *Inorganic Chemistry*, Vol. 53, pp. 4 269-4 271.

[201] Massasso, G., J. Long, C. Guerin, A. Grandjean, B. Onida, Y. Guari, J. Larionova, G. Maurin and S. Devautour-Vinot (2015), "Understanding the host/guest interactions in iodine/Hofmann-type clathrate $Ni(pz)[Ni(CN)_4]$ system", *The Journal of Physical Chemistry C*, Vol. 119/17, pp. 9 395-9 401.

[202] Baron, P. et al. (2019), "A review of separation processes proposed for advanced fuel cycles based on technology readiness level assessments", *Progress in Nuclear Energy*, Vol. 117.

[203] DECC, Department of the Environment Northern Ireland, the Scottish Government and Welsh Assembly (2009), *UK Strategy for Radioactive Discharges*, Department of Energy & Climate Change.

[204] US EPA (1977), "40 CFR 190, Environmental Radiation Protection Standards for Nuclear Power Operations – Final Rule," Federal Register 42 (13 January 1977): 2860, United States Environmental Protection Agency.

[205] Hunt, G.J., B.D. Smith and W.C. Camplin (1998), "Recent changes in liquid radioactive waste discharges from Sellafield to the Irish Sea: Monitoring of the environmental consequences and radiological implications", *Radiation Protection Dosimetry*, Vol. 75/1, pp. 149-154.

[206] NEA (2018), *State-of-the-art Report on the Progress of Nuclear Fuel Cycle Chemistry*, NEA No. 7267, OECD Publishing, Paris, www.oecd-nea.org/jcms/pl_14970.